Modeling and Control of a Quadrotor with Dynamic Inertia

Jared D A Becker

A thesis submitted in partial fulfillment of the requirements for the degree of

Master of Science in Aeronautics & Astronautics

University of Washington

2013

Reading Committee:

Kristi Morgansen

Juris Vagners

Program Authorized to Offer Degree:
Aeronautics & Astronautics

University of Washington

Abstract

Modeling and Control of a Quadrotor with Dynamic Inertia

Jared D A Becker

Chair of the Supervisory Committee:
Associate Professor Kristi Morgansen
Aeronautics & Astronautics

As the support and technology for unmanned vehicles has increased, so have the possible applications for Unmanned Aerial Vehicles (UAVs). From military intelligence gathering missions, to civilian search and rescue missions, the demand for highly capable UAVs is high. Drawing inspiration from biological examples such as the hawkmoth, this research investigates the use of dynamic inertia as a control mechanism for small quadrotor helicopters. Using Lagrangian mechanics, a nonlinear 3D model and a nonlinear 2D model are developed for a quadrotor with dynamic inertia modeled as an actuated pendulum mounted beneath the vehicle. Designing a linear quadratic controller for a linearization of the system about the hovering flight condition and applying this controller to the nonlinear model results in a stabilizing dynamic inertia controller capable of adequate trajectory tracking for a simple desired trajectory. Additional simulations also show that the linear controller has favorable robustness properties to compensate for modeling errors and nonlinearities.

TABLE OF CONTENTS

LIST OF FIGURES

LIST OF TABLES

ACKNOWLEDGMENTS

First I would like to thank my advisor, Kristi Morgansen, for her invaluable guidance and mentoring throughout my time here at the University of Washington, in addition to her help on this thesis. I would also like to thank Brian, Nathan, Jake, and the rest of the nonlinear dynamics and controls lab for their help and willingness to do so that has contributed to this research. Finally, I would like to thank Office of Naval Research which provided a portion of the funding for this research (ONR grant N000141010952).

DEDICATION

To my best friend and loving wife, Paige.

Chapter 1

INTRODUCTION

The application of Unmanned Aerial Vehicles (UAVs) has dramatically increased in recent years as support and technology for unmanned vehicles has increased. For many applications, unmanned vehicles offer a less expensive alternative to manned aircraft and can perform operations considered too dangerous or fatiguing for pilots of manned aircraft. Additionally, unmanned vehicles can be built smaller, quieter, and more maneuverable to operate in environments where manned aircraft cannot operate. In particular, the military has acquired a large array of UAVs varying in size, capability, and functionality for specific roles. UAVs such as the versatile fixed wing U.S. Air Force MQ-9 Reaper [1] with a 66 foot wingspan can perform both offensive and defensive missions including: intelligence, surveillance, and reconnaissance (ISR), close air support (CAS), combat search and rescue (CSAR), and precision strike. In addition to large UAVs, the military employs small fixed wing Micro Air Vehicles (MAVs) such as the Tactical Micro Unmanned Aerial Vehicle (TACMAV) [2] for beyond line-of-sight surveillance. With a flexible composite construction and a small 21 inch wingspan, the TACMAV can be carried in a soldier's backpack and used to by the soldiers to get a bird's eye view of what is beyond the next hill or over the wall. This information is extremely valuable, and otherwise too dangerous to acquire by traditional means. The military also uses rotorcraft UAVs such as the YMQ-18A Hummingbird [3] for various offensive and defensive operations as well as the K-MAX [4] unmanned cargo resupply helicopter that can resupply troops in hostile conditions while keeping manned helicopters safe from danger.

Although UAVs are widely used throughout the military, current UAV applications

are not limited to the military. Various police departments are turning to UAVs as a cost effective alternative to helicopters. The Mesa County, CO Sheriff Department has used both fixed wing and rotorcraft drones to help fire investigators study an arson scene, to search for lost hikers, and to search for a suicidal resident that ran into the wilderness. At approximately $30,000 to $50,000 each, the drones cost about the same price as a squad car, and the operating cost is almost nothing compared to the operating cost of a helicopter [5]. Aerial imagery capabilities of small UAVs are currently used for applications including real estate promotion [6], building inspections [7], geographic surveying [8], and more. As UAV technology matures, the breadth of potential applications will increase further. Small UAVs with the capability to fly in unknown cluttered environments could be sent into forests to search for lost hikers below the tree canopy, or they could be sent into unstable buildings to search for survivors after a natural disaster. UAVs could also be used to asses damage in environments contaminated by chemicals or radiation, or other larger UAVs such as the K-MAX helicopters could be used to carry water to help extinguish forest fires, to name a few of the potential applications for UAVs in the future.

Small UAVs and Micro Aerial Vehicles (MAVs) have also been used throughout the world at both research institutions and engineering companies alike. In particular, quadrotor helicopters, or quadrotors have been used as testbeds for various control algorithms. Quadrotors are small rotorcraft vehicles that utilize two pairs of counter-rotating, fixed-pitch blades to generate lift and provide control to the vehicle. By varying the rotor speed, a quadrotor can change the lift and torque produced by each of the four motors to generate aerodynamic forces on the vehicle. The quadrotor design is simpler and more robust than the traditional helicopter design while maintaining the ability to take off vertically, hover, and operate in tight environments. High manueverability, low weight, low cost, and small size make quadrotors ideal vehicles for indoor testing.

Many different control algorithms have been applied to quadrotors, and both linear

and non-linear methods have been successfully implemented. In [9] nested feedback loop controllers were applied independently to multiple quadrotors. The inner attitude control loop used on-board gyros and accelerometers to control roll, pitch, and yaw via proportional derivative (PD) control laws. The outer position control loop was provided state estimates to control position and velocities via proportional integral derivative (PID) feedback. A VICON Motion Capture System was used to precisely and accurately track the position and velocity of the quadrotors within the test environment and provide state estimates to the position controller. For this experiment all control input and trajectory generation computations were computed on an off-board computer then sent to the quadrotor via XBee radio communication. These controllers with additional formation flight algorithms were simulated then implemented with favorable results. Following the multiple MAV, experiment the individual quadrotor capabilities were expanded in [10]. Using the same PD and PID controller design as in [9], the quadrotors were able to fly through narrow vertical gaps and perform perching maneuvers on inverted surfaces with impressive results. The trajectories were generated in simulation using a sequence of smaller trajectory segments and associated controls, then altered in experimentation using parameter variation. Because the quadrotor performance was not exactly critically damped with the exact settling time as simulated, the pitch and three velocity component parameters commanded in simulation were adjusted. Parameter variation resulted in actual parameter values after the simulated settling time equal to the desired parameter values. Once again, a VICON motion capture system and off-board computations were used in experimentation.

In addition to classic PID controllers, Linear Quadratic (LQ) controllers have been applied to quadrotors. In [11] a nonlinear tilt-wing quadrotor model was simulated using a LQR based controller to stabilize the vertical flight mode with the wings and motors rotated to vertical. Position hold and 3D trajectory tracking performance were evaluated, followed by a robustness test where the trajectory tracking

test was repeated with the addition of Gaussian noise modeled as aerodynamic forces and torques on the vehicle. The LQR controller resulted in good trajectory tracking performance, even with noise added to the system. In [12] both a PD and an LQ attitude controller were simulated, implemented, then compared. Although each controller adequately stabilized the quadrotor in both simulation and experimentation, the PD controller performed better than the LQ controller. This discrepancy in performance was likely a result of modeling imperfections.

Non-linear control methods have also been applied to quadrotors. Both the backstepping and sliding-mode control methods were used to design and implement controllers in [13]. Backstepping controllers were designed and simulated for both the rotation subsystem to control attitude, and the linear translation subsystem to control position with successful results. Only the attitude stabilization controller was implemented. The controller was tested on a fixed altitude test bench and provided stabilization in under five seconds for nearly critical initial conditions. A single sliding-mode controller for attitude stabilization was designed and implemented with average results and suffered from sensor drift. Visual feedback was used as the primary sensor in [14] while implementing backstepping and feedback linearization methods for control. Feedback linearization methods were used to build a model-based controller that could switch between various modes such as hover, take off, land, etc. with the hover mode as the central mode. Additionally, a combination of backstepping controllers and PD controllers were designed for both attitude stabilization as well as moving to an arbitrary heading. Both controllers were simulated, but the backstepping method performed better than the feedback linearization controllers. After comparing the two controllers, the backstepping and PD controller was successfully implemented on a small quadrotor.

The previously mentioned research focused on control algorithms for the vehicle alone, but various groups have developed control algorithms for quadrotors with additional payload. In [15], a PID controller similar to those controllers used in [9],

and [10] were used to control a quadrotor capable of grasping and carrying a wooden board or other static payloads with unknown parameters. A least squares method was used to estimate the payload parameters during flight. Implementing the controller and parameter estimation resulted in good performance for trajectory tracking while carrying a payload. Control algorithms have also been developed for quadrotors carrying suspended loads as seen in [16]. Unlike the grasping quadrotor in [15], the parameters of the suspended load were known, requiring no estimation, and the suspended load was a simple pendulum capable of swinging freely beneath the vehicle instead of a rigid piece of wood. One PD controller and one nonlinear controller based on feedback linearization were used to stabilize the vehicle while a dynamic programming approach was used to generate the optimal swing-free trajectory. The proposed control algorithms were simulated and implemented successfully while keeping the payload from swinging more than approximately five degrees in any direction.

The research presented here is different from the previously mentioned research because this research utilizes a different method of control that is inspired from biology. The contributions of this research include: modeling a quadrotor that utilizes dynamic inertia as the primary control mechanism, developing a linear LQR controller for the quadrotor with dynamic inertia, and evaluating the performance of the linear controller implemented on the nonlinear model.

Chapter 2 outlines the biological inspiration for using dynamic inertia as a control mechanism for a flight vehicle and details the differences between traditional differential thrust control and dynamic inertia control applied to a quadrotor. Both 3D and 2D nonlinear models are developed using Lagrangian mechanics for the quadrotor with dynamic inertia in Chapter 3. In Chapter 4 the nonlinear models are linearized about the hovering flight condition and linear LQR controllers are developed. In Chapter 5 the linear controllers are implemented on the nonlinear quadrotor models and simulated in MATLAB . Finally, Chapter 6 concludes the thesis with important takeaways from the research and discusses opportunities for future work.

Chapter 2

DYNAMIC INERTIA

The primary inspiration for this research comes from biology, specifically insects. The hawkmoth is a large, fast flying, agile insect studied at the University of Washington [17] to investigate the way these insects use their abdomen for flight control. Using a small insect-scaled flight simulator to produce visual pitch stimuli, the resulting abdominal motion was tracked and a transfer function was derived from the results. Comparing the moth transfer function to a derived control strategy for abdominal movement verified that moths actively stabilize pitch rotations using abdominal motion as the only control input. Not only was abdominal motion alone sufficient to stabilize the moth, but abdominal motions were able to stabilize in as little as 50 ms. Results from this research suggested that airframe articulation could be a plausible control mechanism for active flight.

Using the hawkmoth as an example, the purpose of this research is to investigate the use of dynamic inertia as a control mechanism for a quadrotor. In this study dynamic inertia is implemented on the quadrotor through a dynamic mass hanging beneath the quadrotor connected by a rigid rod assumed to be mass-less. At the joint between the quadrotor and the rod are servos capable of actuating the dynamic mass in both the pitch and roll directions. Similar to the abdominal motion of a hawkmoth, actuating the mass underneath the quadrotor changes the moment of inertia of the vehicle and generates a rotational moment on the vehicle. The intent is not to replicate the abdominal stabilization of the hawkmoth, but to use examples from biology to extract engineering principles and learn from nature.

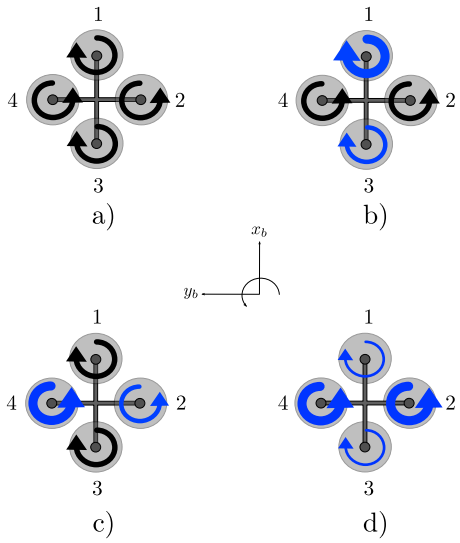

Figure 2.1: Differential thrust for a) steady state, b) pitch, c) roll, and d) yaw.

2.1 Quadrotor Thrust Generation

Before continuing with the dynamic mass it is important to understand more about quadrotors and the traditional differential thrust methods used to control quadrotors. Traditional helicopters utilize a large, horizontally mounted main rotor to provide lift and a smaller, nearly vertically mounted tail rotor to offset the torque generated by the main rotor. Unlike traditional helicopters, all four rotors of a quadrotor rotate in the same plane, and the torque generated by one rotor is offset by opposing torque generated by an adjacent counter rotating rotor, eliminating the need for a tail rotor. Therefore, all four rotors contribute to the lift of the vehicle. Figure 2.1a is a top view diagram of a quadrotor indicating the rotation direction of each of the four rotors. Notice that the front and rear rotors rotate in the clockwise direction, while the left and right rotors rotate in the counterclockwise direction.

Additionally, helicopters have variable pitch rotors used for control, whereas quadrotors have fixed pitch blades and use differential thrust to generate rotational moments. Pitch up is generated by increasing the thrust of the front motor while decreasing the

thrust of the back rotor, shown in Figure 2.1b. Similarly, a positive rolling moment is generated by increasing thrust of the left rotor while decreasing the thrust of the right rotor, Figure 2.1c. A positive yaw moment is generated by increasing the thrust of the left and right rotors rotating counterclockwise while decreasing the thrust of the front and rear rotors rotating in the clockwise direction, resulting in a non-zero torque that generates the yaw moment on the vehicle, Figure 2.1d. The absence of a tail rotor and variable pitch rotors make quadrotors less complex and more robust than traditional helicopters, but this method requires independent control of each of the four rotors.

Using biological examples as inspiration, the purpose of the actuated is mass is to use the dynamic inertia as a control mechanism instead of using differential thrust as the primary method for control. In other words, all motors produce uniform thrust, and any thrust control varies the thrust of all motors equally. The only exception

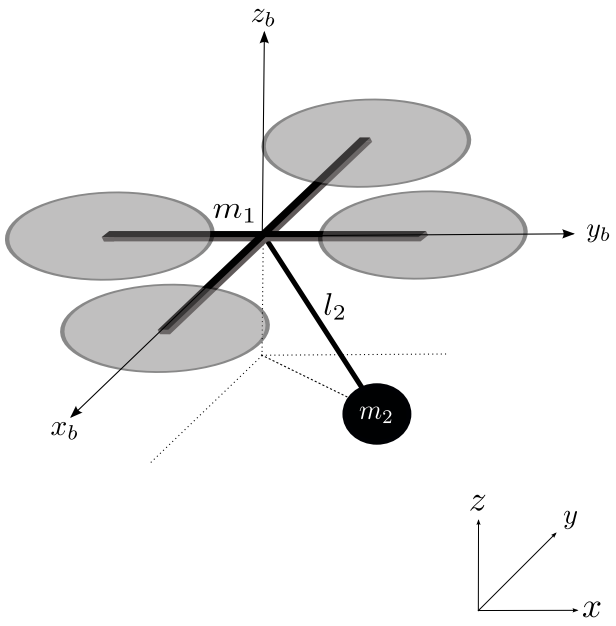

Figure 2.2: Diagram of the quadrotor with actuated dynamic mass (m_2) mounted beneath the vehicle and the axis system.

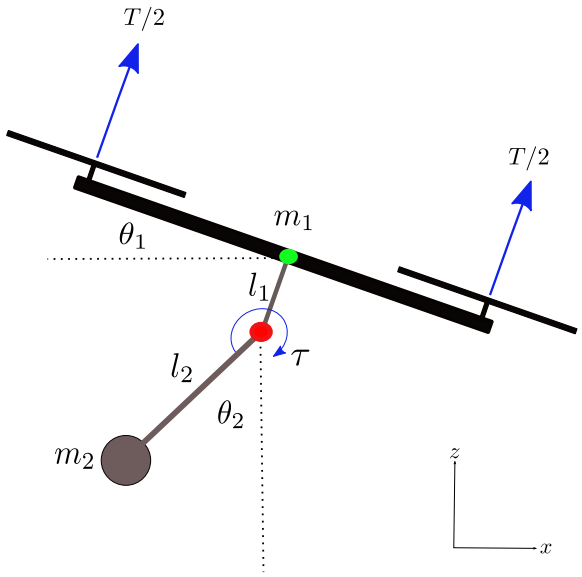

Figure 2.3: Side view diagram of the quadrotor and dynamic mass showing the location of the pendulum joint (red) is not coincidental with the quadrotor center of gravity (green).

to this rule occurs when controlling yaw. Yaw maneuvers are controlled through differential thrust methods. Actuating the mass underneath the quadrotor changes the moment of inertia of the vehicle which will generate a rotational moment on the quadrotor provided all rotors rotate at the same speed.

2.2 Axis System

Important to developing a mathematical model of the quadrotor is defining a suitable coordinate system. A standard inertial reference frame is defined $x,\ y,\ z$ and a body fixed axis is defined $x_b,\ y_b,\ z_b$ shown in Figure 2.2. Notice that the body fixed axis is slightly different than the traditional aircraft body fixed axis system. The x_b axis points out of the front of the vehicle, the y_b axis points out of the left side of the vehicle, and the z_b axis points out of the top of the vehicle. Figure 2.2 also shows the dynamic mass, m_2, underneath the vehicle. The quadrotor is modeled as a rigid body,

and the dynamic mass is modeled as a pendulum consisting of mass m_2 centered at the end of a mass-less rod of length l_2.

Figure 2.3 is a side view diagram of the quadrotor with dynamic mass showing pertinent model parameters. It is important to note that the location of the joint where the dynamic mass is attached to the quadrotor (shown in red) does not coincide with center of gravity of the quadrotor (shown in green). The distance between the center of gravity of the qaudrotor and the joint with the dynamic mass is l_1. Also shown in Figure 2.3 are the planar control inputs. Pure thrust is evenly produced by the motors fixed in the z_b direction, and the servo torque τ is applied at the joint. Although this figure depicts the x-z plane, a similar servo torque is applied at the joint to generate rolling moments in y-z plane. Traditional differential thrust control is only applied for minor yaw corrections.

Chapter 3

QUADROTOR DYNAMICS

For multi-body systems Lagrangian mechanics are better suited than Newtonian mechanics for developing the equations of motion for the complete system. Newtonian mechanics require developing equations of motion for each body, assuming three or six degrees of freedom (DOF) for each body, then reducing the total number of equations of motion to the number of DOF for the complete system using system constraints. The advantage of using Lagrangian mechanics is that the multi-body system is treated as a whole and the number of equations of motion is equal to the number of DOF for the complete system from the start. For multi-body systems with complex interactions between bodies, the Lagrangian approach is a more elegant approach and is better suited for developing the equations of motion than Newtonian mechanics. Due to the complex interactions between the actuated mass and the quadrotor, Lagrangian mechanics are used to develop the equations of motion for the complete system including both the quadrotor and the dynamic mass. The Lagrangian equations of motion are given by

$$\frac{d}{dt}\left(\frac{\partial L}{\partial \dot{q}_i}\right) - \frac{\partial L}{\partial q_i} = Q_{nc,i} \tag{3.1}$$

where $Q_{nc,i}$ are the non-conservative forces on the system, and q_i are the generalized coordinates for the system. The Lagrangian L is equal to the total kinetic energy of the system T minus the total potential energy of the system U,

$$L = T - U \ . \tag{3.2}$$

3.1 Generalized Coordinates

Assuming rigid body dynamics, a multi-body system with n independent bodies requires $6n$ coordinates to describe the position and orientation of each body. When components are linked together the number of coordinates needed and the number of DOF of the system is reduced to $6n - m$, where m is the number of nonholonomic constraints. For this quadrotor model, the dynamic mass is free to rotate in pitch and roll, but the yaw is fixed. Additionally, the translation velocity of the dynamic mass is constrained by its angular positions and velocities as well as the velocity of the quadrotor. Together the fixed yaw and dynamic mass velocity relations constitute four constraints on the system. Therefore, this system has eight degrees of freedom and requires eight generalized coordinates. Let the generalized coordinates be the location of the center of gravity (CG) of the quadrotor $(x,\ y,\ z)$, the rotation angles of the quadrotor $(\theta_1,\ \phi_1,\ \psi_1)$, and the angular position of the dynamic mass $(\theta_2,\ \phi_2)$:

$$
\begin{array}{lll}
q_1 = x & q_4 = \theta_1 & q_7 = \theta_2 \\
q_2 = y & q_5 = \phi_1 & q_8 = \phi_2 \\
q_3 = z & q_6 = \psi_1 &
\end{array}
$$

It is important to clarify that the angular position of the dynamic mass $(\theta_2,\ \phi_2)$ is not measured with respect to the quadrotor attitude but with respect to an inertial frame.

3.2 Kinetic Energy

A simple way to develop the Lagrangian equations of motion for this system is to solve (3.1) term by term and combining the terms at the end. Before solving each term, the total kinetic and potential energy of the system must be found. To simplify the kinetic energy computation, the total kinetic energy of the system can be rewritten as the sum of the kinetic energy of the quadrotor and the kinetic energy of the dynamic

mass, $T = T_1 + T_2$.

The kinetic energy of the quadrotor is given by

$$T_1 = \frac{1}{2}m_1(\bar{v}_1 \cdot \bar{v}_1) + \frac{1}{2}I_{1_y}(\omega_1 \cdot \omega_1) + \frac{1}{2}I_{1_x}(\omega_2 \cdot \omega_2) + \frac{1}{2}I_{1_z}(\omega_3 \cdot \omega_3) \ , \tag{3.3}$$

where the angular velocities are simply the time derivatives of the rotation angles of the quadrotor,

$$\omega_1 = \dot{\theta_1} \qquad \omega_2 = \dot{\phi_1} \qquad \omega_1 = \dot{\psi_1} \ ,$$

and the linear velocity is simply the time derivative of $\bar{r}_1$, the vector from the origin to the center of gravity (CG) of the quadrotor,

$$\bar{r}_1 = (x)\hat{i} + (y)\hat{j} + (z)\hat{k}$$

$$\bar{v}_1 = (\dot{x})\hat{i} + (\dot{y})\hat{j} + (\dot{z})\hat{k} \ .$$

where $\hat{i},\ \hat{j},\ \hat{k}$ are unit vectors for the inertial coordinate system. Substituting the velocity equations into (3.3) results in

$$T_1 = \frac{1}{2}m_1(\dot{x}^2 + \dot{y}^2 + \dot{z}^2) + \frac{1}{2}I_{1_y}(\dot{\theta}_1^2) + \frac{1}{2}I_{1_x}(\dot{\phi}_1^2) + \frac{1}{2}I_{1_z}(\dot{\psi}_1^2) \ , \tag{3.4}$$

the kinetic energy of the quadrotor.

Next, compute the kinetic energy of the dynamic mass. For this model, the dynamic mass is assumed to be a point mass with a center of gravity located at the end of the massless rod, similar to a pendulum, connected to the bottom of the quadrotor chassis. The kinetic energy of the dynamic mass is

$$T_2 = \frac{1}{2}m_2(\bar{v}_2 \cdot \bar{v}_2) + \frac{1}{2}I_{2_y}(\omega_4 \cdot \omega_4) + \frac{1}{2}I_{2_x}(\omega_5 \cdot \omega_5) \ . \tag{3.5}$$

Once again the angular velocities are simply the time derivatives of the angular position of the dynamic mass

$$\omega_1 = \dot{\theta_2},\ \omega_2 = \dot{\phi_2} \ .$$

However, the velocity vector for the dynamic mass is much more complicated than that of the quadrotor. Here, $\bar{r}_2$ is the vector from the origin to the CG of the dynamic mass in terms of the geometric relations and the location of the quadrotor CG. The position and velocity vectors of the dynamic mass are as follows:

$$\bar{r}_2 = (x - l_1 \sin\theta_1 \cos\phi_1 - l_2 \sin\theta_2 \cos\phi_2)\hat{i} + (y + l_1 \cos\theta_1 \sin\phi_1 + l_2 \cos\theta_2 \sin\phi_2)\hat{j} + (z - l_1 \cos\theta_1 \cos\phi_1 - l_2 \cos\theta_2 \cos\phi_2)\hat{k}$$

$$\begin{aligned}\bar{v}_2 = {} & (\dot{x} - \dot{\theta}_1 l_1 \cos\theta_1 \cos\phi_1 + \dot{\phi}_1 l_1 \sin\theta_1 \sin\phi_1 - \dot{\theta}_2 l_2 \cos\theta_2 \cos\phi_2 + \dot{\phi}_2 l_2 \sin\theta_2 \sin\phi_2)\hat{i} \\ & + (\dot{y} + \dot{\phi}_1 l_1 \cos\theta_1 \cos\phi_1 - \dot{\theta}_1 l_1 \sin\theta_1 \sin\phi_1 + \dot{\phi}_2 l_2 \cos\theta_2 \cos\phi_2 - \dot{\theta}_2 l_2 \sin\theta_2 \sin\phi_2)\hat{j} \\ & + (\dot{z} + \dot{\theta}_1 l_1 \sin\theta_1 \cos\phi_1 + \dot{\phi}_1 l_1 \cos\theta_1 \sin\phi_1 + \dot{\theta}_2 l_2 \sin\theta_2 \cos\phi_2 + \dot{\phi}_2 l_2 \cos\theta_2 \sin\phi_2)\hat{k} \ .\end{aligned}$$

Substituting the velocities into (3.5) results in

$$\begin{aligned}T_2 = {} & \frac{1}{2} m_2 [(\dot{x} - \dot{\theta}_1 l_1 \cos\theta_1 \cos\phi_1 + \dot{\phi}_1 l_1 \sin\theta_1 \sin\phi_1 - \dot{\theta}_2 l_2 \cos\theta_2 \cos\phi_2 + \dot{\phi}_2 l_2 \sin\theta_2 \sin\phi_2)^2 \\ & + (\dot{y} + \dot{\phi}_1 l_1 \cos\theta_1 \cos\phi_1 - \dot{\theta}_1 l_1 \sin\theta_1 \sin\phi_1 + \dot{\phi}_2 l_2 \cos\theta_2 \cos\phi_2 - \dot{\theta}_2 l_2 \sin\theta_2 \sin\phi_2)^2 \\ & + (\dot{z} + \dot{\theta}_1 l_1 \sin\theta_1 \cos\phi_1 + \dot{\phi}_1 l_1 \cos\theta_1 \sin\phi_1 + \dot{\theta}_2 l_2 \sin\theta_2 \cos\phi_2 + \dot{\phi}_2 l_2 \cos\theta_2 \sin\phi_2)^2] \\ & + \frac{1}{2} I_{2_y} (\dot{\theta}_2^2) + \frac{1}{2} I_{2_x} (\dot{\phi}_2^2) \ , \quad (3.6)\end{aligned}$$

the kinetic energy of the dynamic mass. Finally the total kinetic energy of the system is the sum of the kinetic energy of the quadrotor (3.4) and the kinetic energy of the dynamic mass (3.6).

3.3 Potential Energy

With the kinetic energy computed, the total potential energy of the system is the last component that must be computed before solving for each term of the Lagrange equation. The total potential energy of the system is straightforward:

$$U = m_1 g h_1 + m_2 g h_2 \ ,$$

where $h_1 = z$ is the height of the quadrotor CG, and h_2 is the height of the dynamic mass CG. Substituting the height equations results in

$$U = g\big(m_1 z + m_2(z - l_1\cos\theta_1\cos\phi_1 - l_2\cos\theta_2\cos\phi_2)\big)\ , \tag{3.7}$$

the total potential energy of the system.

The Lagrangian is then computed $L = T_1 + T_2 - U$ resulting in

$$\begin{aligned} L = \frac{1}{2}m_2((\dot{x} - l_1\dot{\theta}_1\cos\theta_1\cos\phi_1 - l_2\dot{\theta}_2\cos\theta_2\cos\phi_2 + l_1\dot{\phi}_1\sin\theta_1\sin\phi_1 + l_2\dot{\phi}_2\sin\theta_2\sin\phi_2)^2 \\ + (\dot{y} + l_1\dot{\phi}_1\cos\theta_1\cos\phi_1 + l_2\dot{\phi}_2\cos\theta_2\cos\phi_2 - l_1\dot{\theta}_1\sin\theta_1\sin\phi_1 - l_2\dot{\theta}_2\sin\theta_2\sin\phi_2)^2 \\ + (\dot{z} + l_1\dot{\theta}_1\cos\phi_1\sin\theta_1 + l_1\dot{\phi}_1\cos\theta_1\sin\phi_1 + l_2\dot{\theta}_2\cos\phi_2\sin\theta_2 + l_2\dot{\phi}_2\cos\theta_2\sin\phi_2)^2) \\ + \frac{1}{2}I_{1y}\dot{\theta}_1^2 + \frac{1}{2}I_{1x}\dot{\phi}_1^2 + \frac{1}{2}I_{1z}\dot{\psi}_1^2 + \frac{1}{2}I_{2y}\dot{\theta}_2^2 + \frac{1}{2}I_{2x}\dot{\phi}_2^2 \\ + \frac{1}{2}m_1(\dot{x}^2 + \dot{y}^2 + \dot{z}^2) - gm_1 z + gm_2(l_1\cos\theta_1\cos\phi_1 - z + l_2\cos\theta_2\cos\phi_2) \end{aligned} \tag{3.8}$$

Next, the Lagrange equations of motion are computed term by term beginning with the first term in (3.1) which is the time derivative of the canonical momenta

$$\frac{d}{dt}\frac{\partial L}{\partial \dot{q}_i}\ . \tag{3.9}$$

Note that (3.1) is written in index notation, meaning there is an equation of motion for each generalized coordinate, and each term in the equation actually represents eight terms, one for each equation. Considering the complexity of the Lagrangian (3.8), computing (3.9) is not a trivial task. The symbolic tool box in MATLAB is used to differentiate the Lagrangian with respect to the time derivatives of the generalized coordinates. The resultant term in the x direction is

$$\begin{aligned} \frac{d}{dt}\frac{\partial L}{\partial \dot{x}} = m_2 l_1\cos\phi_1\sin\theta_1\dot{\theta}_1^2 + 2m_2 l_1\cos\theta_1\sin\phi_1\dot{\theta}_1\dot{\phi}_1 + m_2 l_1\cos\phi_1\sin\theta_1\dot{\phi}_1^2 \\ + l_2 m_2\cos\phi_2\sin\theta_2\dot{\theta}_2^2 + 2l_2 m_2\cos\theta_2\sin\phi_2\dot{\theta}_2\dot{\phi}_2 + l_2 m_2\cos\phi_2\sin\theta_2\dot{\phi}_2^2 + (m_1 + m_2)\ddot{x} \\ -l_1 m_2\ddot{\theta}_1\cos\theta_1\cos\phi_1 - l_2 m_2\ddot{\theta}_2\cos\theta_2\cos\phi_2 + l_1 m_2\ddot{\phi}_1\sin\theta_1\sin\phi_1 + l_2 m_2\ddot{\phi}_2\sin\theta_2\sin\phi_2\ , \end{aligned}$$

and the resultant term in the θ_2 direction is,

$$\begin{aligned}
\frac{d}{dt}\frac{\partial L}{\partial \dot{\theta}_2} &= I_{2y}\ddot{\theta}_2 - l_2m_2\ddot{x}\cos\theta_2\cos\phi_2 + l_2m_2\ddot{z}\cos\phi_2\sin\theta_2 + l_2^2m_2\ddot{\theta}_2\cos^2\theta_2\cos^2\phi_2 \\
&-l_2m_2\ddot{y}\sin\theta_2\sin\phi_2 + l_2^2m_2\ddot{\theta}_2\cos^2\phi_2\sin^2\theta_2 + l_2^2m_2\ddot{\theta}_2\sin^2\theta_2\sin^2\phi_2 - l_2^2m_2\cos\theta_2\cos^2\phi_2\sin\theta_2\dot{\phi}_2^2 \\
&+ 2l_2^2m_2\cos\theta_2\sin\theta_2\sin^2\phi_2\dot{\theta}_2^2 + l_2^2m_2\cos\theta_2\sin\theta_2\sin^2\phi_2\dot{\phi}_2^2 + l_2m_2\cos\theta_2\cos\phi_2\dot{z}\dot{\theta}_2 \\
&+ l_2m_2\cos\phi_2\sin\theta_2\dot{x}\dot{\theta}_2 + l_2m_2\cos\theta_2\sin\phi_2\dot{x}\dot{\phi}_2 - l_2m_2\cos\theta_2\sin\phi_2\dot{y}\dot{\theta}_2 - l_2m_2\cos\phi_2\sin\theta_2\dot{y}\dot{\phi}_2 \\
&- l_2m_2\sin\theta_2\sin\phi_2\dot{z}\dot{\phi}_2 - l_2^2m_2\ddot{\phi}_2\cos\theta_2\cos\phi_2\sin\theta_2\sin\phi_2 - 3l_2^2m_2\cos^2\theta_2\cos\phi_2\sin\phi_2\dot{\theta}_2\dot{\phi}_2 \\
&+ l_2^2m_2\cos\phi_2\sin^2\theta_2\sin\phi_2\dot{\theta}_2\dot{\phi}_2 + l_1l_2m_2\cos\theta_1\cos\phi_1\cos\phi_2\sin\theta_2\dot{\theta}_1^2 \\
&- l_1l_2m_2\cos\phi_1\cos\theta_2\cos\phi_2\sin\theta_1\dot{\theta}_1^2 + l_1l_2m_2\cos\theta_1\cos\phi_1\cos\phi_2\sin\theta_2\dot{\phi}_1^2 \\
&- l_1l_2m_2\cos\phi_1\cos\theta_2\cos\phi_2\sin\theta_1\dot{\phi}_1^2 + l_1l_2m_2\ddot{\theta}_1\cos\theta_1\cos\phi_1\cos\theta_2\cos\phi_2 \\
&+ l_1l_2m_2\cos\theta_1\sin\phi_1\sin\theta_2\sin\phi_2\dot{\theta}_1^2 + l_1l_2m_2\cos\theta_1\sin\phi_1\sin\theta_2\sin\phi_2\dot{\phi}_1^2 \\
&+ l_1l_2m_2\ddot{\theta}_1\cos\phi_1\cos\phi_2\sin\theta_1\sin\theta_2 - l_1l_2m_2\ddot{\phi}_1\cos\theta_1\cos\phi_1\sin\theta_2\sin\phi_2 \\
&+ l_1l_2m_2\ddot{\phi}_1\cos\theta_1\cos\phi_2\sin\phi_1\sin\theta_2 - l_1l_2m_2\ddot{\phi}_1\cos\theta_2\cos\phi_2\sin\theta_1\sin\phi_1 \\
&+ l_1l_2m_2\ddot{\theta}_1\sin\theta_1\sin\phi_1\sin\theta_2\sin\phi_2 - 2l_1l_2m_2\cos\theta_1\cos\theta_2\cos\phi_2\sin\phi_1\dot{\theta}_1\dot{\phi}_1 \\
&- l_1l_2m_2\cos\theta_1\cos\phi_1\cos\phi_2\sin\theta_2\dot{\theta}_1\dot{\theta}_2 + l_1l_2m_2\cos\phi_1\cos\theta_2\cos\phi_2\sin\theta_1\dot{\theta}_1\dot{\theta}_2 \\
&- l_1l_2m_2\cos\theta_1\cos\phi_1\cos\theta_2\sin\phi_2\dot{\theta}_1\dot{\phi}_2 - l_1l_2m_2\cos\theta_1\cos\phi_1\cos\theta_2\sin\phi_2\dot{\phi}_1\dot{\theta}_2 \\
&+ l_1l_2m_2\cos\theta_1\cos\theta_2\cos\phi_2\sin\phi_1\dot{\phi}_1\dot{\theta}_2 - l_1l_2m_2\cos\theta_1\cos\phi_1\cos\phi_2\sin\theta_2\dot{\phi}_1\dot{\phi}_2 \\
&+ 2l_1l_2m_2\cos\phi_1\sin\theta_1\sin\theta_2\sin\phi_2\dot{\theta}_1\dot{\phi}_1 - 2l_1l_2m_2\cos\phi_2\sin\theta_1\sin\phi_1\sin\theta_2\dot{\theta}_1\dot{\phi}_1 \\
&+ l_1l_2m_2\cos\theta_2\sin\theta_1\sin\phi_1\sin\phi_2\dot{\theta}_1\dot{\theta}_2 - l_1l_2m_2\cos\phi_1\sin\theta_1\sin\theta_2\sin\phi_2\dot{\theta}_1\dot{\phi}_2 \\
&+ l_1l_2m_2\cos\phi_2\sin\theta_1\sin\phi_1\sin\theta_2\dot{\theta}_1\dot{\phi}_2 + l_1l_2m_2\cos\phi_2\sin\theta_1\sin\phi_1\sin\theta_2\dot{\phi}_1\dot{\theta}_2 \\
&- l_1l_2m_2\cos\theta_1\sin\phi_1\sin\theta_2\sin\phi_2\dot{\phi}_1\dot{\phi}_2 + l_1l_2m_2\cos\theta_2\sin\theta_1\sin\phi_1\sin\phi_2\dot{\phi}_1\dot{\phi}_2 \ .
\end{aligned}$$

For the sake of brevity, the remaining terms can be found in Appendix A.1. The two terms shown above indicate the complexity of the dynamics and the extensive amount of coupling within the system.

The second term in (3.1) represents the canonical forces:

$$\frac{\partial L}{\partial q_i} \ . \tag{3.10}$$

As with the canonical momenta terms (3.9), computing the canonical forces is not a trivial computation. Similarly the symbolic tool box in MATLAB is used to compute (3.10). Since the Lagrangian is not a function of the positional coordinates or the ψ_1 coordinate many terms are equal to zero:

$$\frac{\partial L}{\partial x} = \frac{\partial L}{\partial y} = \frac{\partial L}{\partial z} = \frac{\partial L}{\partial \psi_1} = 0 \ .$$

The remaining terms that do not evaluate to zero are exceedingly long, highly coupled expressions. For example, the canonical force with respect to the θ_2 direction is,

$$\begin{aligned}
\frac{\partial L}{\partial \theta_2} &= l_2^2 m_2 \dot{\theta}_2^2 \cos\theta_2 \sin\theta_2 \sin^2\phi_2 - l_2^2 m_2 \dot{\phi}_2^2 \cos\theta_2 \cos^2\phi_2 \sin\theta_2 - g l_2 m_2 \cos\phi_2 \sin\theta_2 \\
&+ l_2 m_2 \dot{z}\dot{\theta}_2 \cos\theta_2 \cos\phi_2 + l_2 m_2 \dot{x}\dot{\theta}_2 \cos\phi_2 \sin\theta_2 + l_2 m_2 \dot{x}\dot{\phi}_2 \cos\theta_2 \sin\phi_2 - l_2 m_2 \dot{y}\dot{\theta}_2 \cos\theta_2 \sin\phi_2 \\
&- l_2 m_2 \dot{y}\dot{\phi}_2 \cos\phi_2 \sin\theta_2 - l_2 m_2 \dot{z}\dot{\phi}_2 \sin\theta_2 \sin\phi_2 - l_2^2 m_2 \dot{\theta}_2 \dot{\phi}_2 \cos^2\theta_2 \cos\phi_2 \sin\phi_2 \\
&+ l_2^2 m_2 \dot{\theta}_2 \dot{\phi}_2 \cos\phi_2 \sin^2\theta_2 \sin\phi_2 + l_1 l_2 m_2 \dot{\theta}_1 \dot{\theta}_2 \cos\theta_2 \sin\theta_1 \sin\phi_1 \sin\phi_2 \\
&- l_1 l_2 m_2 \dot{\theta}_1 \dot{\phi}_2 \cos\phi_1 \sin\theta_1 \sin\theta_2 \sin\phi_2 + l_1 l_2 m_2 \dot{\theta}_1 \dot{\phi}_2 \cos\phi_2 \sin\theta_1 \sin\phi_1 \sin\theta_2 \\
&+ l_1 l_2 m_2 \dot{\phi}_1 \dot{\theta}_2 \cos\phi_2 \sin\theta_1 \sin\phi_1 \sin\theta_2 - l_1 l_2 m_2 \dot{\phi}_1 \dot{\phi}_2 \cos\theta_1 \sin\phi_1 \sin\theta_2 \sin\phi_2 \\
&+ l_1 l_2 m_2 \dot{\phi}_1 \dot{\phi}_2 \cos\theta_2 \sin\theta_1 \sin\phi_1 \sin\phi_2 - l_1 l_2 m_2 \dot{\theta}_1 \dot{\theta}_2 \cos\theta_1 \cos\phi_1 \cos\phi_2 \sin\theta_2 \\
&+ l_1 l_2 m_2 \dot{\theta}_1 \dot{\theta}_2 \cos\phi_1 \cos\theta_2 \cos\phi_2 \sin\theta_1 - l_1 l_2 m_2 \dot{\theta}_1 \dot{\phi}_2 \cos\theta_1 \cos\phi_1 \cos\theta_2 \sin\phi_2 \\
&- l_1 l_2 m_2 \dot{\phi}_1 \dot{\theta}_2 \cos\theta_1 \cos\phi_1 \cos\theta_2 \sin\phi_2 + l_1 l_2 m_2 \dot{\phi}_1 \dot{\theta}_2 \cos\theta_1 \cos\theta_2 \cos\phi_2 \sin\phi_1 \\
&- l_1 l_2 m_2 \dot{\phi}_1 \dot{\phi}_2 \cos\theta_1 \cos\phi_1 \cos\phi_2 \sin\theta_2 \ . \qquad (3.11)
\end{aligned}$$

Once again, for the sake the of brevity, the remaining terms can be found in Appendix A.2.

3.4 Generalized Forces

The final terms in the Lagrangian equations of motion are the non-conservative forces on the system acting in the directions of the generalized coordinates. These forces are known as the generalized forces on the system.

Cumulative thrust T_r generated by the quadrotor is fixed in direction along the z_b axis that points directly out of the top of the quadrotor. Therefore, the forces in the $x,\ y$ and z directions are dependent on the rotation angles of the quadrotor in addition to thrust. These forces are given by

$$Q_{nc_x} = T_r \sin\theta_1 \cos\phi_1 \cos\psi_1 \quad Q_{nc_y} = -T_r \cos\theta_1 \sin\phi_1 \cos\psi_1 \quad Q_{nc_z} = T_r \cos\theta_1 \cos\phi_1 \ .$$

Let τ_1 be the servo torque used to actuate the dynamic mass in the θ_2 direction. Although θ_1 and θ_2 are independent generalized coordinates, τ_1 is equally and oppositely applied to both the quadrotor and the dynamic mass as it is an internal torque. These equal and opposite torques could be shown with a simple free body diagram. Therefore, the generalized forces in the θ_1 and θ_2 directions are

$$Q_{nc_{\theta_1}} = -\tau_1 \qquad\qquad Q_{nc_{\theta_2}} = \tau_1 \ .$$

Similarly, let τ_2 be the servo torque used to actuate the dynamic mass in the ϕ_2 direction. Once again τ_2 is an internal torque meaning it is equally and oppositely applied in the ϕ_1 and ϕ_2 directions, resulting in

$$Q_{nc_{\phi_1}} = -\tau_2 \qquad\qquad Q_{nc_{\phi_2}} = \tau_2 \ .$$

Unlike the roll and pitch of the quadrotor, yaw is not controlled by actuating the dynamic mass but by traditional differential thrust methods. Let τ_3 be a virtual input equivalent to the yaw torque generated through differential thrust. The resulting generalized force in the ψ_1 direction is

$$Q_{nc_{\psi_1}} = \tau_3 \ .$$

3-D Nonlinear Equations of Motion with Dynamic Mass

With the terms of the Lagrangian equations of motion computed, these terms can be substituted into (3.1) to solve for the equations of motion of the quadrotor with

the dynamic mass mounted beneath it. Carrying out the substitution and canceling appropriate terms results in the following eight equations of motion, one for each direction defined by the generalized coordinates.

With respect to the x direction,

$$\begin{aligned} &l_1 m_2 \cos\phi_1 \sin\theta_1 \dot{\theta}_1^2 + 2 l_1 m_2 \cos\theta_1 \sin\phi_1 \dot{\theta}_1 \dot{\phi}_1 + l_1 m_2 \cos\phi_1 \sin\theta_1 \dot{\phi}_1^2 + l_2 m_2 \cos\phi_2 \sin\theta_2 \dot{\theta}_2^2 \\ &+ 2 l_2 m_2 \cos\theta_2 \sin\phi_2 \dot{\theta}_2 \dot{\phi}_2 + l_2 m_2 \cos\phi_2 \sin\theta_2 \dot{\phi}_2^2 + m_1 \ddot{x} + m_2 \ddot{x} - l_1 m_2 \ddot{\theta}_1 \cos\theta_1 \cos\phi_1 \\ &- l_2 m_2 \ddot{\theta}_2 \cos\theta_2 \cos\phi_2 + l_1 m_2 \ddot{\phi}_1 \sin\theta_1 \sin\phi_1 + l_2 m_2 \ddot{\phi}_2 \sin\theta_2 \sin\phi_2 \\ &= u_1 \sin\theta_1 \cos\phi_1 \cos(\psi_1) \ . \end{aligned} \tag{3.12a}$$

With respect to the y direction,

$$\begin{aligned} &- l_1 m_2 \cos\theta_1 \sin\phi_1 \dot{\theta}_1^2 - 2 l_1 m_2 \cos\phi_1 \sin\theta_1 \dot{\theta}_1 \dot{\phi}_1 - l_1 m_2 \cos\theta_1 \sin\phi_1 \dot{\phi}_1^2 \\ &- l_2 m_2 \cos\theta_2 \sin\phi_2 \dot{\theta}_2^2 - 2 l_2 m_2 \cos\phi_2 \sin\theta_2 \dot{\theta}_2 \dot{\phi}_2 - l_2 m_2 \cos\theta_2 \sin\phi_2 \dot{\phi}_2^2 + m_1 \ddot{y} + m_2 \ddot{y} \\ &+ l_1 m_2 \ddot{\phi}_1 \cos\theta_1 \cos\phi_1 + l_2 m_2 \ddot{\phi}_2 \cos\theta_2 \cos\phi_2 - l_1 m_2 \ddot{\theta}_1 \sin\theta_1 \sin\phi_1 \\ &- l_2 m_2 \ddot{\theta}_2 \sin\theta_2 \sin\phi_2 = -u_1 \cos\theta_1 \sin\phi_1 \cos(\psi_1) \ . \end{aligned} \tag{3.12b}$$

With respect to the z direction,

$$\begin{aligned} &l_1 m_2 \cos\theta_1 \cos\phi_1 \dot{\theta}_1^2 - 2 l_1 m_2 \sin\theta_1 \sin\phi_1 \dot{\theta}_1 \dot{\phi}_1 + l_1 m_2 \cos\theta_1 \cos\phi_1 \dot{\phi}_1^2 + l_2 m_2 \cos\theta_2 \cos\phi_2 \dot{\theta}_2^2 \\ &- 2 l_2 m_2 \sin\theta_2 \sin\phi_2 \dot{\theta}_2 \dot{\phi}_2 + l_2 m_2 \cos\theta_2 \cos\phi_2 \dot{\phi}_2^2 + g m_1 + g m_2 + m_1 \ddot{z} + m_2 \ddot{z} \\ &+ l_1 m_2 \ddot{\theta}_1 \cos\phi_1 \sin\theta_1 + l_1 m_2 \ddot{\phi}_1 \cos\theta_1 \sin\phi_1 + l_2 m_2 \ddot{\theta}_2 \cos\phi_2 \sin\theta_2 + l_2 m_2 \ddot{\phi}_2 \cos\theta_2 \sin\phi_2 \\ &= u_1 \cos\theta_1 \cos\phi_1 \ . \end{aligned} \tag{3.12c}$$

With respect to the ψ_1 direction,

$$I_{1z} \ddot{\psi}_1 = u_4 \ . \tag{3.12d}$$

With respect to the θ_1 direction,

$$
\begin{aligned}
&I_{1y}\ddot{\theta}_1 - l_1 m_2 \ddot{x}\cos\theta_1\cos\phi_1 + g l_1 m_2 \cos\phi_1\sin\theta_1 + l_1 m_2 \ddot{z}\cos\phi_1\sin\theta_1 \\
&+ l_1^2 m_2 \ddot{\theta}_1\cos^2\theta_1\cos^2\phi_1 - l_1 m_2 \ddot{y}\sin\theta_1\sin\phi_1 + l_1^2 m_2 \ddot{\theta}_1\cos^2\phi_1\sin^2\theta_1 + l_1^2 m_2 \ddot{\theta}_1\sin^2\theta_1\sin^2\phi_1 \\
&+ l_1^2 m_2 \dot{\theta}_1^2\cos\theta_1\sin\theta_1\sin^2\phi_1 + l_1^2 m_2 \dot{\phi}_1^2\cos\theta_1\sin\theta_1\sin^2\phi_1 - 2 l_1^2 m_2 \dot{\theta}_1\dot{\phi}_1\cos^2\theta_1\cos\phi_1\sin\phi_1 \\
&- l_1^2 m_2 \ddot{\phi}_1\cos\theta_1\cos\phi_1\sin\theta_1\sin\phi_1 + l_1 l_2 m_2 \ddot{\theta}_2\cos\theta_1\cos\phi_1\cos\theta_2\cos\phi_2 \\
&+ l_1 l_2 m_2 \ddot{\theta}_2\cos\phi_1\cos\phi_2\sin\theta_1\sin\theta_2 - l_1 l_2 m_2 \ddot{\phi}_2\cos\theta_1\cos\phi_1\sin\theta_2\sin\phi_2 \\
&+ l_1 l_2 m_2 \ddot{\phi}_2\cos\phi_1\cos\theta_2\sin\theta_1\sin\phi_2 - l_1 l_2 m_2 \ddot{\phi}_2\cos\theta_2\cos\phi_2\sin\theta_1\sin\phi_1 \\
&+ l_1 l_2 m_2 \ddot{\theta}_2\sin\theta_1\sin\phi_1\sin\theta_2\sin\phi_2 - l_1 l_2 m_2 \dot{\theta}_2^2\cos\theta_1\cos\phi_1\cos\phi_2\sin\theta_2 \\
&+ l_1 l_2 m_2 \dot{\theta}_2^2\cos\phi_1\cos\theta_2\cos\phi_2\sin\theta_1 - l_1 l_2 m_2 \dot{\phi}_2^2\cos\theta_1\cos\phi_1\cos\phi_2\sin\theta_2 \\
&+ l_1 l_2 m_2 \dot{\phi}_2^2\cos\phi_1\cos\theta_2\cos\phi_2\sin\theta_1 + l_1 l_2 m_2 \dot{\theta}_2^2\cos\theta_2\sin\theta_1\sin\phi_1\sin\phi_2 \\
&+ l_1 l_2 m_2 \dot{\phi}_2^2\cos\theta_2\sin\theta_1\sin\phi_1\sin\phi_2 - 2 l_1 l_2 m_2 \dot{\theta}_2\dot{\phi}_2\cos\phi_1\sin\theta_1\sin\theta_2\sin\phi_2 \\
&+ 2 l_1 l_2 m_2 \dot{\theta}_2\dot{\phi}_2\cos\phi_2\sin\theta_1\sin\phi_1\sin\theta_2 - 2 l_1 l_2 m_2 \dot{\theta}_2\dot{\phi}_2\cos\theta_1\cos\phi_1\cos\theta_2\sin\phi_2 = -u_2 \ .
\end{aligned}
\tag{3.12e}
$$

With respect to the ϕ_1 direction,

$$
\begin{aligned}
&I_{1x}\ddot{\phi}_1 + l_1 m_2 \ddot{y}\cos\theta_1\cos\phi_1 + g l_1 m_2 \cos\theta_1\sin\phi_1 + l_1 m_2 \ddot{z}\cos\theta_1\sin\phi_1 \\
&+ l_1^2 m_2 \ddot{\phi}_1\cos^2\theta_1\cos^2\phi_1 + l_1 m_2 \ddot{x}\sin\theta_1\sin\phi_1 + l_1^2 m_2 \ddot{\phi}_1\cos^2\theta_1\sin^2\phi_1 \\
&+ l_1^2 m_2 \ddot{\phi}_1\sin^2\theta_1\sin^2\phi_1 + l_1^2 m_2 \dot{\theta}_1^2\cos\phi_1\sin^2\theta_1\sin\phi_1 + l_1^2 m_2 \dot{\phi}_1^2\cos\phi_1\sin^2\theta_1\sin\phi_1 \\
&- 2 l_1^2 m_2 \dot{\theta}_1\dot{\phi}_1\cos\theta_1\cos^2\phi_1\sin\theta_1 - l_1^2 m_2 \ddot{\theta}_1\cos\theta_1\cos\phi_1\sin\theta_1\sin\phi_1 \\
&+ l_1 l_2 m_2 \ddot{\phi}_2\cos\theta_1\cos\phi_1\cos\theta_2\cos\phi_2 - l_1 l_2 m_2 \ddot{\theta}_2\cos\theta_1\cos\phi_1\sin\theta_2\sin\phi_2 \\
&+ l_1 l_2 m_2 \ddot{\theta}_2\cos\theta_1\cos\phi_2\sin\phi_1\sin\theta_2 - l_1 l_2 m_2 \ddot{\theta}_2\cos\theta_2\cos\phi_2\sin\theta_1\sin\phi_1 \\
&+ l_1 l_2 m_2 \ddot{\phi}_2\cos\theta_1\cos\theta_2\sin\phi_1\sin\phi_2 + l_1 l_2 m_2 \ddot{\phi}_2\sin\theta_1\sin\phi_1\sin\theta_2\sin\phi_2 \\
&- l_1 l_2 m_2 \dot{\theta}_2^2\cos\theta_1\cos\phi_1\cos\theta_2\sin\phi_2 + l_1 l_2 m_2 \dot{\theta}_2^2\cos\theta_1\cos\theta_2\cos\phi_2\sin\phi_1 \\
&- l_1 l_2 m_2 \dot{\phi}_2^2\cos\theta_1\cos\phi_1\cos\theta_2\sin\phi_2 + l_1 l_2 m_2 \dot{\phi}_2^2\cos\theta_1\cos\theta_2\cos\phi_2\sin\phi_1 \\
&+ l_1 l_2 m_2 \dot{\theta}_2^2\cos\phi_2\sin\theta_1\sin\phi_1\sin\theta_2 + l_1 l_2 m_2 \dot{\phi}_2^2\cos\phi_2\sin\theta_1\sin\phi_1\sin\theta_2 \\
&- 2 l_1 l_2 m_2 \dot{\theta}_2\dot{\phi}_2\cos\theta_1\sin\phi_1\sin\theta_2\sin\phi_2 + 2 l_1 l_2 m_2 \dot{\theta}_2\dot{\phi}_2\cos\theta_2\sin\theta_1\sin\phi_1\sin\phi_2 \\
&- 2 l_1 l_2 m_2 \dot{\theta}_2\dot{\phi}_2\cos\theta_1\cos\phi_1\cos\phi_2\sin\theta_2 = -u_3 \ .
\end{aligned}
\tag{3.12f}
$$

With respect to the θ_2 direction,

$$
\begin{aligned}
&I_{2y}\ddot{\theta}_2 - l_2m_2\ddot{x}\cos\theta_2\cos\phi_2 + gl_2m_2\cos\phi_2\sin\theta_2 + l_2m_2\ddot{z}\cos\phi_2\sin\theta_2 + l_2^2m_2\ddot{\theta}_2\cos^2\theta_2\cos^2\phi_2 \\
&-l_2m_2\ddot{y}\sin\theta_2\sin\phi_2 + l_2^2m_2\ddot{\theta}_2\cos^2\phi_2\sin^2\theta_2 + l_2^2m_2\ddot{\theta}_2\sin^2\theta_2\sin^2\phi_2 + l_2^2m_2\dot{\theta}_2^2\cos\theta_2\sin\theta_2\sin^2\phi_2 \\
&+l_2^2m_2\dot{\phi}_2^2\cos\theta_2\sin\theta_2\sin^2\phi_2 - 2l_2^2m_2\dot{\theta}_2\dot{\phi}_2\cos^2\theta_2\cos\phi_2\sin\phi_2 - l_2^2m_2\ddot{\phi}_2\cos\theta_2\cos\phi_2\sin\theta_2\sin\phi_2 \\
&+ l_1l_2m_2\ddot{\theta}_1\cos\theta_1\cos\phi_1\cos\theta_2\cos\phi_2 + l_1l_2m_2\ddot{\theta}_1\cos\phi_1\cos\phi_2\sin\theta_1\sin\theta_2 \\
&- l_1l_2m_2\ddot{\phi}_1\cos\theta_1\cos\phi_1\sin\theta_2\sin\phi_2 + l_1l_2m_2\ddot{\phi}_1\cos\theta_1\cos\phi_2\sin\phi_1\sin\theta_2 \\
&- l_1l_2m_2\ddot{\phi}_1\cos\theta_2\cos\phi_2\sin\theta_1\sin\phi_1 + l_1l_2m_2\ddot{\theta}_1\sin\theta_1\sin\phi_1\sin\theta_2\sin\phi_2 \\
&+ l_1l_2m_2\dot{\theta}_1^2\cos\theta_1\cos\phi_1\cos\phi_2\sin\theta_2 - l_1l_2m_2\dot{\theta}_1^2\cos\phi_1\cos\theta_2\cos\phi_2\sin\theta_1 \\
&+ l_1l_2m_2\dot{\phi}_1^2\cos\theta_1\cos\phi_1\cos\phi_2\sin\theta_2 - l_1l_2m_2\dot{\phi}_1^2\cos\phi_1\cos\theta_2\cos\phi_2\sin\theta_1 \\
&+ l_1l_2m_2\dot{\theta}_1^2\cos\theta_1\sin\phi_1\sin\theta_2\sin\phi_2 + l_1l_2m_2\dot{\phi}_1^2\cos\theta_1\sin\phi_1\sin\theta_2\sin\phi_2 \\
&+ 2l_1l_2m_2\dot{\theta}_1\dot{\phi}_1\cos\phi_1\sin\theta_1\sin\theta_2\sin\phi_2 - 2l_1l_2m_2\dot{\theta}_1\dot{\phi}_1\cos\phi_2\sin\theta_1\sin\phi_1\sin\theta_2 \\
&- 2l_1l_2m_2\dot{\theta}_1\dot{\phi}_1\cos\theta_1\cos\theta_2\cos\phi_2\sin\phi_1 = u_2\ . \qquad \text{(3.12g)}
\end{aligned}
$$

With respect to the ϕ_2 direction,

$$
\begin{aligned}
&I_{2x}\ddot{\phi}_2 + l_2m_2\ddot{y}\cos\theta_2\cos\phi_2 + gl_2m_2\cos\theta_2\sin\phi_2 + l_2m_2\ddot{z}\cos\theta_2\sin\phi_2 + l_2^2m_2\ddot{\phi}_2\cos^2\theta_2\cos^2\phi_2 \\
&+l_2m_2\ddot{x}\sin\theta_2\sin\phi_2 + l_2^2m_2\ddot{\phi}_2\cos^2\theta_2\sin^2\phi_2 + l_2^2m_2\ddot{\phi}_2\sin^2\theta_2\sin^2\phi_2 + l_2^2m_2\dot{\theta}_2^2\cos\phi_2\sin^2\theta_2\sin\phi_2 \\
&+l_2^2m_2\dot{\phi}_2^2\cos\phi_2\sin^2\theta_2\sin\phi_2 - 2l_2^2m_2\dot{\theta}_2\dot{\phi}_2\cos\theta_2\cos^2\phi_2\sin\theta_2 - l_2^2m_2\ddot{\theta}_2\cos\theta_2\cos\phi_2\sin\theta_2\sin\phi_2 \\
&+ l_1l_2m_2\ddot{\phi}_1\cos\theta_1\cos\phi_1\cos\theta_2\cos\phi_2 - l_1l_2m_2\ddot{\theta}_1\cos\theta_1\cos\phi_1\sin\theta_2\sin\phi_2 \\
&+ l_1l_2m_2\ddot{\theta}_1\cos\phi_1\cos\theta_2\sin\theta_1\sin\phi_2 - l_1l_2m_2\ddot{\theta}_1\cos\theta_2\cos\phi_2\sin\theta_1\sin\phi_1 \\
&+ l_1l_2m_2\ddot{\phi}_1\cos\theta_1\cos\theta_2\sin\phi_1\sin\phi_2 + l_1l_2m_2\ddot{\phi}_1\sin\theta_1\sin\phi_1\sin\theta_2\sin\phi_2 \\
&+ l_1l_2m_2\dot{\theta}_1^2\cos\theta_1\cos\phi_1\cos\theta_2\sin\phi_2 - l_1l_2m_2\dot{\theta}_1^2\cos\theta_1\cos\theta_2\cos\phi_2\sin\phi_1 \\
&+ l_1l_2m_2\dot{\phi}_1^2\cos\theta_1\cos\phi_1\cos\theta_2\sin\phi_2 - l_1l_2m_2\dot{\phi}_1^2\cos\theta_1\cos\theta_2\cos\phi_2\sin\phi_1 \\
&+ l_1l_2m_2\dot{\theta}_1^2\cos\phi_1\sin\theta_1\sin\theta_2\sin\phi_2 + l_1l_2m_2\dot{\phi}_1^2\cos\phi_1\sin\theta_1\sin\theta_2\sin\phi_2 \\
&+ 2l_1l_2m_2\dot{\theta}_1\dot{\phi}_1\cos\theta_1\sin\phi_1\sin\theta_2\sin\phi_2 - 2l_1l_2m_2\dot{\theta}_1\dot{\phi}_1\cos\theta_2\sin\theta_1\sin\phi_1\sin\phi_2 \\
&- 2l_1l_2m_2\dot{\theta}_1\dot{\phi}_1\cos\phi_1\cos\theta_2\cos\phi_2\sin\theta_1 = u_3\ . \qquad \text{(3.12h)}
\end{aligned}
$$

These equations of motion show that the dynamics associated with quadrotor and dynamic mass control mechanism are highly non-linear and highly coupled as expected.

Let the first control input be equal to the sum total thrust generated equally by all four rotors, $u_1 = T_r$. As mentioned previously, let the second and third control inputs be the servo torque used to actuate the dynamic mass in the θ_2 and ϕ_2 directions respectively, $u_2 = \tau_1$ and $u_3 = \tau_2$. Finally, let the fourth control input be a virtual control input that is equivalent to the yawing torque on the vehicle generated by differential thrust. This control input is the only instance where differential thrust is used to generate a rotational moment on the vehicle. Pitch and roll moments are generated by actuating the dynamic mass. With eight degrees of freedom and only four control inputs, this system is an underactuated system.

3.5 Planar Nonlinear Equations of Motion

In addition to a full three dimensional model, a planar model is developed to examine the quadrotor dynamics constrained to the x-z plane. To develop the planar model, the 3D nonlinear equations are simplified by considering only the states contained in the x-z plane, or $x,\ z,\ \theta_1,\ \theta_2$ and their derivatives. The equations of motion corresponding to $y,\ \phi_1,\ \psi_1,\ \phi_2$ are disregarded and these variables are considered equal to zero in the remaining equations of motion.

After canceling the out of plane terms, the equations of motion for the planar quadrotor model can be reduced to the following four nonlinear equations of motion,

$$m_1\ddot{x} + m_2(\ddot{x} + l_1 sin\theta_1\dot{\theta}_1^2 + l_2 sin\theta_2\dot{\theta}_2^2 - l_1\ddot{\theta}_1 cos\theta_1 - l_2\ddot{\theta}_2 cos\theta_2) = u_1 \sin\theta_1 \tag{3.13a}$$

$$m_1\ddot{z} + m_2(\ddot{z} + l_1 cos\theta_1\dot{\theta}_1^2 + l_2 cos\theta_2\dot{\theta}_2^2 + l_1\ddot{\theta}_1 sin\theta_1 + l_2\ddot{\theta}_2 sin\theta_2) + g(m_1 + m_2) = u_1 \cos\theta_1 \tag{3.13b}$$

$$I_{1_y}\ddot{\theta}_1 + l_1^2 m_2 \ddot{\theta}_1 - l_1 m_2 \ddot{x} cos\theta_1 + g l_1 m_2 sin\theta_1 + l_1 m_2 \ddot{z} sin\theta_1 + l_1 l_2 m_2 \ddot{\theta}_2 cos(\theta_1 - \theta_2) + l_1 l_2 m_2 \dot{\theta}_2^2 sin(\theta_1 - \theta_2) = -u_2 \quad (3.13c)$$

$$I_{2_y}\ddot{\theta}_2 + l_2^2 m_2 \ddot{\theta}_2 - l_2 m_2 \ddot{x} cos\theta_2 + g l_2 m_2 sin\theta_2 + l_2 m_2 \ddot{z} sin\theta_2 + l_1 l_2 m_2 \ddot{\theta}_1 cos(\theta_1 - \theta_2) - l_1 l_2 m_2 \dot{\theta}_1^2 sin(\theta_1 - \theta_2)) = u_2 \ . \quad (3.13d)$$

Similar to the three dimensional model, the first control input u_1 is equal to pure thrust, and the second control input u_2 is the servo torque in the θ_2 direction. The equations of motion are then rearranged into matrix form,

$$\begin{bmatrix} m_1 + m_2 & 0 & -m_2 l_1 \cos\theta_1 & -m_2 l_2 \cos\theta_2 \\ 0 & m_1 + m_2 & m_2 l_1 \sin\theta_1 & m_2 l_2 \sin\theta_2 \\ -m_2 l_1 \cos\theta_1 & m_2 l_1 \sin\theta_1 & m_2 l_1^2 + I_{1_y} & m_2 l_1 l_2 \cos(\theta_1 - \theta_2) \\ -m_2 l_2 \cos\theta_2 & m_2 l_2 \sin\theta_2 & m_2 l_1 l_2 \cos(\theta_1 - \theta_2) & m_2 l_2^2 + I_{2_y} \end{bmatrix} \begin{bmatrix} \ddot{x} \\ \ddot{z} \\ \ddot{\theta}_1 \\ \ddot{\theta}_2 \end{bmatrix}$$

$$= \begin{bmatrix} u_1 \sin\theta_1 - m_2 \dot{\theta}_1^2 l_1 \sin\theta_1 - m_2 \dot{\theta}_2^2 l_2 \sin\theta_2 \\ u_1 \cos\theta_1 - g(m_1 + m_2) - m_2 \dot{\theta}_1^2 \cos\theta_1 l_1 - m_2 \dot{\theta}_2^2 l_2 \cos\theta_2 \\ -u_2 - g m_2 l_1 \sin\theta_1 - m_2 \dot{\theta}_2^2 l_1 l_2 \sin(\theta_1 - \theta_2) \\ u_2 - g m_2 l_2 \sin\theta_2 + m_2 \dot{\theta}_1^2 l_1 l_2 \sin(\theta_1 - \theta_2) \end{bmatrix} . \quad (3.14)$$

Once again, the planar model has fewer control inputs than degrees of freedom, making the planar system an underactuated system.

Chapter 4

CONTROLLER DEVELOPMENT

Like traditional helicopters, quadrotors are dynamically unstable systems requiring the use of controllers for stable flight. With many different control techniques ranging from a classical PID approach, modern linear optimal control methods, various nonlinear methods, or a combination of multiple approaches, the controller possibilities are endless. However, LQR methods are chosen to develop the controllers for this research for several reasons. LQR controllers have many attractive properties but most important are the strong robustness and stability properties. These robustness properties provide good tolerance of nonlinearities, which is very helpful for this system in particular as nonlinear affects such as aerodynamics were not included in the model development. Also, the LQR solution is an optimal solution for the linearized system according to the cost function that can be varied through the Q and R matrices. Unlike PID controllers which require tuning each gain, all adjustable parameters in the LQR method are contained in the Q and R weighting matrices making LQR controllers relatively easy to implement.

The purpose of the controllers for this research are to stabilize the system and to follow simple trajectories. Although the equations of motion for the quadrotor with dynamic inertia are highly nonlinear, controllers developed on a linear approximation of the system are acceptable considering the purpose of the controller.

An LQR controller would likely fail if the quadrotor was required to achieve large pitch and roll angles or perform aggressive maneuvers which are outside the region of attraction of the linearization. The purpose of the controllers for this research are to stabilize the system and to follow simple trajectories in which no high roll and pitch

angles or aggressive maneuvers are required. Before developing the LQR controller the nonlinear equations of motion must be linearized.

4.1 2D Planar Model Linearization

Both the full three dimensional equations of motion (3.12) and the planar equations of motion (3.13) are linearized in this research, although, for the sake of clarity, the linearization process is shown only for the planar model. Linearization of the three dimensional equations of motion follows the exact procedure as the planar equations of motion, the only difference being the number of states and equations. Using perturbation theory, an approximation to a full solution A is written in terms of a power series such as

$$A = A_0 + \epsilon^1 A_1 + \epsilon^2 A_2 + ... \quad .$$

Truncating the higher order terms of the power series results in an approximate solution $A \approx A_0 + \delta A$. How well this approximation represents the full solution is dependent on the nonlinearity of the full solution A and the distance from the initial condition A_0. Using perturbation theory to linearize the planar equations of motion (3.13), substitute the states and inputs for an initial condition and a perturbation,

$$\dot{X} \rightarrow \dot{X}_0 + \delta\dot{X} \qquad X \rightarrow X_0 + \delta X \qquad U \rightarrow U_0 + \delta U \ .$$

After making the previous substitution to the nonlinear planar equations of motion (3.13), simplifications are made to the perturbed equations of motion. Trigonometric terms are expanded using the addition formula for the sum of two angles. The small angle approximation is applied such that $\sin(\delta X) \approx \delta X$ and $\cos(\delta X) \approx 1$. Assuming small perturbations, the product of two perturbations is approximately zero, $(\delta X)(\delta X) \approx 0$. The previous simplifications reduce the perturbed equation of motion

(3.13a) to

$$(m_1+m_2)\ddot{x}_0+(m_1+m_2)\delta\ddot{x}-\delta\ddot{\theta}_1 l_1 m_2\cos\theta_{1_0}-\delta\ddot{\theta}_2 l_2 m_2\cos\theta_{2_0}-l_1 m_2\ddot{\theta}_{1_0}\cos\theta_{1_0}$$
$$-l_2 m_2\ddot{\theta}_{2_0}\cos\theta_{2_0}+l_1 m_2\dot{\theta}_{1_0}^2\sin\theta_{1_0}+l_2 m_2\dot{\theta}_{2_0}^2\sin\theta_{2_0}+\delta\theta_1 l_1 m_2\ddot{\theta}_{1_0}\sin\theta_{1_0}+\delta\theta_2 l_2 m_2\ddot{\theta}_{2_0}\sin\theta_{2_0}$$
$$=\delta u_1\sin\theta_{1_0}+u_{1_0}\sin\theta_{1_0}+\delta\theta_1 u_{1_0}\cos\theta_{1_0}-\delta\dot{\theta}_1^2 l_1 m_2\sin\theta_{1_0}-\delta\dot{\theta}_2^2 l_2 m_2\sin\theta_{2_0}$$
$$-\delta\theta_1 l_1 m_2\dot{\theta}_{1_0}^2\cos\theta_{1_0}-\delta\theta_2 l_2 m_2\dot{\theta}_{2_0}^2\cos\theta_{2_0}-2\delta\dot{\theta}_1 l_1 m_2\dot{\theta}_{1_0}\sin\theta_{1_0}-2\delta\dot{\theta}_2 l_2 m_2\dot{\theta}_{2_0}\sin\theta_{2_0}\ .$$

Likewise equations (3.13b - 3.13d) are reduced in the same manner. Further simplifications can be made by comparing the linearized equations of motion to the original equations of motion. For example, the previous reduced perturbed equation of motion is rearranged to the following,

$$\underbrace{(m_1+m_2)\ddot{x}_0}+(m_1+m_2)\delta\ddot{x}-\delta\ddot{\theta}_1 l_1 m_2\cos\theta_{1_0}-\delta\ddot{\theta}_2 l_2 m_2\cos\theta_{2_0}\underbrace{-l_1 m_2\ddot{\theta}_{1_0}\cos\theta_{1_0}}$$
$$\underbrace{-l_2 m_2\ddot{\theta}_{2_0}\cos\theta_{2_0}+l_1 m_2\dot{\theta}_{1_0}^2\sin\theta_{1_0}+l_2 m_2\dot{\theta}_{2_0}^2\sin\theta_{2_0}}+\delta\theta_1 l_1 m_2\ddot{\theta}_{1_0}\sin\theta_{1_0}+\delta\theta_2 l_2 m_2\ddot{\theta}_{2_0}\sin\theta_{2_0}$$
$$=\delta u_1\sin\theta_{1_0}+\underbrace{u_{1_0}\sin\theta_{1_0}}+\delta\theta_1 u_{1_0}\cos\theta_{1_0}-\delta\dot{\theta}_1^2 l_1 m_2\sin\theta_{1_0}-\delta\dot{\theta}_2^2 l_2 m_2\sin\theta_{2_0}$$
$$-\delta\theta_1 l_1 m_2\dot{\theta}_{1_0}^2\cos\theta_{1_0}-\delta\theta_2 l_2 m_2\dot{\theta}_{2_0}^2\cos\theta_{2_0}-2\delta\dot{\theta}_1 l_1 m_2\dot{\theta}_{1_0}\sin\theta_{1_0}-2\delta\dot{\theta}_2 l_2 m_2\dot{\theta}_{2_0}\sin\theta_{2_0}$$

The underlined terms can be rearranged into the same form of the original nonlinear equation of motion (3.13a). In fact, when rearranged, the underlined terms combine to form (3.13a) evaluated at the linearization conditions. Therefore, when combined, the underlined terms cancel according to the original nonlinear equations of motion. Similar cancellations are made to the remaining perturbed equations of motion. Finally, a flight condition is chosen about which to linearize the perturbed equations of motion. The hovering flight condition is a logical choice for the linearization condition because quadrotor movements can be considered perturbations from a static hover. Translational velocities, rotational velocities, and orientation angles of the system are equal to zero during the hover condition. Positional states do not have an effect on the linearized system dynamics, and therefore these states are arbitrarily set to zero for simplicity. Maintaining a hover requires a nonzero thrust

input to counter the force of gravity, but the second input is zero. These linearization conditions are written as

$$X_0 = 0 \qquad u_{1_0} = g(m_1 + m_2) \qquad u_{2_0} = 0 \ .$$

Evaluating the perturbed equations of motion at the linearization conditions produces the linearized equations of motion for the quadrotor and dynamic mass constrained to the x-z plane. These equations of motion are then rearranged into matrix form:

$$\begin{bmatrix} m_1+m_2 & 0 & -m_2 l_1 & -m_2 l_2 \\ 0 & m_1+m_2 & 0 & 0 \\ -m2l_1 & 0 & m_2 l_1^2 + I_{1y} & m_2 l_1 l_2 \\ -m_2 l_2 & 0 & m_2 l_1 l_2 & m_2 l_2^2 + I_{2y} \end{bmatrix} \begin{bmatrix} \delta\ddot{x} \\ \delta\ddot{z} \\ \delta\ddot{\theta}_1 \\ \delta\ddot{\theta}_2 \end{bmatrix}$$

$$+ \begin{bmatrix} 0 & 0 & -g(m_1+m_2) & 0 \\ 0 & 0 & 0 & 0 \\ 0 & 0 & m_2 l_1 g & 0 \\ 0 & 0 & 0 & m_2 l_2 g \end{bmatrix} \begin{bmatrix} \delta x \\ \delta z \\ \delta\theta_1 \\ \delta\theta_2 \end{bmatrix} = \begin{bmatrix} 0 & 0 \\ 1 & 0 \\ 0 & -1 \\ 0 & 1 \end{bmatrix} \begin{bmatrix} \delta u_1 \\ \delta u_2 \end{bmatrix} \ . \quad (4.1)$$

A final step remains in the linearization process. The linearized equations of motion in (4.1) are all second order ordinary differential equations (ODEs) and must be transformed into a system of first order ODEs in standard linear form,

$$\dot{\mathbf{x}} = \mathbf{A}\mathbf{x} + \mathbf{B}\mathbf{u} \ .$$

The result of the transformation is a state space model with eight states containing the generalized coordinates and the their velocities, with the corresponding state vector and control input vector,

$$\mathbf{x} = \begin{bmatrix} x & z & \theta_1 & \theta_2 & \dot{x} & \dot{z} & \dot{\theta}_1 & \dot{\theta}_2 \end{bmatrix}^T \qquad \mathbf{u} = \begin{bmatrix} u_1 & u_2 \end{bmatrix}^T \ .$$

The **A** and **B** matrices for the planar model in symbolic form is found in Appendix B.1, Equations (B.1) and (B.2) respectively.

4.2 Linearized 3D Model

Using the same small perturbation linearization process used to linearize the planar model, the three dimensional quadrotor model is also linearized about the hovering flight condition. As before all translational and rotational velocities as well as roll and pitch angles are zero during hover, leaving the positional states and the yaw angle undefined as these states do not affect the dynamics of the system. For simplicity these states are arbitrarily set equal to zero. Once again a thrust input equal to the gravitational force on the system is required to maintain hover, but all other control inputs are equal to zero. The linearization condition is written as

$$X_0 = 0 \qquad u_{1_0} = g(m_1 + m_2) \qquad u_{2_0} = 0 \qquad u_{3_0} = 0 \qquad u_{4_0} = 0 \ .$$

After applying the linearization condition substitutions, the linearized equations for the three dimensional model of the quadrotor and dynamic inertia are rearranged into matrix form:

$$\begin{bmatrix} m_1+m_2 & 0 & 0 & -m_2l_1 & 0 & 0 & m_2l_2 & 0 \\ 0 & m_1+m_2 & 0 & 0 & m_2l_1 & 0 & 0 & m_2l_2 \\ 0 & 0 & m_1+m_2 & 0 & 0 & 0 & 0 & 0 \\ -m_2l_1 & 0 & 0 & m_2l_1^2+I_{1y} & 0 & 0 & m_2l_1l_2 & 0 \\ 0 & m_2l_1 & 0 & 0 & m_2l_1^2+I_{1x} & 0 & 0 & m_2l_1l_2 \\ 0 & 0 & 0 & 0 & 0 & I_{1z} & 0 & 0 \\ -m_2l_2 & 0 & 0 & m_2l_1l_2 & 0 & 0 & m_2l_2^2+I_{2y} & 0 \\ 0 & m_2l_2 & 0 & 0 & m_2l_1l_2 & 0 & 0 & m_2l_2^2+I_{2x} \end{bmatrix} \begin{bmatrix} \delta\ddot{x} \\ \delta\ddot{y} \\ \delta\ddot{z} \\ \delta\ddot{\theta}_1 \\ \delta\ddot{\phi}_1 \\ \delta\ddot{\psi}_1 \\ \delta\ddot{\theta}_2 \\ \delta\ddot{\phi}_2 \end{bmatrix}$$

$$+ \begin{bmatrix} 0 & 0 & 0 & -g(m_1+m_2) & 0 & 0 & 0 & 0 \\ 0 & 0 & 0 & 0 & g(m_1+m_2) & 0 & 0 & 0 \\ 0 & 0 & 0 & 0 & 0 & 0 & 0 & 0 \\ 0 & 0 & 0 & m_2l_1g & 0 & 0 & 0 & 0 \\ 0 & 0 & 0 & 0 & m_2l_1g & 0 & 0 & 0 \\ 0 & 0 & 0 & 0 & 0 & 0 & 0 & 0 \\ 0 & 0 & 0 & 0 & 0 & 0 & m_2l_2g & 0 \\ 0 & 0 & 0 & 0 & 0 & 0 & 0 & m_2l_2g \end{bmatrix} \begin{bmatrix} \delta x \\ \delta y \\ \delta z \\ \delta\theta_1 \\ \delta\phi_1 \\ \delta\psi_1 \\ \delta\theta_2 \\ \delta\psi_2 \end{bmatrix} = \begin{bmatrix} 0 & 0 & 0 & 0 \\ 0 & 0 & 0 & 0 \\ 1 & 0 & 0 & 0 \\ 0 & -1 & 0 & 0 \\ 0 & 0 & -1 & 0 \\ 0 & 0 & 0 & 1 \\ 0 & 1 & 0 & 0 \\ 0 & 0 & 1 & 0 \end{bmatrix} \begin{bmatrix} \delta u_1 \\ \delta u_2 \\ \delta u_3 \\ \delta u_4 \end{bmatrix} . \quad (4.2)$$

The final step of the linearization process is transforming the linearized equations of motion into a system in standard linear form using the same approach used to

transform the planar model. Using the linearized dynamics of the three dimensional quadrotor model (3.14), the second order system of ODEs is transformed into a system of first order ODEs with the state vector and control vector:

$$\mathbf{x} = \begin{bmatrix} x & y & z & \theta_1 & \phi_1 & \psi_1 & \theta_2 & \phi_2 & \dot{x} & \dot{y} & \dot{z} & \dot{\theta}_1 & \dot{\phi}_1 & \dot{\psi}_1 & \dot{\theta}_2 & \dot{\phi}_2 \end{bmatrix}^T$$

$$\mathbf{u} = \begin{bmatrix} u_1 & u_2 & u_3 & u_4 \end{bmatrix}^T \ .$$

4.3 LQR Controller

The linear quadratic control approach was used to develop an optimal controller that minimizes a given cost function for a dynamic system assumed to be linear in the form

$$\dot{\mathbf{x}} = \mathbf{A}\mathbf{x} + \mathbf{B}\mathbf{u} \ . \tag{4.3}$$

The linear quadratic approach generates an optimal control law, but optimal in the sense that the control law minimizes the given cost function. This cost function must be defined. Following the approach in [18], the cost function for the infinite horizon or steady state regulator problem takes the form

$$V = \int_{t_0}^{\infty} \left(\mathbf{x}^T \mathbf{Q} \mathbf{x} + \mathbf{u}^T \mathbf{R} \mathbf{u} \right) dt \ . \tag{4.4}$$

For this research, all quadrotor motion is considered a perturbation from the hovering flight condition. For example, when navigating from waypoint to waypoint, the quadrotor begins in the hovering condition, then a combination of non-zero rotation angles and velocities cause the quadrotor to move toward the desired waypoint. The non-zero rotation angles and velocities are not desired, but these non-zero states are required to navigate to the next waypoint. Upon arriving at the desired position, the quadrotor returns to the hovering condition and the process is repeated. Since the purpose of this controller is to stabilize the system back to the hover condition and all motion of the quadrotor is considered a perturbation from the hover condition, there is no completion time.

In (4.4), the term $x'Qx$ in is a measure of control accuracy, and $u'Ru$ is a measure of control effort, where Q and R are, respectively, positive semi-definite and positive definite weighting matrices. Increasing elements of Q increases the cost of error associated with regulating the corresponding state to zero. Similarly, increasing elements of R increases the cost of using the associated control input. While increasing elements in the weighting matrices does increase costs, the ratio Q/R is more important than the individual values themselves. Therefore, the goal of minimizing the cost function is to keep the state x as close to the state $x_r = 0$ as possible using as little control input as possible.

The state-feedback control law that minimizes the cost function in (4.4) takes the form

$$\mathbf{u}(t)^* = -\mathbf{K}\mathbf{x}(t) \ , \tag{4.5}$$

where the optimal feedback gain K is equal to

$$\mathbf{K} = \mathbf{R}^{-1}\mathbf{B}^T\mathbf{P} \ , \tag{4.6}$$

where the matrix P is a symmetric matrix satisfying the Ricatti equation. For the infinite horizon problem, the Ricatti equation is reduced to the algebraic Ricatti equation

$$0 = \mathbf{A}^T\mathbf{P} + \mathbf{P}\mathbf{A} + \mathbf{Q} - \mathbf{P}\mathbf{B}\mathbf{R}^{-1}\mathbf{B}^T\mathbf{P} \ . \tag{4.7}$$

Solving the algebraic Ricatti equation (4.7) for the matrix P, using the result to find the optimal feedback gain (4.6), and substituting back into (4.5) results in the optimal state-feedback control law

$$\mathbf{u}(t)^* = -\mathbf{R}^{-1}\mathbf{B}^T\mathbf{P}\mathbf{x}(t) \ . \tag{4.8}$$

MATLAB is a numerical computing environment and programming language that is a standard in engineering industry. MATLAB is based on matrix manipulation making it the ideal choice for developing the controllers and simulating the quadrotor

response. In addition to the matrix manipulation tools, MATLAB has a function that solves the algebraic Ricatti equation to compute the optimal feedback gain matrix for a given time invariant system. This tool is used to compute the optimal feedback gain matrix for this research.

4.4 Quadrotor Parameters

At this point the quadrotor parameters must be specified. For this research, the quadrotor parameters are representative of the Ascending Technologies Hummingbird quadrotor with additional electronics required for onboard sensing, computing, and dynamic mass control. The quadrotor parameters are listed in Table 4.1. This modified quadrotor will be one of the primary testbeds for implementing sensing and control methods in the Nonlinear Dynamics and Controls Lab at the University of Washington. Not only is the Hummingbird quadrotor the current platform used in the Nonlinear Dynamics and Controls Lab, the Hummingbird is used by industry and research institutions across the world making it a good choice for specifying the quadrotor parameters.

The quadrotor, battery, additional electronics, as well as a prototype of the dynamic mass pendulum were weighed in the lab to obtain an estimate for the weights of the vehicle and final dynamic mass system. Also, inertia values of the quadrotor were roughly estimated through experiments where the vehicle was mounted in a test stand that recorded the oscillatory frequencies of the quadrotor as it pivoted freely about a single axis. Dynamic mass inertia values were estimated by assuming the dynamic mass acts like a point mass with the center of gravity located at the end of the pendulum.

In addition to vehicle parameters, control saturation limits are also specified. Table 4.2 contains the control saturation limits based on testing, manufacturer specifications, and estimations. The thrust limit is determined by mounting the vehicle to a unidirectional force balance and recording thrust measurements at various throttle

Table 4.1: Quadrotor Parameters.

Parameter	Value	Description
m_1	0.70 kg	Quadrotor Mass
m_2	0.20 kg	Dynamic Mass
l_1	0.02 m	Distance from joint to the quadrotor CG
l_2	0.10 m	Distance from joint to dynamic mass CG
I_{1_y}	4.60×10^{-3} $kg\ m^2$	Quadrotor inertia about the y axis
I_{1_x}	4.60×10^{-3} $kg\ m^2$	Quadrotor inertia about the x axis
I_{1_z}	8.20×10^{-3} $kg\ m^2$	Quadrotor inertia about the z axis
I_{2_y}	2.0×10^{-3} $kg\ m^2$	Quadrotor inertia about the y axis
I_{2_x}	2.0×10^{-3} $kg\ m^2$	Quadrotor inertia about the x axis

settings. The data measurements are then characterized by a third order polynomial, and the maximum thrust is estimated. Servo torque limits for HiTEC HS-35HD Ultra Nano servos are specified on the manufacturer website. Finally, the yaw torque is estimated based on inertial values and the manufacturer specified yaw rates. There is a minimum thrust specified to ensure smooth decreases in altitude and prevent the vehicle from reducing thrust to zero in order to drop at a maximum rate. This could lead to dangerously quick drops in altitude and larger controller overshoots in the negative z direction. Should the control inputs reach the saturation limits during simulations, the input will be limited to the saturation limit until acceptable inputs are required.

4.5 Controllability Check

Before computing the solution to the algebraic Ricatti equation P and the optimal feedback gain matrix, it is important to verify that the solution P exists. If a system is controllable there always exists a constant control law in the form $u = -Kx$ that

Table 4.2: Control Saturation Limits.

Parameter	Value	Description
$u_{1,max}$	15 N	Maximum thrust
$u_{1,min}$	5 N	Minimum thrust
$u_{2,max}$	0.8 Nm	Maximum servo torque
$u_{3,max}$	0.8 Nm	Maximum servo torque
$u_{4,max}$	0.035 Nm	Maximum yaw torque from differential thrust

makes the closed loop system asymptotically stable. A linear system is controllable if the rank of the controllability matrix is equal to the number of states of the system, that is

$$\text{rank} \begin{bmatrix} B & AB & ... & A^{n-1}B \end{bmatrix} = n \ . \tag{4.9}$$

When the A and B matrices for the linearized three dimensional quadrotor model shown in Appendix B.1 are used to build the controllability matrix, the rank of the resulting matrix is $n = 16$. Therefore, the linear 3D model is controllable and a stabilizing LQR feedback controller exists. Similarly, the rank of the controllability matrix for the 2D model is $n = 8$, meaning the system is controllable, and a stabilizing feedback controller exists.

4.6 Optimal Gain Matrix

MATLAB is used to solve the algebraic Ricatti equation and compute the optimal state feedback gain matrix for the 3D quadrotor model, but first the linearized A and B matrices are specified. The A and B matrices evaluated using the parameters in Table 4.1 are shown in Appendix B.1. In addition to the A and B matrices, the weighting matrices Q and R are defined. Bryson's rule is a common method for assigning values to the weighting matrix that uses the maximum values of the states and inputs of the

system:

$$Q_{ii} = \frac{1}{(\text{max value } x_i)^2} \qquad\qquad R_{ii} = \frac{1}{(\text{max value } u_i)^2} \ ,$$

where the maximum value of x_i is replaced by the maximum acceptable tracking error in state x_i for a trajectory tracking problem.

Stabilization and trajectory tracking are the most important performance measures for this research, which is dependent on the control accuracy term of the cost function and the Q matrix in particular. A significant quadrotor behavior that is not captured in linearized dynamics is the relationship between vertical thrust and roll or pitch. Since the thrust vector is fixed to the z_b axis in the body frame, when the quadrotor is at a non-zero roll or pitch angle the vehicle loses thrust in the inertial z direction. As a result the quadrotor must increase thrust, or the vehicle will lose altitude. This coupling occurs whenever the quadrotor translates in the x y plane but is not captured in the linearized dynamics used to generate the controller. To compensate for this loss of altitude, the control accuracy cost associated with the z positional state is increased by increasing the associated element in the Q matrix. Using Bryson's rule and decreasing the maximum acceptable tracking error to $z_{error} = 0.1\ m$,

$$Q_{33} = \frac{1}{(\text{acceptable error } z)^2} = \frac{1}{(0.1)^2} = 100 \ .$$

Tracking in the z direction is more sensitive due to the force of gravity acting in that direction, but the tracking accuracy in the $x,\ y$ states is important as well. Without the thrust loss behavior seen in the z axis and without fear of crashing into the ground in the x and y axis, the acceptable tracking error in the $x,\ y$ positions can be relaxed. Using Bryson's rule with an acceptable tracking error $x_{error} = y_{error} = 0.3m$,

$$Q_{11,22} = \frac{1}{(\text{acceptable error})^2} = \frac{1}{(0.3)^2} \approx 10 \ .$$

Tracking accuracy in the remaining states is not as important for this research, and the corresponding element in the weighting matrix is set to unity. The resulting

Q matrix is diagonal in form with the following elements along the diagonal:

$$\mathbf{Q} = diag\begin{bmatrix}10 & 10 & 100 & 1 & 1 & 1 & 1 & 1 & 1 & 1 & 1 & 1 & 1 & 1 & 1 & 1\end{bmatrix}.$$

Thrust is the most important control input of the quadrotor. Not only does thrust keep the vehicle airborne, all translational acceleration of the vehicle is coupled with the thrust input. Therefore increased excess thrust results in increased maneuverability. For these reasons, the control cost of the thrust input is decreased, and the control cost weighting matrix is

$$\mathbf{R} = \begin{bmatrix} 0.044 & 0 & 0 & 0 \\ 0 & 1.56 & 0 & 0 \\ 0 & 0 & 1.56 & 0 \\ 0 & 0 & 0 & 1.56 \end{bmatrix}.$$

Solving the algebraic Ricatti equation results in the optimal feedback gain matrix:

$$K = \begin{bmatrix} 0 & 0 & 47.67 & 0 & 0 & 0 & 0 & 0 & \cdots \\ -2.53 & 0 & 0 & -15.15 & 0 & 0 & 4.43 & 0 & \\ 0 & 2.53 & 0 & 0 & -15.15 & 0 & 0 & 4.43 & \\ 0 & 0 & 0 & 0 & 0 & 1.00 & 0 & 0 & \end{bmatrix}$$

$$\begin{bmatrix} 0 & 0 & 10.33 & 0 & 0 & 0 & 0 & 0 \\ -2.48 & 0 & 0 & -2.04 & 0 & 0 & -0.47 & 0 \\ 0 & 2.48 & 0 & 0 & -2.04 & 0 & 0 & -0.47 \\ 0 & 0 & 0 & 0 & 0 & 1.01 & 0 & 0 \end{bmatrix}.$$

In a similar way to the 3D model, the optimal feedback gain is computed for the 2D planar quadrotor model. The linearized 2D A matrix (B.1) and B matrix (B.2) are evaluated using the quadrotor parameters in Table 4.1 and shown in Appendix B.1. Once again the control accuracy cost is increased for the z positional state to compensate for a reduction in vertical thrust. The control accuracy cost for the x

positional state is also slightly increased to improve trajectory tracking performance. The resulting Q and R matrices for the 2D planar model are

$$\mathbf{Q} = \begin{bmatrix} 10 & 0 & 0 & 0 & 0 & 0 & 0 & 0 \\ 0 & 100 & 0 & 0 & 0 & 0 & 0 & 0 \\ 0 & 0 & 1 & 0 & 0 & 0 & 0 & 0 \\ 0 & 0 & 0 & 1 & 0 & 0 & 0 & 0 \\ 0 & 0 & 0 & 0 & 1 & 0 & 0 & 0 \\ 0 & 0 & 0 & 0 & 0 & 1 & 0 & 0 \\ 0 & 0 & 0 & 0 & 0 & 0 & 1 & 0 \\ 0 & 0 & 0 & 0 & 0 & 0 & 0 & 1 \end{bmatrix} \quad \text{and} \quad \mathbf{R} = \begin{bmatrix} 0.044 & 0 \\ 0 & 1.56 \end{bmatrix}.$$

The resulting optimal feedback gain matrix is

$$K = \begin{bmatrix} 0 & 47.67 & 0 & 0 & 0 & 10.33 & 0 & 0 \\ -2.53 & 0 & -15.15 & 4.43 & -2.49 & 0 & -2.04 & -0.47 \end{bmatrix}.$$

The computed gain matrices can now be substituted into (4.5) to develop the optimal feedback control law for the quadrotor models. Although the optimal feedback gain matrices are computed using the linearized dynamics, the gain matrices are not limited to use with only the linearized quadrotor models. The optimal feedback control laws can be applied to the nonlinear quadrotor models individually or in combination with other controllers to provide stability and robustness to the system.

Chapter 5

SIMULATION

In order to evaluate the performance of the controllers, the linear controllers are implemented on the nonlinear quadrotor models, then MATLAB is used to simulate the behaviors of the controlled systems. The nonlinear dynamics are propagated forward through time using the `ode45` function, which is a standard function in MATLAB that solves a system of ordinary differential equations using the 4th order Runge-Kutta iterative approximation method. In this section the behaviors of both the 2D and 3D controlled systems are presented. The behaviors of interest include: stabilization, linear motion, and trajectory tracking. Following the performance evaluations, the trajectory tracking performance of the quadrotor using dynamic inertia control is compared to the performance of the quadrotor without dynamic inertia using traditional differential thrust control methods.

5.1 Stabilization

Since quadrotors are inherently unstable, the first task of any controller is stabilizing the vehicle. To evaluate the stabilizing performance of the controller, the quadrotor is given the task of hovering at an arbitrary location where all states, including positional states are set equal to zero for simplicity. With the hovering condition specified, the quadrotor is started at a non-zero initial condition, forcing the quadrotor to stabilize and move to the desired hovering position at the origin,

$$X_d = \begin{bmatrix} 0 & 0 & 0 & 0 & 0 & 0 & 0 & 0 \end{bmatrix}^T .$$

Recall the state vector for the planar model is,

$$X = \begin{bmatrix} x & z & \theta_1 & \theta_2 & \dot{x} & \dot{z} & \dot{\theta}_1 & \dot{\theta}_2 \end{bmatrix}^T .$$

Figure 5.1 shows the stabilizing performance of the LQR controller implemented on the nonlinear 2D quadrotor model given the initial conditions

$$X_0 = \begin{bmatrix} 1 & 2 & -15 & 20 & 0 & 0 & 0 & 0 \end{bmatrix}^T .$$

Starting at the specified initial conditions, the LQR controller stabilizes the vehicle in a favorable manner. Overshoot with feedback controllers is to be expected, but the overshoot in the z direction is increased by the gravitational force acting in the z direction. The overshoot in the z direction is 0.53 meters before leveling out at $z = -0.086\ m$. Even though the z position is initially displaced further from the hover set point than the x position, stabilization in the z direction occurs more quickly. Stabilization occurs in approximately 1.8 seconds for the z position, and approximately 3 seconds for the x position. This difference in stabilization time is not surprising considering the z position is directly controlled with the thrust input u_1, whereas the x position is coupled with both thrust u_1 and the dynamic mass position u_2. Although stabilization in the x position is slower, the overshoot is only 0.096 meters which is much smaller than the overshoot in the z direction.

The lower graph in Figure 5.1 shows the stabilizing behavior on the angular states. Note that the quadrotor has a negative initial pitch whereas the dynamic mass has a positive initial pitch. Despite initial differences, the pitch of the quadrotor and the dynamic mass quickly transition to motion that is nearly in phase. As expected stabilization is slower in the angular states because nonzero pitch angles are required to stop the motion in the x direction. With the exception of the initial conditions, the quadrotor pitch reaches a maximum magnitude of approximately 10 degrees, and the dynamic mass reaches a maximum magnitude of approximately 20 degrees. Stabilization in the angular position states occurs approximately in approximately 4

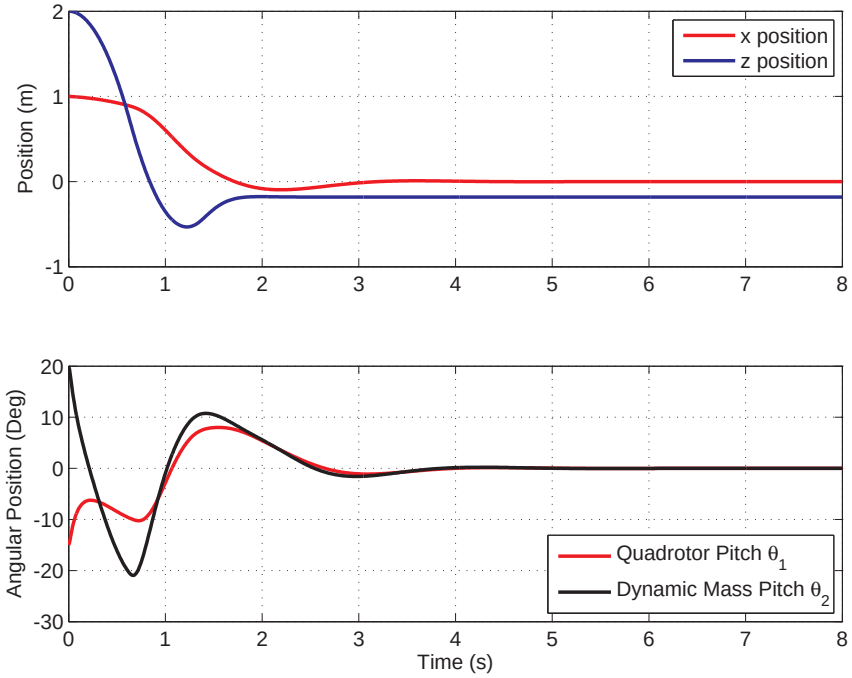

Figure 5.1: Simulation of the nonlinear 2D quadrotor model using dynamic inertia stabilization given nonzero initial conditions.

seconds. Figure 5.2 shows the stabilization behavior of the $x,\ y,\ z$ positional states for the nonlinear 3D model. Once again the desired hovering position is at the origin, with initial conditions,

$$X_0 = \begin{bmatrix} 1 & 1 & 2 & -15 & 15 & 0 & 20 & -20 & 0 & 0 & 0 & 0 & 0 & 0 & 0 & 0 \end{bmatrix}^T .$$

These initial conditions are identical to the initial conditions used in the 2D simulation with mirrored $x,\ z$ plane and $y,\ z$ plane initial conditions. Recall that the state vector for the 3D model is,

$$\mathbf{x} = \begin{bmatrix} x & y & z & \theta_1 & \phi_1 & \psi_1 & \theta_2 & \phi_2 & \dot{x} & \dot{y} & \dot{z} & \dot{\theta}_1 & \dot{\phi}_1 & \dot{\psi}_1 & \dot{\theta}_2 & \dot{\phi}_2 \end{bmatrix}^T .$$

As with the 2D simulation, the controller provides favorable stabilization for the 3D model. Due to the symmetry of the quadrotor, nearly identical responses in the x and y directions are expected. Also expected is nearly identical behavior to the

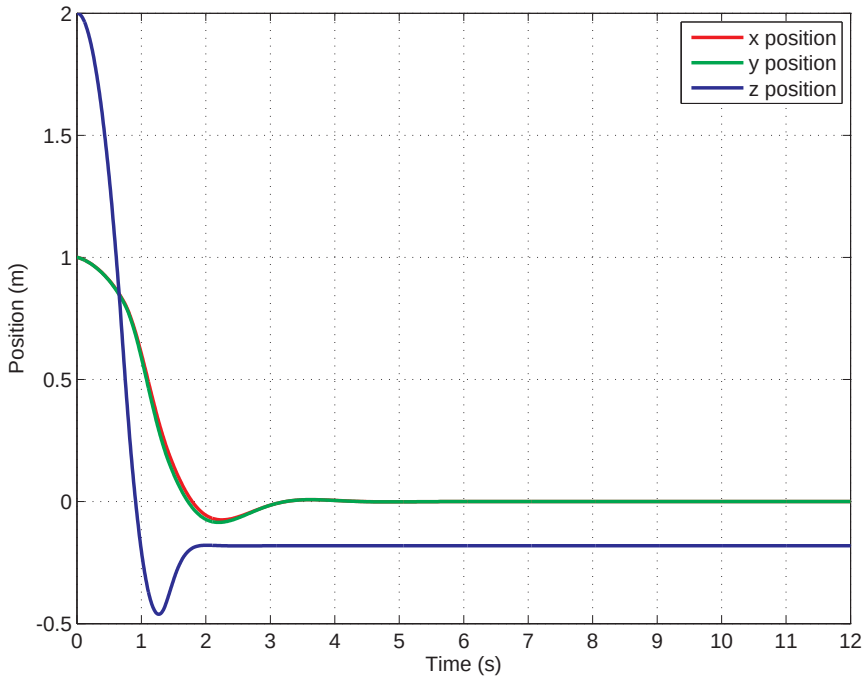

Figure 5.2: Stabilization of the positional states of the nonlinear 3D quadrotor model using dynamic inertia stabilization given nonzero initial conditions.

2D simulation seen in the responses of the x and z states. Figure 5.3 shows the response of the angular positions of the vehicle. Notice that the pitch, θ, responses are identical to the responses seen in the 2D simulations. The roll, ϕ, responses are nearly identical to the pitch responses except that the roll response is inverted. This inversion is a result of the defined axis system in which a positive pitch results in motion in the positive x direction, whereas a positive roll results in motion in the negative y direction. Also, the magnitude of the angular states and the stabilization time for the 3D simulation is a close match to the 2D simulation.

Figure 5.3 does not show the response for the ψ_1 state because this state remained approximately equal to zero for all testing. During testing the yaw initial conditions and all yaw trajectories are equal to zero. Zero yaw angle is desired for this research because yaw is not dependent on dynamic inertia control. The states affected by the

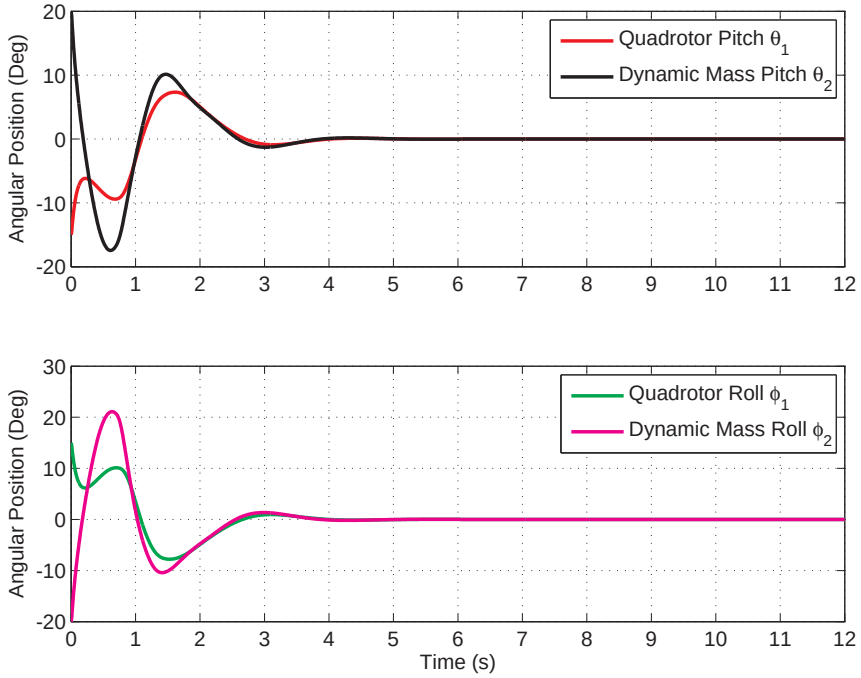

Figure 5.3: Stabilization of the attitude states of the nonlinear 3D quadrotor model using dynamic inertia stabilization given nonzero initial conditions.

dynamic inertia are most important for this research, and minimal response is desired for all other states in order to isolate the responses of those states affected by the dynamic inertia. Due to the zero state desired for ψ_1, the fourth control input u_4 is approximately zero for all time and not displayed in these results.

The results from the stabilization simulations show that the linear controllers provide good stabilization to the nonlinear models. In addition to stabilization, the results show that the more complicated 3D controller produces results that closely match the results of the simpler 2D controller on the respective nonlinear models. This similarity shows the planar dynamics seen in the 2D simulations do not change when the model is extended to three dimensions.

For the remainder of this thesis only the 3D model results are presented because the 2D simulations mimic the in-plane results of the 3D simulations.

5.2 Linear Motion

Once stabilization has been established, the next potential task for the quadrotor is a simple linear movement, where a step response of the positional states is desired. The desired flight profile begins at the origin, hovers for 2 seconds, followed by a step response to $x = 5\ m$ and $y = 5\ m$, and hover at the new location. Figure 5.4 shows the response of the $x,\ y,\ z$ states of the 3D model for this linear movement profile.

As expected, the x and y states have the same response due to vehicle symmetry and matching desired responses. Both the x and y states overshoot approximately $0.16\ m$ before stabilizing after approximately 3 seconds of motion. The z state remains close to zero for the duration of the maneuver with two slight dips during the transition. These dips are a result of the thrust loss that occurs when the vehicle is at a nonzero pitch or roll as discussed earlier. The z state drops to a minimum of $-0.11\ m$ at the peak of each depression. The peak of each dip in the z state corresponds to the time at which the quadrotor is at a maximum pitch and roll angle. This correlation is shown by comparing the peak times in Figure 5.4 and Figure 5.5.

Figure 5.5 shows the angular response to the linear motion. As expected from the stabilization results, the pitch response and roll response are extremely similar with the exception that the roll response is inverted. Figure 5.5 clearly shows the relative motion of the quadrotor and dynamic mass at the start of the motion at 2 seconds. For example, the pitch of the quadrotor is opposite of the pitch of the dynamic mass at the beginning of the motion, and likewise with the roll response. In order to generate a positive pitch on the quadrotor, a negative, opposing torque must be applied to the dynamic mass pendulum. The result is a positive quadrotor pitch and a temporarily negative pitch of the dynamic mass before swinging back the other way and staying generally in phase with the quadrotor. The same behavior occurs in the roll response, and both roll and pitch responses stabilize approximately 3.5 seconds after the motion begins.

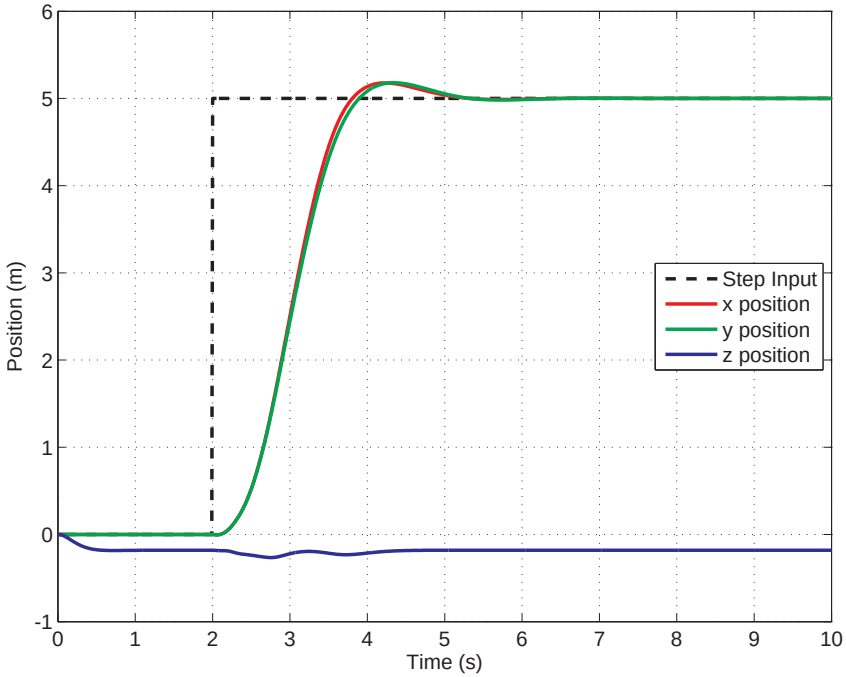

Figure 5.4: Positional state traces for the 3D quadrotor model given a step input to move 5 meters forward in the x and y directions.

During development of the linearized model and linear LQR controller, attitude angles were assumed to be small, but Figure 5.5 clearly shows large pitch and roll angles. The presence of large angles in the simulation does not invalidate the controller, rather the presence of large angles in the vehicle response suggests the applied control may not be the optimal control for the nonlinear model. Although the controller was developed as an optimal controller, the control is only optimal for the linear model used to compute the feedback gain matrix. Therefore, the controller can result in non-optimal control when applied to the nonlinear model which is likely what is happening in this response.

In addition to the state responses to the linear motion, the control inputs are recorded and shown in Figure 5.6. The inputs to the system are important for choosing various components for the final version of the quadrotor used in the lab. The top

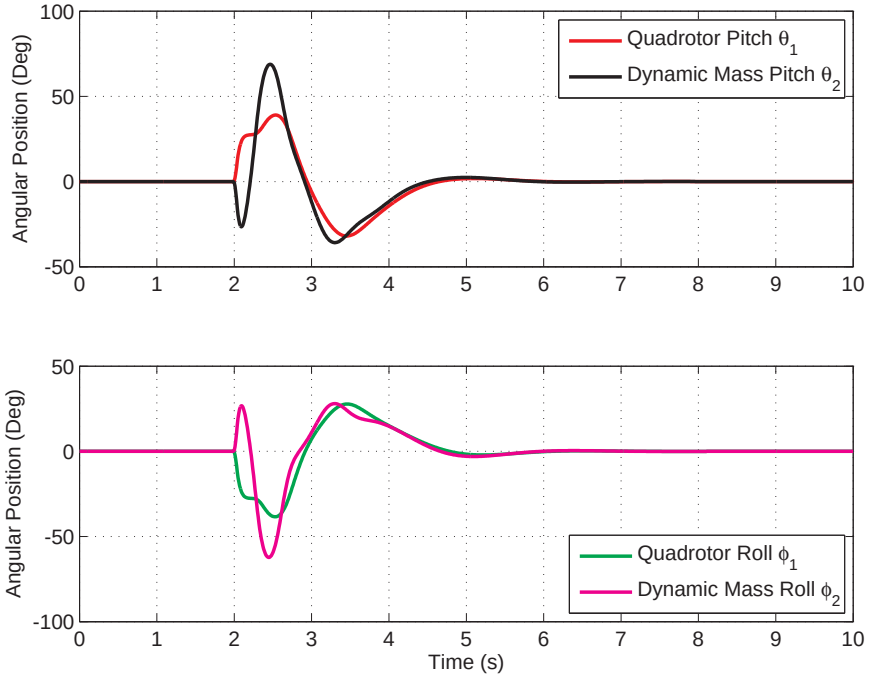

Figure 5.5: Positional state traces for the 3D quadrotor model given a step input to move 5 meters forward in the x and y directions.

graph shows the cumulative thrust input in blue and the maximum thrust limit of the quadrotor in red. Thrust increases when the quadrotor transitions to the desired location with peaks corresponding to the times when the vehicle is at maximum pitch and roll angles. These thrust peaks are a result of the controller compensating for the thrust loss that occurs at nonzero pitch and roll angles. Throughout the maneuver, the thrust input of the quadrotor remains below the maximum thrust produced by the vehicle.

The lower two graphs show the servo torque in the pitch and roll directions. Note the maximum servo torque in each case occurs during the initial movements of the vehicle when the dynamic mass pendulum is torqued in the opposite direction to generate the required pitch or roll for the quadrotor. Servo torque spikes during this initial movement and saturates the control limit of 0.8 $N\ m$. There is also a significant

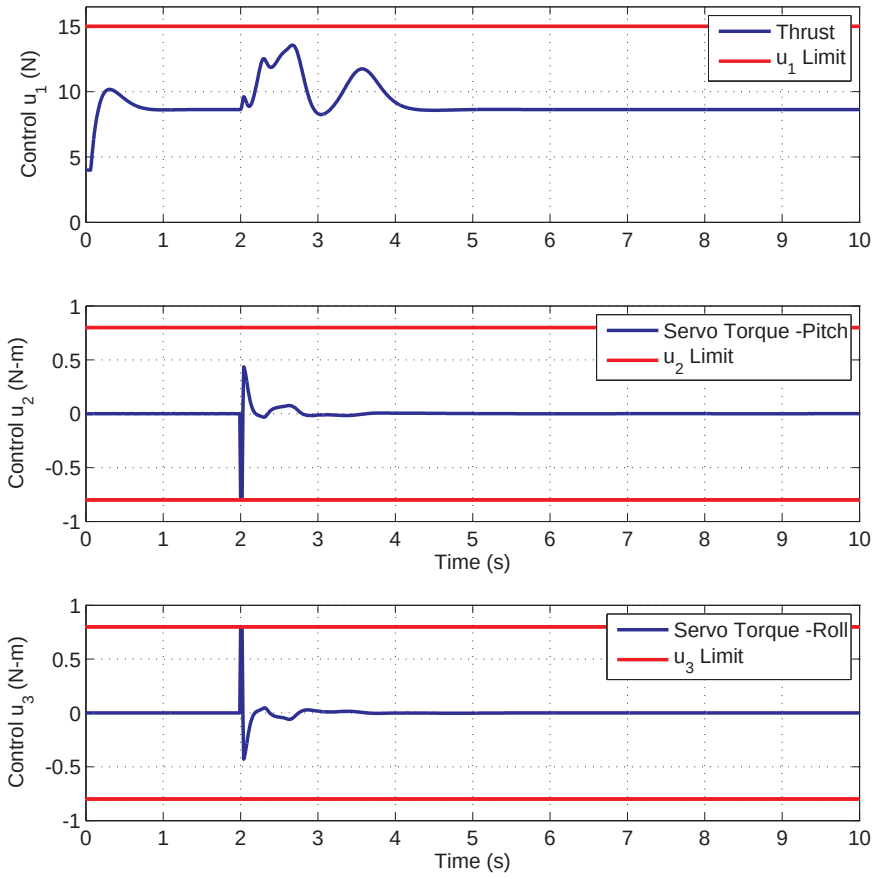

Figure 5.6: Control inputs during the linear movement of the 3D quadrotor model.

spike immediately after the initial torque, which redirects the dynamic mass in the opposite direction as the quadrotor and dynamic mass transition to in phase motion. The remaining torque inputs are much smaller, and all inputs reach a steady state approximately 2 seconds after the maneuver starts.

In Figure 5.5 the angular positions do not stabilize until approximately 4 seconds after the initial movement, but Figure 5.6 shows the inputs reach a steady state at approximately 2 seconds after the initial movement. This time difference shows that the controlled system exhibits dynamics with a slow settling time that take additional time to stabilize after the inputs cease. In addition to this time difference, there is a

noticeable lag between the time the servo torques are applied and the time the vehicle attitude is affected.

The simulations for linear motion show that the controlled system behaves favorably when a step response is desired. The quadrotor reaches the desired position in approximately 3.5 seconds with 13% overshoot and minimal oscillations.

5.3 Trajectory Tracking

After stabilization and a simple linear motion are simulated, the next step is to track a simple trajectory. For this research the desired trajectory for tracking is involves flying in a straight line 10 m in the $x,\ y$ plane, stopping, increasing altitude by 10 m, flying another 10 m in the $x,\ y$ plane, then hovering. A visual of this desired trajectory is shown in Figure 5.7.

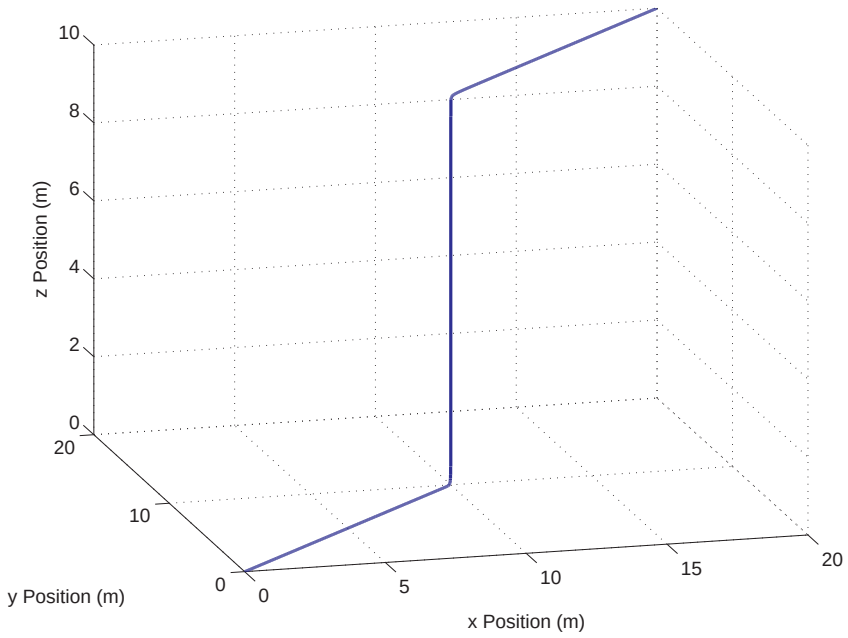

Figure 5.7: Desired 3D trajectory for tracking performance evaluation.

A major difference between this trajectory and the previous step response desired trajectory is that step responses are not desired for this trajectory. The time profiles of the $x,\ y,\ z$ states for this desired trajectory is shown in Figure 5.8.

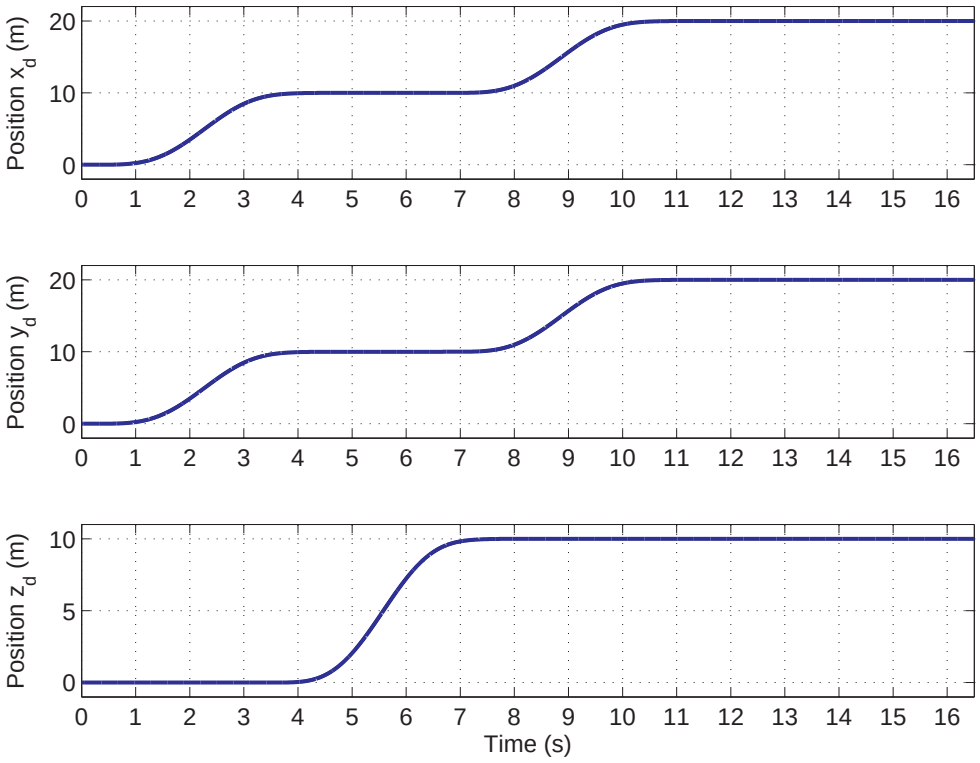

Figure 5.8: Time profiles for the desired trajectory.

The transition time for the movements in not instantaneous as in the linear motion; instead the transition is 3.3 seconds for each 10 m segment of the desired trajectory.

Figure 5.9 shows the positional tracking performance of the quadrotor. The top two graphs show the $x,\ y$ state traces and the desired trajectory. As seen previously, there is a small lag in in tracking that is inherent with feedback controllers as well as a single overshoot with of approximately 1.3 m in both states at each 10 m movement. This overshoot also corresponds to the maximum tracking error in the x and y states.

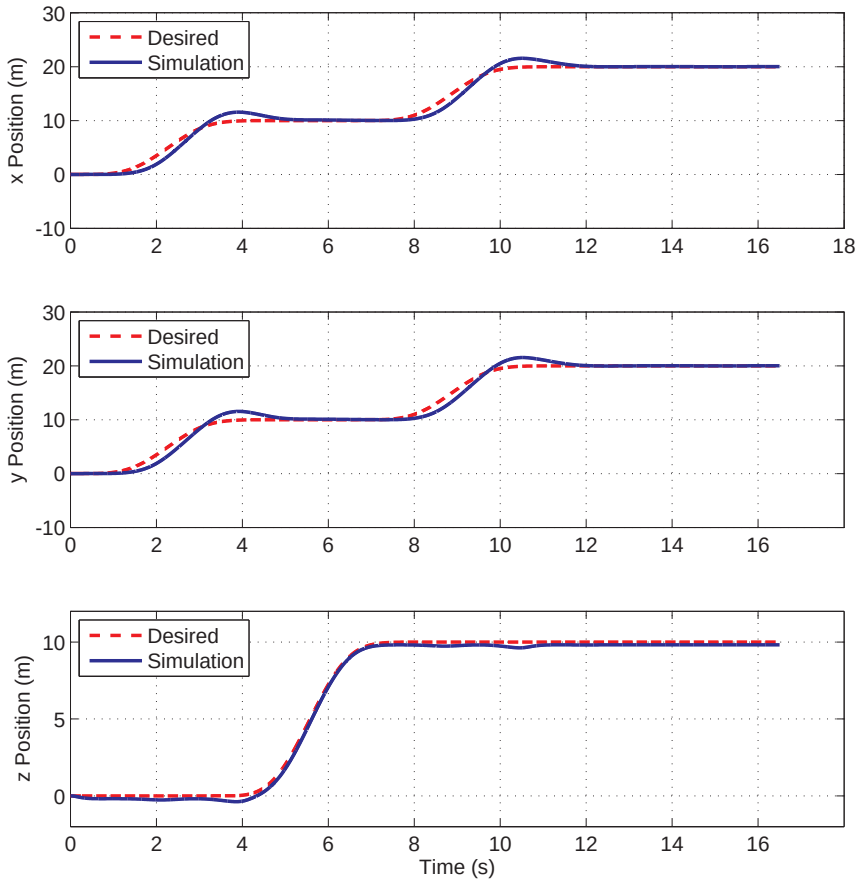

Figure 5.9: Trajectory tracking performance of the 3D quadrotor in the $x,\ y,\ z$ states.

The bottom graph in Figure 5.9 shows the trajectory tracking in the z state. Due to the high control accuracy cost in the weighting matrix, the z state tracks very well with a maximum tracking error of 0.016 %. The high tracking accuracy in the z direction is not surprising because the z state is controlled by thrust, which affects the z state nearly instantaneously unlike pitch and roll which are affected by servo torques more slowly. For this trajectory the linear LQR controller provides adequate tracking in the $x,\ y$ positional states and good tracking in the z state.

Figure 5.10 shows the pitch and roll state traces for both the quadrotor and dynamic mass during the trajectory tracking. The pitch response of the quadrotor

and dynamic mass are as expected with a positive pitch to generate forward motion followed by a negative pitch to bring the quadrotor to a stop. Different from the previous simulation is the degree to which the quadrotor and dynamic mass move in phase together. This higher degree of in phase movement is a result of a slower trajectory.

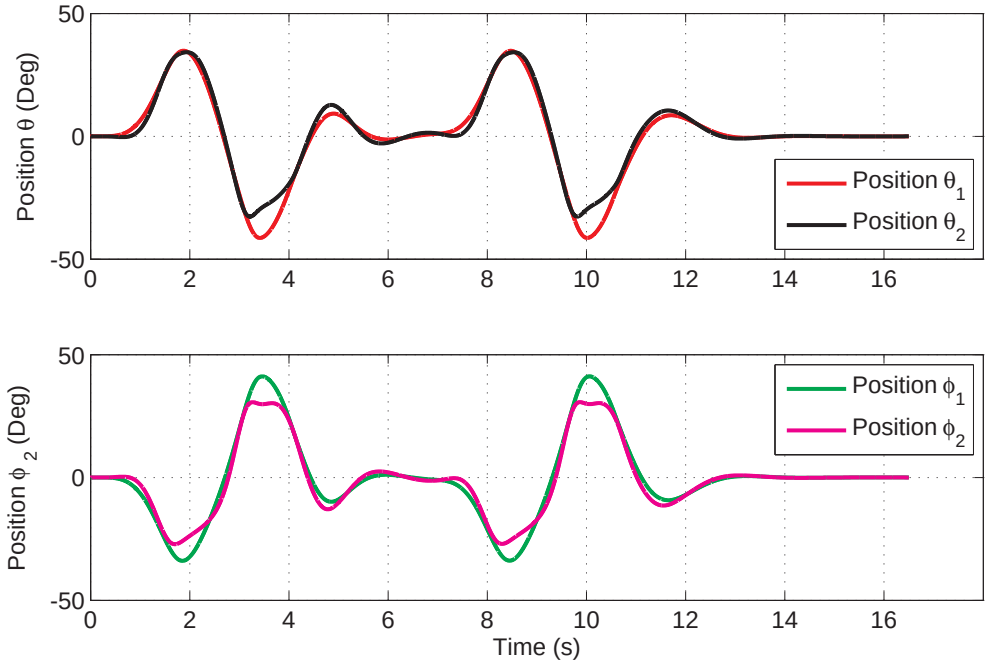

Figure 5.10: Trajectory tracking performance in the pitch and roll sates.

5.4 Comparison to Differential Thrust

After using dynamic inertia as the control mechanism for trajectory tracking, it is useful to compare the results to trajectory tracking using differential thrust as the control mechanism. A model for the quadrotor without dynamic inertia is developed using the nonlinear equations of motion for the 3D model of the quadrotor with dynamic inertia in (3.12). Replacing the terms corresponding to the dynamic mass with zero reduces the system of equations to six nonlinear equations of motion represent-

ing the dynamics of the quadrotor without dynamic inertia. The resulting equations of motion are linearized using small perturbation analysis, and a linear LQR controller is developed using nearly identical weighting matrices. The development of the quadrotor models with out dynamic inertia can be found in Appendix C.

Figure 5.11 shows the tracking performance of the quadrotor using differential thrust for control. The top two graphs show the tracking in the x and y states with a maximum tracking error of 0.13 m in each state. This tracking error is an order of magnitude smaller than the 1.3 m tracking error incurred in the x and y states when using dynamic inertia for control.

The bottom graph shows the tracking performance in the z state which incurs a maximum tracking error of 0.23 m. The tracking performance using differential thrust is only slightly better than the performance when using dynamic inertia control which results in a maximum error of 0.35 m. The thrust input u_1 is cumulative thrust for both dynamic inertia and differential thrust control quadrotor models. Because the input u_1 represents the same force on the vehicle when using both control methods, the similar tracking performance is not surprising.

The comparison between the tracking performance using dynamic inertia control versus differential thrust control shows that tracking performance is superior when using differential thrust. Tracking in the z state is nearly equivalent between the two control methods, but x and y state tracking results in 13% and 1.3% tracking error in both states for dynamic inertia and differential thrust control respectively.

Although differential thrust control provides superior tracking performance to dynamic inertia control, differential thrust control requires a independent control to all four motors. Dynamic inertia control does not require independent control of each motor, instead only cumulative thrust is varied.

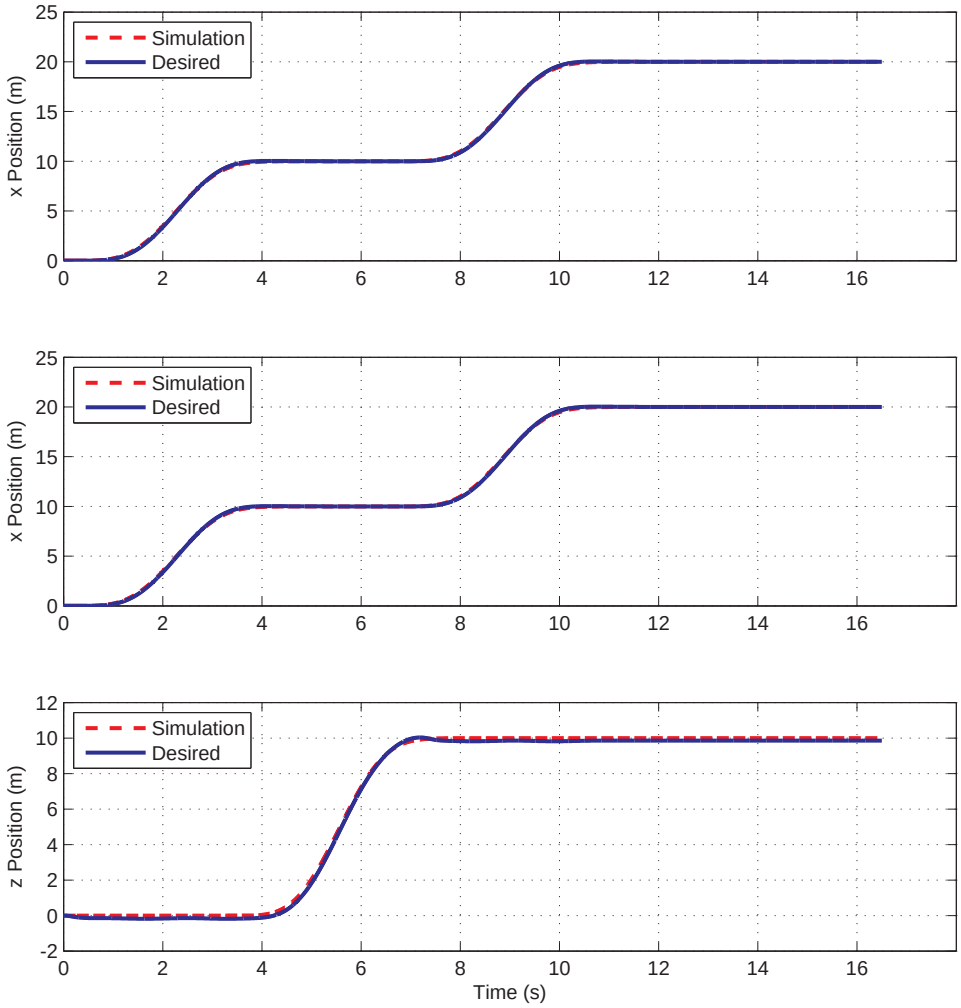

Figure 5.11: Trajectory tracking performance of the 3D quadrotor in the x, y, z states using differential thrust for control.

5.5 Robustness

One of the reasons linear LQR controllers were chosen to control the nonlinear quadrotor systems is the robustness of LQR controllers. This robustness is important because the quadrotor models are highly nonlinear, meaning small modeling errors can cause large instabilities in the system response. Good tolerance of nonlinearities found in LQR controllers help reduce the impact of modeling errors and uncertainties on the

controllability of the system.

To examine the robustness of the 3D controller, a Monte Carlo approach is used to determine the stability bounds of the system. Various quadrotor parameters are selected for the study, then the designed controller is simulated on the nonlinear model with modified parameters. The quadrotor parameters are varied one at a time for each simulation until the system response is unstable.

The most probable modeling errors for this system involve inertia values for the vehicle because they are difficult to compute and difficult to obtain experimentally. When the inertia values I_{1y} and I_{1x} are varied individually, the results are identical to results when these inertia values are varied together. The system remains stable when even when inertia modeling errors greater than 160% are present.

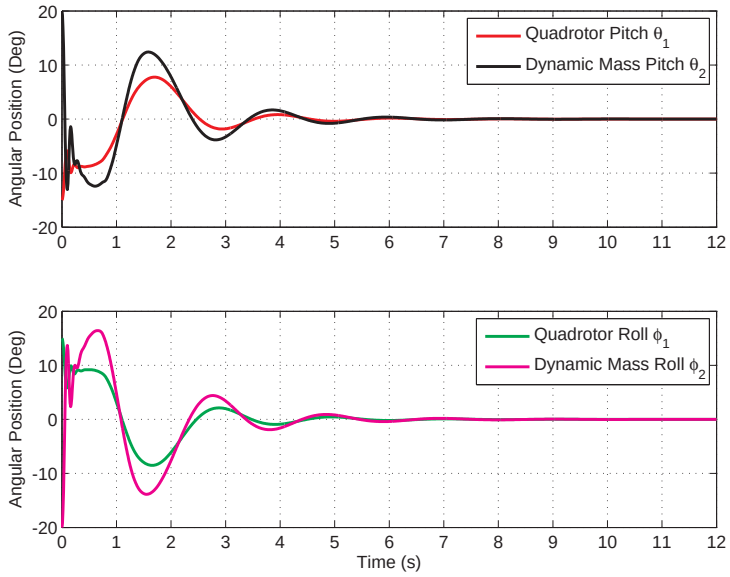

Figure 5.12: Stabilization behavior with 160% inertia modeling error, $I_{1y} = I_{1x} = 1.2 \times 10^{-2} kg\ m^2$.

Figure 5.12 shows the stabilization of the angular states with a 160% inertia modeling error. The controller was designed for inertia values $I_{1y} = I_{1x} = 4.6 \times 10^{-3} kg\ m^2$ and simulated on a nonlinear model with inertia values equal to $I_{1y} =$

$I_{1x} = 1.2 \times 10^{-2} kg\ m^2$. Note the beginning of instabilities are present during the first 1/4 second of the simulation. Increasing inertia values further results in the system becoming uncontrollable. The system also remains stable when the inertia values are reduced to $I_{1y} = I_{1x} = 1.0 \times 10^{-4} kg\ m^2$.

In addition to inertia values, mass modeling errors are simulated for both the quadrotor mass and the dynamic mass values. At approximately $m_2 = 0.06\ kg$, the dynamic mass becomes too light to adequateness change the inertia of the system, making the system uncontrollable.

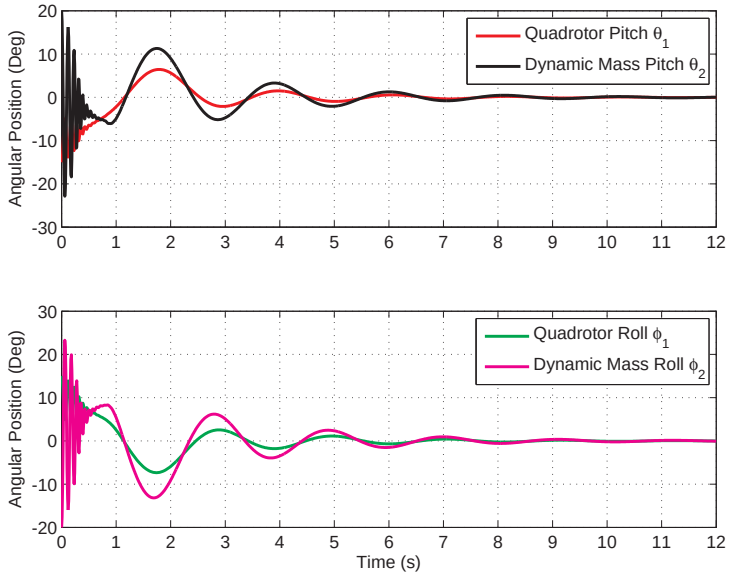

Figure 5.13: Stabilization behavior with dynamic mass modeling error, $m_2 = 0.057kg$.

Figure 5.13 shows the stabilization of the pitch and roll states of the vehicle with a dynamic mass modeling error greater than 70%. In this simulation, $m_2 = 0.057\ kg$ instead of the value $m_2 = 0.20\ kg$ for which the controller was designed. Instabilities are present during the initial 0.5 second of the system response. As the dynamic mass is decreased further the system becomes uncontrollable.

Increasing the dynamic mass does not reduce the stability or controllability of

the system, but increasing the dynamic mass reduces the tracking accuracy in the z state. When increasing the mass of the system, there is little difference in the system response between increasing the quadrotor mass m_1 versus increasing the dynamic mass m_2. The most important parameter is the total mass of the system $m_1 + m_2$. When the total mass of the system reaches 1.4 kg, the quadrotor cannot produce enough thrust to stabilize the z state in a reasonable amount of time without extremely excessive overshoots.

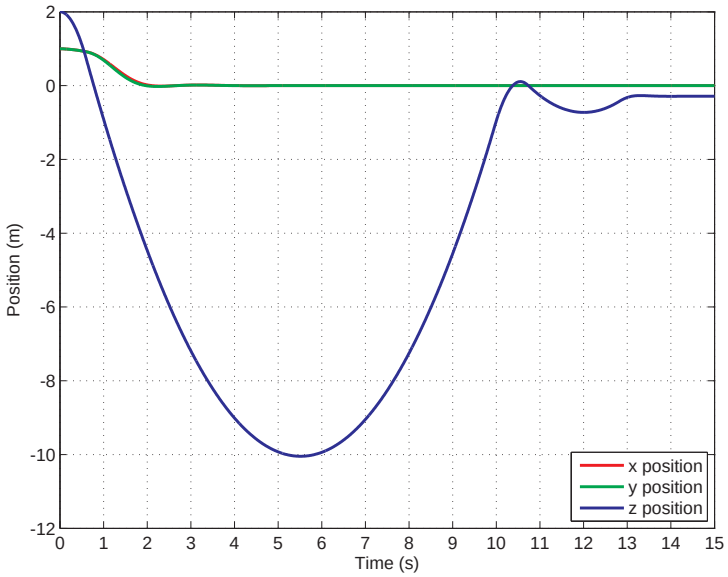

Figure 5.14: Stabilization behavior of the system with large total mass modeling error, $m_1 + m_2 = 1.4\ kg$.

Figure 5.14 shows the stabilization of the positional states when the total mass of the system is equal to $m_1 + m_2 = 1.4\ kg$. Not only does the system require approximately 14 seconds to stabilize the z state, the overshoot is equal to approximately 10 m. However, decreasing the quadrotor mass m_1 does not negatively affect the stabilizing performance of the quadrotor as long as there is no minimum thrust limit. A minimum thrust limit would result in an uncontrollable climb if the quadrotor mass is too low.

These results show that the controller can accommodate for significant modeling error in quadrotor mass and dynamic mass. Although increasing the total mass does not result in the system becoming uncontrollable, increasing the total mass reduces the performance of the vehicle.

The length between the quadrotor CG and the joint with the dynamic mass l_1 is difficult to measure or compute because the exact location of the quadrotor CG is hard to determine. Because l_1 is difficult to determine, the ability to compensate for modeling errors in l_1 is an important characteristic of the controller. Simulation results show that the controller has good tolerance for modeling errors in l_1. The controller remains effective even when $l_1 = -0.12$, or in other words the dynamic mass joint is 12 cm above the CG, which is practically impossible. The controller also remains effective up to $l_1 = 0.33$ m. The system response when $l_1 = 0.34$ m is shown in Figure 5.15.

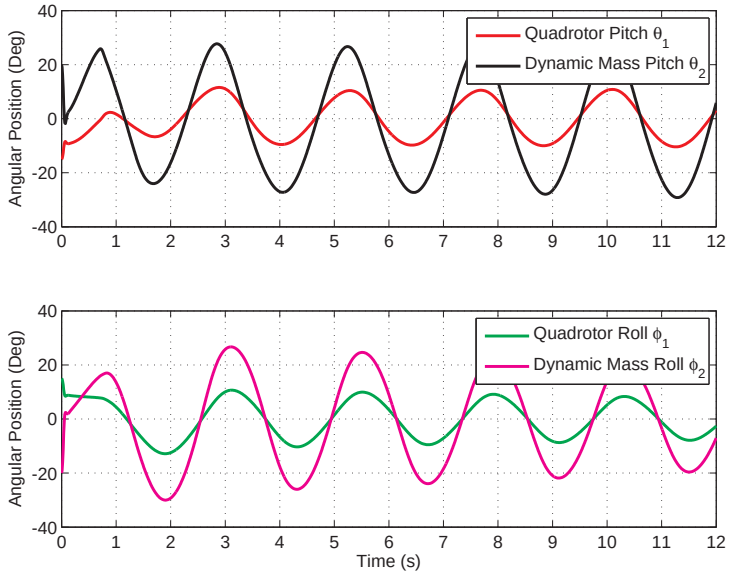

Figure 5.15: Stabilization behavior of the system when $l_1 = 0.34$ m.

These results show that the location of the of the dynamic mass joint does not

need to be extremely precise because the controller will compensate for the modeling error. This compensation is good because it reduces the need for determining the exact location of the quadrotor CG.

The final parameter varied in the robustness study is the length of the dynamic mass pendulum l_2. Increasing the length of the pendulum increases the stability of the vehicle, but in reality increasing the pendulum length increases the total vehicle weight. Additionally, a longer pendulum increases the servo torque required for dynamic mass actuation. Decreasing the pendulum length reduces the stability of the system.

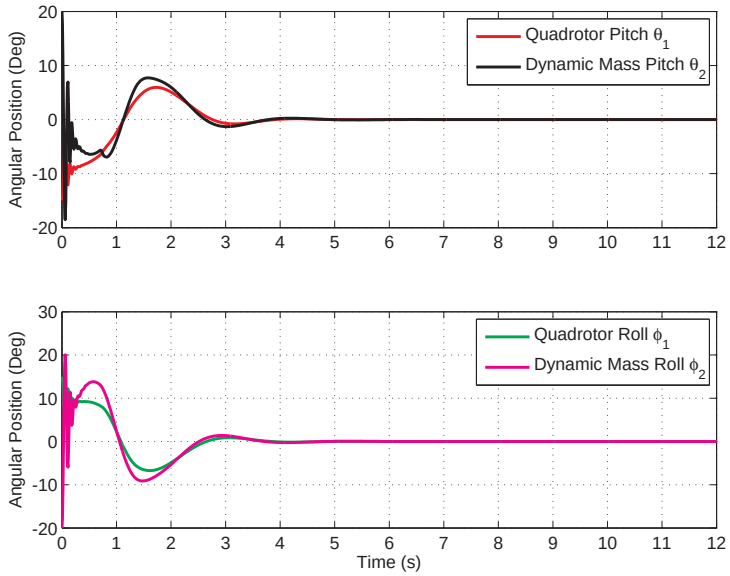

Figure 5.16: Stabilization behavior of the system when $l_2 = 0.056\ m$.

Figure 5.16 shows the system response when l_2 is decreased to $l_2 = 0.055\ m$. Decreasing l_2 any further results in the system becoming uncontrollable. The instabilities developing as a result of the decreased l_2 can be seen during the initial second of the stabilization maneuver above. Therefore the controller can compensate for decreased pendulum lengths up to 45% before the system becomes unstable.

The results of the robustness study show that the linear LQR controller has favorable robustness properties. The controller is able to compensate for significant modeling errors in various quadrotor parameters while keeping the system stable.

Chapter 6

CONCLUSIONS AND FUTURE WORK

With rising demand for UAVs and increasing UAV technology, the possible applications for unmanned vehicles are ever increasing. From military intelligence and reconnaissance missions, search and rescue, to civilian aerial photography, small UAVs will have a large presence in the future. With more UAVs flying there has been a considerable amount of research done around the globe exploring new control methods for these vehicles. In particular, quadrotor helicopters are a popular test bed for implementing new control methods. Using the hawkmoth and other biological examples as inspiration, the objective of this research was to apply dynamic inertia control to a quadrotor.

Dynamic inertia control was implemented on the quadrotor through the use of a dynamic mass mounted beneath the quadrotor. Similar to a pendulum, the dynamic mass was modeled as a point mass attached to the quadrotor by a mass-less rod with actuation in both the pitch and roll directions. Using Lagrangian mechanics, the equations of motion for the quadrotor with dynamic inertia were developed for a three dimensional model as well as a planar model in the $x,\ z$ plane.

Using small perturbation analysis, the nonlinear quadrotor models were linearized about a hovering flight condition. The linearized models were then used to develop linear LQR controllers utilizing dynamic inertia for control instead of the traditional differential thrust control methods. To evaluate the performance of the developed controllers, the linear controllers were simulated on the nonlinear models.

Results from the simulations showed that the linear controllers and dynamic inertia control provided good stabilization to the system. Not surprisingly, the angular

states required more time for stabilization than the positional states, but the vehicle was stabilized in under 4 seconds. Simulations were also conducted for a desired step response where the vehicle beginning from a hover moves 5 m in the x and y direction. Results from this simulation showed that the controller generated a favorable response for the vehicle during the maneuver. In addition, the simulation identified the situation requiring the maximum servo torque. Trajectory tracking performance was also evaluated for a simple trajectory resulting in maximum tracking errors of approximately 13%. When compared to trajectory tracking performance using differential thrust control methods, tracking errors generated from dynamic inertia control were significantly larger.

Finally, the robustness of the 3D linear controller was evaluated through parameter variations to simulate modeling error. Results of the robustness study showed that the linear controller has good robustness properties. The controller was able to compensate for large modeling errors in mass, length, and inertia values in order to stabilize the vehicle.

The results from this research showed promise that using a dynamic inertia for control is a viable control method for UAVs, but there is still future work to be done. Simulations on a full nonlinear model such as the simulations completed in this research are a great start. The next step is implementing the controller on a real quadrotor. To simplify the mechanical challenges of building a 2D pendulum, building a 1D pendulum that can be actuated in the pitch direction only should be the first step. Currently the Nonlinear Dynamics and Controls Lab at the University of Washington is testing a prototype dynamic mass control mechanism to be installed on an Ascending Technologies Hummingbird quadrotor in the future.

During the development of the equations of motion for the quadrotor with dynamic inertia, the values for the dynamic mass m_2 and pendulum length l_2 were chosen somewhat arbitrarily based on relative size of the quadrotor. Future work should include experimenting with different m_2 and l_2 values to find optimal values for the

vehicle.

Finally, developing nonlinear models for the quadrotor with dynamic inertia makes simulations for different controllers more accessible. Future work can also include developing new controllers using different methods from simple PID controllers, to more complicated nonlinear controllers. Simulations can then be conducted on the nonlinear model with the new controllers and compared to existing controllers to further improve future controllers.

BIBLIOGRAPHY

[1] U. S. Air Force Factsheets, "MQ-9 Reaper." www.af.mil/information/factsheets.

[2] U. Lance Cpl. Bernadette L. Ainsworth, "Mini-plane Newest Addition to Unmanned Family." www.defense.gov/transformation/articles/2005-10/ta101705a.html, October 2005.

[3] D. I. Daily, "A160 Hummingbird: Boeing's Variable-Rotor VTUAV." http://www.defenseindustrydaily.com/a160-hummingbird-boeings-variable-rotor-vtuav-03989/, January 2012.

[4] C. Dillow, "Marines in Afghanistan Execute the World's First Cargo Resupply with an Unmanned Helicopter," *Popular Mechanics*, December 2011.

[5] D. Preston, "Drones Take to American Skies on Police, Search Missions," *Bloomberg News*, May 2012.

[6] N. Wingfield and S. Sengupta, "Drones Set Sights on U.S. Skies," *New York Times*, February 2012.

[7] J. Hampton, "Flying Drone Gives Inside Scoop on Cathedral Damage," *3 News, New Zealand*, June 2011.

[8] U. G. Survey, "National Unmanned Aircraft Systems (UAS) Project Office." http://uas.usgs.gov/.

[9] N. Michael, D. Mellinger, Q. Lindsey, and V. Kumar, "The GRASP Multiple Micro-UAV Testbed," *Robotics Automation Magazine, IEEE*, vol. 17, pp. 56 –65, sept. 2010.

[10] D. Mellinger, N. Michael, and V. Kumar, "Trajectory Generation and Control for Precise Aggressive Maneuvers with Quadrotors," *The International Journal of Robotics Research*, vol. 31, no. 5, pp. 664–674, 2012.

[11] K. Oner, E. Cetinsoy, M. Unel, M. Aksit, I. Kandemir, and K. Gulez, "Dynamic Model and Control of a New Quadrotor Unmanned Aerial Vehicle with Tilt-Wing Mechanism," in *2008 International Conference on Control, Automation, Robotics, and Vision (ICCARV)*, November 2008.

[12] S. Bouabdallah, A. Noth, and R. Siegwart, "PID vs LQ Control Techniques Applied to an Indoor Micro Quadrotor," in *Intelligent Robots and Systems, 2004. (IROS 2004). Proceedings. 2004 IEEE/RSJ International Conference on*, vol. 3, pp. 2451 – 2456 vol.3, sept.-2 oct. 2004.

[13] S. Bouabdallah and R. Siegwart, "Backstepping and Sliding-mode Techniques Applied to an Indoor Micro Quadrotor," in *Robotics and Automation, 2005. ICRA 2005. Proceedings of the 2005 IEEE International Conference on*, pp. 2247 – 2252, april 2005.

[14] E. Altug, J. P. Ostrowski, and R. Mahony, "Control of a Quadrotor Helicopter Using Visual Feedback," in *Proceedings of the 2002 IEE International Conference on Robotics and Automation*, GRASP Lab. University of Pennsylvania, May 2002.

[15] D. Mellinger, Q. Lindsey, M. Shomin, and V. Kumar, "Design, Modeling, Estimation and Control for Aerial Grasping and Manipulation," in *2011 IEEE/RSJ International Conference on Intelligent Robots and Systems*, pp. 2668–2673, september 2011.

[16] I. Palunko, R. Fierro, and P. Cruz, "Trajectory Generation for Swing-Free Maneuvers of a Quadrotor with Suspended Payload: A Dynamic Programming Approach," in *Robotics and Automation (ICRA), 2012 IEEE International Conference on*, pp. 2691 –2697, may 2012.

[17] J. P. Dyhr, N. J. Cowan, D. J. Colmenares, K. A. Morgansen, and T. L. Daniel, "Autostabilizing Airframe Articulation: Animal Inspired Air Vehicle Control," in *51st IEEE Conference on Decision and Control*, University of Washington, March 2012.

[18] B. D. O. Anderson and J. B. Moore, *Optimal Control: Linear Quadratic Methods*. Mineola, NY, USA: Dover Publications, Inc., 2007.

Appendix A

LAGRANGIAN DYNAMICS

A.1 Canonical Momenta Time Derivatives

Below are all the time derivatives of the canonical momenta (3.9) referred to in Chapter 3.

With respect to the x direction,

$$\frac{d}{dt}\frac{\partial L}{\partial \dot{x}} = m_2 l_1 \cos\phi_1 \sin\theta_1 \dot{\theta}_1^2 + 2m_2 l_1 \cos\theta_1 \sin\phi_1 \dot{\theta}_1 \dot{\phi}_1 + m_2 l_1 \cos\phi_1 \sin\theta_1 \dot{\phi}_1^2$$
$$+ l_2 m_2 \cos\phi_2 \sin\theta_2 \dot{\theta}_2^2 + 2 l_2 m_2 \cos\theta_2 \sin\phi_2 \dot{\theta}_2 \dot{\phi}_2 + l_2 m_2 \cos\phi_2 \sin\theta_2 \dot{\phi}_2^2 + (m_1 + m_2)\ddot{x}$$
$$- l_1 m_2 \ddot{\theta}_1 \cos\theta_1 \cos\phi_1 - l_2 m_2 \ddot{\theta}_2 \cos\theta_2 \cos\phi_2 + l_1 m_2 \ddot{\phi}_1 \sin\theta_1 \sin\phi_1 + l_2 m_2 \ddot{\phi}_2 \sin\theta_2 \sin\phi_2 \ .$$

With respect to the y direction,

$$\frac{d}{dt}\frac{\partial L}{\partial \dot{y}} = -l_1 m_2 \cos\theta_1 \sin\phi_1 * \dot{\theta}_1^2 - 2 l_1 m_2 \cos\phi_1 \sin\theta_1 \dot{\theta}_1 \dot{\phi}_1 - l_1 m_2 \cos\theta_1 \sin\phi_1 \dot{\phi}_1^2$$
$$- l_2 m_2 \cos\theta_2 \sin\phi_2 \dot{\theta}_2^2 - 2 l_2 m_2 \cos\phi_2 \sin\theta_2 \dot{\theta}_2 \dot{\phi}_2 - l_2 m_2 \cos\theta_2 \sin\phi_2 \dot{\phi}_2^2 + m_1 \ddot{y} + m_2 \ddot{y}$$
$$+ l_1 m_2 \ddot{\phi}_1 \cos\theta_1 \cos\phi_1 + l_2 m_2 \ddot{\phi}_2 \cos\theta_2 \cos\phi_2 - l_1 m_2 \ddot{\theta}_1 \sin\theta_1 \sin\phi_1 - l_2 m_2 \ddot{\theta}_2 \sin\theta_2 \sin\phi_2 \ .$$

With respect to the z direction,

$$\frac{d}{dt}\frac{\partial L}{\partial \dot{z}} = l_1 m_2 \cos\theta_1 \cos\phi_1 \dot{\theta}_1^2 - 2 l_1 m_2 \sin\theta_1 \sin\phi_1 \dot{\theta}_1 \dot{\phi}_1 + l_1 m_2 \cos\theta_1 \cos\phi_1 \dot{\phi}_1^2$$
$$+ l_2 m_2 \cos\theta_2 \cos\phi_2 \dot{\theta}_2^2 - 2 l_2 m_2 \sin\theta_2 \sin\phi_2 \dot{\theta}_2 \dot{\phi}_2 + l_2 m_2 \cos\theta_2 \cos\phi_2 \dot{\phi}_2^2 + m_1 \ddot{z} + m_2 \ddot{z}$$
$$+ l_1 m_2 \ddot{\theta}_1 \cos\phi_1 \sin\theta_1 + l_1 m_2 \ddot{\phi}_1 \cos\theta_1 \sin\phi_1 + l_2 m_2 \ddot{\theta}_2 \cos\phi_2 \sin\theta_2 + l_2 m_2 \ddot{\phi}_2 \cos\theta_2 \sin\phi_2 \ .$$

With respect to the θ_1 direction,

$$\frac{d}{dt}\frac{\partial L}{\partial \dot{\theta}_1} = I_{1y}\ddot{\theta}_1 - l_1 m_2 \ddot{x}\cos\theta_1\cos\phi_1 + l_1 m_2 \ddot{z}\cos\phi_1\sin\theta_1 + l_1^2 m_2 \ddot{\theta}_1\cos^2\theta_1\cos^2\phi_1$$
$$-l_1 m_2 \ddot{y}\sin\theta_1\sin\phi_1 + l_1^2 m_2 \ddot{\theta}_1\cos^2\phi_1\sin^2\theta_1 + l_1^2 m_2 \ddot{\theta}_1\sin^2\theta_1\sin^2\phi_1 - l_1^2 m_2\cos\theta_1\cos^2\phi_1\sin\theta_1$$
$$\dot{\phi}_1^2 + 2l_1^2 m_2\cos\theta_1\sin\theta_1\sin^2\phi_1\dot{\theta}_1^2 + l_1^2 m_2\cos\theta_1\sin\theta_1\sin^2\phi_1\dot{\phi}_1^2 + l_1 m_2\cos\theta_1\cos\phi_1\dot{z}\dot{\theta}_1$$
$$+ l_1 m_2\cos\phi_1\sin\theta_1\dot{x}\dot{\theta}_1 + l_1 m_2\cos\theta_1\sin\phi_1\dot{x}\dot{\phi}_1$$
$$- l_1 m_2\cos\theta_1\sin\phi_1\dot{y}\dot{\theta}_1 - l_1 m_2\cos\phi_1\sin\theta_1\dot{y}\dot{\phi}_1$$
$$- l_1 m_2\sin\theta_1\sin\phi_1\dot{z}\dot{\phi}_1 - l_1^2 m_2\ddot{\phi}_1\cos\theta_1\cos\phi_1\sin\theta_1\sin\phi_1$$
$$- 3l_1^2 m_2\cos^2\theta_1\cos\phi_1\sin\phi_1\dot{\theta}_1\dot{\phi}_1 + l_1^2 m_2\cos\phi_1\sin\theta_1^2\sin\phi_1\dot{\theta}_1\dot{\phi}_1$$
$$- l_1 l_2 m_2\cos\theta_1\cos\phi_1\cos\phi_2\sin\theta_2\dot{\theta}_2^2 + l_1 l_2 m_2\cos\phi_1\cos\theta_2\cos\phi_2\sin\theta_1\dot{\theta}_2^2$$
$$- l_1 l_2 m_2\cos\theta_1\cos\phi_1\cos\phi_2\sin\theta_2\dot{\phi}_2^2 + l_1 l_2 m_2\cos\phi_1\cos\theta_2\cos\phi_2\sin\theta_1\dot{\phi}_2^2$$
$$+ l_1 l_2 m_2\ddot{\theta}_2\cos\theta_1\cos\phi_1\cos\theta_2\cos\phi_2 + l_1 l_2 m_2\cos\theta_2\sin\theta_1\sin\phi_1\sin\phi_2\dot{\theta}_2^2$$
$$+ l_1 l_2 m_2\cos\theta_2\sin\theta_1\sin\phi_1\sin\phi_2\dot{\phi}_2^2 + l_1 l_2 m_2\ddot{\theta}_2\cos\phi_1\cos\phi_2\sin\theta_1\sin\theta_2$$
$$- l_1 l_2 m_2\ddot{\phi}_2\cos\theta_1\cos\phi_1\sin\theta_2\sin\phi_2 + l_1 l_2 m_2\ddot{\phi}_2\cos\phi_1\cos\theta_2\sin\theta_1\sin\phi_2$$
$$- l_1 l_2 m_2\ddot{\phi}_2\cos\theta_2\cos\phi_2\sin\theta_1\sin\phi_1 + l_1 l_2 m_2\ddot{\theta}_2\sin\theta_1\sin\phi_1\sin\theta_2\sin\phi_2$$
$$+ l_1 l_2 m_2\cos\theta_1\cos\phi_1\cos\phi_2\sin\theta_2\dot{\theta}_1\dot{\theta}_2 - l_1 l_2 m_2\cos\phi_1\cos\theta_2\cos\phi_2\sin\theta_1\dot{\theta}_1\dot{\theta}_2$$
$$+ l_1 l_2 m_2\cos\theta_1\cos\phi_1\cos\theta_2\sin\phi_2\dot{\theta}_1\dot{\phi}_2 - l_1 l_2 m_2\cos\theta_1\cos\theta_2\cos\phi_2\sin\phi_1\dot{\theta}_1\dot{\phi}_2$$
$$- l_1 l_2 m_2\cos\theta_1\cos\theta_2\cos\phi_2\sin\phi_1\dot{\phi}_1\dot{\theta}_2 - l_1 l_2 m_2\cos\phi_1\cos\theta_2\cos\phi_2\sin\theta_1\dot{\phi}_1\dot{\phi}_2$$
$$- 2l_1 l_2 m_2\cos\theta_1\cos\phi_1\cos\theta_2\sin\phi_2\dot{\theta}_2\dot{\phi}_2 + l_1 l_2 m_2\cos\theta_1\sin\phi_1\sin\theta_2\sin\phi_2\dot{\theta}_1\dot{\theta}_2$$
$$+ l_1 l_2 m_2\cos\phi_1\sin\theta_1\sin\theta_2\sin\phi_2\dot{\theta}_1\dot{\phi}_2 + l_1 l_2 m_2\cos\phi_1\sin\theta_1\sin\theta_2\sin\phi_2\dot{\phi}_1\dot{\theta}_2$$
$$- l_1 l_2 m_2\cos\phi_2\sin\theta_1\sin\phi_1\sin\theta_2\dot{\phi}_1\dot{\theta}_2 + l_1 l_2 m_2\cos\theta_1\sin\phi_1\sin\theta_2\sin\phi_2\dot{\phi}_1\dot{\phi}_2$$
$$- l_1 l_2 m_2\cos\theta_2\sin\theta_1\sin\phi_1\sin\phi_2\dot{\phi}_1\dot{\phi}_2 - 2l_1 l_2 m_2\cos\phi_1\sin\theta_1\sin\theta_2\sin\phi_2\dot{\theta}_2\dot{\phi}_2$$
$$+ 2l_1 l_2 m_2\cos\phi_2\sin\theta_1\sin\phi_1\sin\theta_2\dot{\theta}_2\dot{\phi}_2 \ .$$

With respect to the ϕ_1 direction,

$$\begin{aligned}
\frac{d}{dt}\frac{\partial L}{\partial \dot{\phi}_1} &= I_{1x}\ddot{\phi}_1 + l_1 m_2 \ddot{y}\cos\theta_1\cos\phi_1 + l_1 m_2 \ddot{z}\cos\theta_1\sin\phi_1 + l_1^2 m_2 \ddot{\phi}_1\cos\theta_1^2\cos^2\phi_1 \\
&\quad + l_1 m_2 \ddot{x}\sin\theta_1\sin\phi_1 + l_1^2 m_2 \ddot{\phi}_1\cos^2\theta_1\sin^2\phi_1 + l_1^2 m_2 \ddot{\phi}_1\sin^2\theta_1\sin^2\phi_1 \\
&\quad - l_1^2 m_2\cos^2\theta_1\cos\phi_1\sin\phi_1\dot{\theta}_1^2 + l_1^2 m_2\cos\phi_1\sin^2\theta_1\sin\phi_1\dot{\theta}_1^2 + 2l_1^2 m_2\cos\phi_1\sin^2\theta_1\sin\phi_1\dot{\phi}_1^2 \\
&\quad + l_1 m_2\cos\theta_1\cos\phi_1\dot{z}\dot{\phi}_1 + l_1 m_2\cos\theta_1\sin\phi_1\dot{x}\dot{\theta}_1 + l_1 m_2\cos\phi_1\sin\theta_1\dot{x}\dot{\phi}_1 - l_1 m_2\cos\phi_1\sin\theta_1\dot{y}\dot{\theta}_1 \\
&\quad - l_1 m_2\cos\theta_1\sin\phi_1\dot{y}\dot{\phi}_1 - l_1 m_2\sin\theta_1\sin\phi_1\dot{z}\dot{\theta}_1 - l_1^2 m_2\ddot{\theta}_1\cos\theta_1\cos\phi_1\sin\theta_1\sin\phi_1 \\
&\quad - 3l_1^2 m_2\cos\theta_1\cos^2\phi_1\sin\theta_1\dot{\theta}_1\dot{\phi}_1 + l_1^2 m_2\cos\theta_1\sin\theta_1\sin^2\phi_1\dot{\theta}_1\dot{\phi}_1 \\
&\quad - l_1 l_2 m_2\cos\theta_1\cos\phi_1\cos\theta_2\sin\phi_2\dot{\theta}_2^2 + l_1 l_2 m_2\cos\theta_1\cos\theta_2\cos\phi_2\sin\phi_1\dot{\theta}_2^2 \\
&\quad - l_1 l_2 m_2\cos\theta_1\cos\phi_1\cos\theta_2\sin\phi_2\dot{\phi}_2^2 + l_1 l_2 m_2\cos\theta_1\cos\theta_2\cos\phi_2\sin\phi_1\dot{\phi}_2^2 \\
&\quad + l_1 l_2 m_2\ddot{\phi}_2\cos\theta_1\cos\phi_1\cos\theta_2\cos\phi_2 + l_1 l_2 m_2\cos\phi_2\sin\theta_1\sin\phi_1\sin\theta_2\dot{\theta}_2^2 \\
&\quad + l_1 l_2 m_2\cos\phi_2\sin\theta_1\sin\phi_1\sin\theta_2\dot{\phi}_2^2 - l_1 l_2 m_2\ddot{\theta}_2\cos\theta_1\cos\phi_1\sin\theta_2\sin\phi_2 \\
&\quad + l_1 l_2 m_2\ddot{\theta}_2\cos\theta_1\cos\phi_2\sin\phi_1\sin\theta_2 - l_1 l_2 m_2\ddot{\theta}_2\cos\theta_2\cos\phi_2\sin\theta_1\sin\phi_1 \\
&\quad + l_1 l_2 m_2\ddot{\phi}_2\cos\theta_1\cos\theta_2\sin\phi_1\sin\phi_2 + l_1 l_2 m_2\ddot{\phi}_2\sin\theta_1\sin\phi_1\sin\theta_2\sin\phi_2 \\
&\quad - l_1 l_2 m_2\cos\theta_1\cos\theta_2\cos\phi_2\sin\phi_1\dot{\theta}_1\dot{\theta}_2 + l_1 l_2 m_2\cos\theta_1\cos\phi_1\cos\phi_2\sin\theta_2\dot{\phi}_1\dot{\theta}_2 \\
&\quad - l_1 l_2 m_2\cos\phi_1\cos\theta_2\cos\phi_2\sin\theta_1\dot{\theta}_1\dot{\phi}_2 - l_1 l_2 m_2\cos\phi_1\cos\theta_2\cos\phi_2\sin\theta_1\dot{\phi}_1\dot{\theta}_2 \\
&\quad + l_1 l_2 m_2\cos\theta_1\cos\phi_1\cos\theta_2\sin\phi_2\dot{\phi}_1\dot{\phi}_2 - l_1 l_2 m_2\cos\theta_1\cos\theta_2\cos\phi_2\sin\phi_1\dot{\phi}_1\dot{\phi}_2 \\
&\quad - 2l_1 l_2 m_2\cos\theta_1\cos\phi_1\cos\phi_2\sin\theta_2\dot{\theta}_2\dot{\phi}_2 + l_1 l_2 m_2\cos\phi_1\sin\theta_1\sin\theta_2\sin\phi_2\dot{\theta}_1\dot{\theta}_2 \\
&\quad - l_1 l_2 m_2\cos\phi_2\sin\theta_1\sin\phi_1\sin\theta_2\dot{\theta}_1\dot{\theta}_2 + l_1 l_2 m_2\cos\theta_1\sin\phi_1\sin\theta_2\sin\phi_2\dot{\theta}_1\dot{\phi}_2 \\
&\quad + l_1 l_2 m_2\cos\theta_1\sin\phi_1\sin\theta_2\sin\phi_2\dot{\phi}_1\dot{\theta}_2 - l_1 l_2 m_2\cos\theta_2\sin\theta_1\sin\phi_1\sin\phi_2\dot{\theta}_1\dot{\phi}_2 \\
&\quad + l_1 l_2 m_2\cos\phi_1\sin\theta_1\sin\theta_2\sin\phi_2\dot{\phi}_1\dot{\phi}_2 - 2l_1 l_2 m_2\cos\theta_1\sin\phi_1\sin\theta_2\sin\phi_2\dot{\theta}_2\dot{\phi}_2 \\
&\quad + 2l_1 l_2 m_2\cos\theta_2\sin\theta_1\sin\phi_1\sin\phi_2\dot{\theta}_2\dot{\phi}_2 \ .
\end{aligned}$$

With respect to the ϕ_1 direction,

$$\frac{d}{dt}\frac{\partial L}{\partial \dot{\psi}_1} = I_{1z}\ddot{\psi}_1 \ .$$

With respect to the θ_2 direction,

$$\begin{aligned}
\frac{d}{dt}\frac{\partial L}{\partial \dot{\theta}_2} &= I_{2y}\ddot{\theta}_2 - l_2 m_2 \ddot{x}\cos\theta_2\cos\phi_2 + l_2 m_2 \ddot{z}\cos\phi_2\sin\theta_2 + l_2^2 m_2 \ddot{\theta}_2\cos^2\theta_2\cos^2\phi_2 \\
&\quad - l_2 m_2 \ddot{y}\sin\theta_2\sin\phi_2 + l_2^2 m_2 \ddot{\theta}_2\cos^2\phi_2\sin^2\theta_2 + l_2^2 m_2 \ddot{\theta}_2\sin^2\theta_2\sin^2\phi_2 \\
&\quad - l_2^2 m_2\cos\theta_2\cos^2\phi_2\sin\theta_2\dot{\phi}_2^2 + 2l_2^2 m_2\cos\theta_2\sin\theta_2\sin^2\phi_2\dot{\theta}_2^2 \\
&\quad + l_2^2 m_2\cos\theta_2\sin\theta_2\sin^2\phi_2\dot{\phi}_2^2 + l_2 m_2\cos\theta_2\cos\phi_2\dot{z}\dot{\theta}_2 + l_2 m_2\cos\phi_2\sin\theta_2\dot{x}\dot{\theta}_2 \\
&\quad + l_2 m_2\cos\theta_2\sin\phi_2\dot{x}\dot{\phi}_2 - l_2 m_2\cos\theta_2\sin\phi_2\dot{y}\dot{\theta}_2 - l_2 m_2\cos\phi_2\sin\theta_2\dot{y}\dot{\phi}_2 - l_2 m_2\sin\theta_2\sin\phi_2\dot{z}\dot{\phi}_2 \\
&\quad - l_2^2 m_2\ddot{\phi}_2\cos\theta_2\cos\phi_2\sin\theta_2\sin\phi_2 - 3l_2^2 m_2\cos^2\theta_2\cos\phi_2\sin\phi_2\dot{\theta}_2\dot{\phi}_2 \\
&\quad + l_2^2 m_2\cos\phi_2\sin^2\theta_2\sin\phi_2\dot{\theta}_2\dot{\phi}_2 + l_1 l_2 m_2\cos\theta_1\cos\phi_1\cos\phi_2\sin\theta_2\dot{\theta}_1^2 \\
&\quad - l_1 l_2 m_2\cos\phi_1\cos\theta_2\cos\phi_2\sin\theta_1\dot{\theta}_1^2 + l_1 l_2 m_2\cos\theta_1\cos\phi_1\cos\phi_2\sin\theta_2\dot{\phi}_1^2 \\
&\quad - l_1 l_2 m_2\cos\phi_1\cos\theta_2\cos\phi_2\sin\theta_1\dot{\phi}_1^2 + l_1 l_2 m_2\ddot{\theta}_1\cos\theta_1\cos\phi_1\cos\theta_2\cos\phi_2 \\
&\quad + l_1 l_2 m_2\cos\theta_1\sin\phi_1\sin\theta_2\sin\phi_2\dot{\theta}_1^2 + l_1 l_2 m_2\cos\theta_1\sin\phi_1\sin\theta_2\sin\phi_2\dot{\phi}_1^2 \\
&\quad + l_1 l_2 m_2\ddot{\theta}_1\cos\phi_1\cos\phi_2\sin\theta_1\sin\theta_2 - l_1 l_2 m_2\ddot{\phi}_1\cos\theta_1\cos\phi_1\sin\theta_2\sin\phi_2 \\
&\quad + l_1 l_2 m_2\ddot{\phi}_1\cos\theta_1\cos\phi_2\sin\phi_1\sin\theta_2 - l_1 l_2 m_2\ddot{\phi}_1\cos\theta_2\cos\phi_2\sin\theta_1\sin\phi_1 \\
&\quad + l_1 l_2 m_2\ddot{\theta}_1\sin\theta_1\sin\phi_1\sin\theta_2\sin\phi_2 - 2l_1 l_2 m_2\cos\theta_1\cos\theta_2\cos\phi_2\sin\phi_1\dot{\theta}_1\dot{\phi}_1 \\
&\quad - l_1 l_2 m_2\cos\theta_1\cos\phi_1\cos\phi_2\sin\theta_2\dot{\theta}_1\dot{\theta}_2 + l_1 l_2 m_2\cos\phi_1\cos\theta_2\cos\phi_2\sin\theta_1\dot{\theta}_1\dot{\theta}_2 \\
&\quad - l_1 l_2 m_2\cos\theta_1\cos\phi_1\cos\theta_2\sin\phi_2\dot{\theta}_1\dot{\phi}_2 - l_1 l_2 m_2\cos\theta_1\cos\phi_1\cos\theta_2\sin\phi_2\dot{\phi}_1\dot{\theta}_2 \\
&\quad + l_1 l_2 m_2\cos\theta_1\cos\theta_2\cos\phi_2\sin\phi_1\dot{\phi}_1\dot{\theta}_2 - l_1 l_2 m_2\cos\theta_1\cos\phi_1\cos\phi_2\sin\theta_2\dot{\phi}_1\dot{\phi}_2 \\
&\quad + 2l_1 l_2 m_2\cos\phi_1\sin\theta_1\sin\theta_2\sin\phi_2\dot{\theta}_1\dot{\phi}_1 - 2l_1 l_2 m_2\cos\phi_2\sin\theta_1\sin\phi_1\sin\theta_2\dot{\theta}_1\dot{\phi}_1 \\
&\quad + l_1 l_2 m_2\cos\theta_2\sin\theta_1\sin\phi_1\sin\phi_2\dot{\theta}_1\dot{\theta}_2 - l_1 l_2 m_2\cos\phi_1\sin\theta_1\sin\theta_2\sin\phi_2\dot{\theta}_1\dot{\phi}_2 \\
&\quad + l_1 l_2 m_2\cos\phi_2\sin\theta_1\sin\phi_1\sin\theta_2\dot{\theta}_1\dot{\phi}_2 + l_1 l_2 m_2\cos\phi_2\sin\theta_1\sin\phi_1\sin\theta_2\dot{\phi}_1\dot{\theta}_2 \\
&\quad - l_1 l_2 m_2\cos\theta_1\sin\phi_1\sin\theta_2\sin\phi_2\dot{\phi}_1\dot{\phi}_2 + l_1 l_2 m_2\cos\theta_2\sin\theta_1\sin\phi_1\sin\phi_2\dot{\phi}_1\dot{\phi}_2 \ .
\end{aligned}$$

With respect to the ϕ_2 direction,

$$\begin{aligned}
\frac{d}{dt}\frac{\partial L}{\partial \dot{\phi}_2} &= I_{2x}\ddot{\phi}_2 + l_2 m_2 \ddot{y}\cos\theta_2\cos\phi_2 + l_2 m_2 \ddot{z}\cos\theta_2\sin\phi_2 + l_2^2 m_2 \ddot{\phi}_2\cos^2\theta_2\cos^2\phi_2 \\
&\quad + l_2 m_2 \ddot{x}\sin\theta_2\sin\phi_2 + l_2^2 m_2 \ddot{\phi}_2\cos^2\theta_2\sin^2\phi_2 + l_2^2 m_2 \ddot{\phi}_2\sin^2\theta_2\sin^2\phi_2 \\
&\quad - l_2^2 m_2\cos^2\theta_2\cos\phi_2\sin\phi_2\dot{\theta}_2^2 + l_2^2 m_2\cos\phi_2\sin^2\theta_2\sin\phi_2\dot{\theta}_2^2 + 2l_2^2 m_2\cos\phi_2\sin^2\theta_2\sin\phi_2\dot{\phi}_2^2 \\
&\quad + l_2 m_2\cos\theta_2\cos\phi_2\dot{z}\dot{\phi}_2 + l_2 m_2\cos\theta_2\sin\phi_2\dot{x}\dot{\theta}_2 + l_2 m_2\cos\phi_2\sin\theta_2\dot{x}\dot{\phi}_2 - l_2 m_2\cos\phi_2\sin\theta_2\dot{y}\dot{\theta}_2 \\
&\quad - l_2 m_2\cos\theta_2\sin\phi_2\dot{y}\dot{\phi}_2 - l_2 m_2\sin\theta_2\sin\phi_2\dot{z}\dot{\theta}_2 - l_2^2 m_2\ddot{\theta}_2\cos\theta_2\cos\phi_2\sin\theta_2\sin\phi_2 \\
&\quad - 3l_2^2 m_2\cos\theta_2\cos^2\phi_2\sin\theta_2\dot{\theta}_2\dot{\phi}_2 + l_2^2 m_2\cos\theta_2\sin\theta_2\sin^2\phi_2\dot{\theta}_2\dot{\phi}_2 \\
&\quad + l_1 l_2 m_2\cos\theta_1\cos\phi_1\cos\theta_2\sin\phi_2\dot{\theta}_1^2 - l_1 l_2 m_2\cos\theta_1\cos\theta_2\cos\phi_2\sin\phi_1\dot{\theta}_1^2 \\
&\quad + l_1 l_2 m_2\cos\theta_1\cos\phi_1\cos\theta_2\sin\phi_2\dot{\phi}_1^2 - l_1 l_2 m_2\cos\theta_1\cos\theta_2\cos\phi_2\sin\phi_1\dot{\phi}_1^2 \\
&\quad + l_1 l_2 m_2\ddot{\phi}_1\cos\theta_1\cos\phi_1\cos\theta_2\cos\phi_2 + l_1 l_2 m_2\cos\phi_1\sin\theta_1\sin\theta_2\sin\phi_2\dot{\theta}_1^2 \\
&\quad + l_1 l_2 m_2\cos\phi_1\sin\theta_1\sin\theta_2\sin\phi_2\dot{\phi}_1^2 - l_1 l_2 m_2\ddot{\theta}_1\cos\theta_1\cos\phi_1\sin\theta_2\sin\phi_2 \\
&\quad + l_1 l_2 m_2\ddot{\theta}_1\cos\phi_1\cos\theta_2\sin\theta_1\sin\phi_2 - l_1 l_2 m_2\ddot{\theta}_1\cos\theta_2\cos\phi_2\sin\theta_1\sin\phi_1 \\
&\quad + l_1 l_2 m_2\ddot{\phi}_1\cos\theta_1\cos\theta_2\sin\phi_1\sin\phi_2 + l_1 l_2 m_2\ddot{\phi}_1\sin\theta_1\sin\phi_1\sin\theta_2\sin\phi_2 \\
&\quad - 2l_1 l_2 m_2\cos\phi_1\cos\theta_2\cos\phi_2\sin\theta_1\dot{\theta}_1\dot{\phi}_1 - l_1 l_2 m_2\cos\theta_1\cos\phi_1\cos\theta_2\sin\phi_2\dot{\theta}_1\dot{\theta}_2 \\
&\quad - l_1 l_2 m_2\cos\theta_1\cos\phi_1\cos\phi_2\sin\theta_2\dot{\theta}_1\dot{\phi}_2 - l_1 l_2 m_2\cos\theta_1\cos\phi_1\cos\phi_2\sin\theta_2\dot{\phi}_1\dot{\theta}_2 \\
&\quad + l_1 l_2 m_2\cos\phi_1\cos\theta_2\cos\phi_2\sin\theta_1\dot{\theta}_1\dot{\phi}_2 - l_1 l_2 m_2\cos\theta_1\cos\phi_1\cos\theta_2\sin\phi_2\dot{\phi}_1\dot{\phi}_2 \\
&\quad + l_1 l_2 m_2\cos\theta_1\cos\theta_2\cos\phi_2\sin\phi_1\dot{\phi}_1\dot{\phi}_2 + 2l_1 l_2 m_2\cos\theta_1\sin\phi_1\sin\theta_2\sin\phi_2\dot{\theta}_1\dot{\phi}_1 \\
&\quad - 2l_1 l_2 m_2\cos\theta_2\sin\theta_1\sin\phi_1\sin\phi_2\dot{\theta}_1\dot{\phi}_1 - l_1 l_2 m_2\cos\phi_1\sin\theta_1\sin\theta_2\sin\phi_2\dot{\theta}_1\dot{\theta}_2 \\
&\quad + l_1 l_2 m_2\cos\phi_2\sin\theta_1\sin\phi_1\sin\theta_2\dot{\theta}_1\dot{\theta}_2 - l_1 l_2 m_2\cos\theta_1\sin\phi_1\sin\theta_2\sin\phi_2\dot{\phi}_1\dot{\theta}_2 \\
&\quad + l_1 l_2 m_2\cos\theta_2\sin\theta_1\sin\phi_1\sin\phi_2\dot{\theta}_1\dot{\phi}_2 + l_1 l_2 m_2\cos\theta_2\sin\theta_1\sin\phi_1\sin\phi_2\dot{\phi}_1\dot{\theta}_2 \\
&\quad + l_1 l_2 m_2\cos\phi_2\sin\theta_1\sin\phi_1\sin\theta_2\dot{\phi}_1\dot{\phi}_2 \ .
\end{aligned}$$

A.2 Canonical Forces

Below are all the computed canonical forces (3.10) referred in the Chapter 3.

With respect to the x direction,

$$\frac{\partial L}{\partial x} = 0 \ . \tag{A.1}$$

With respect to the y direction,

$$\frac{\partial L}{\partial y} = 0 \ . \tag{A.2}$$

With respect to the z direction,

$$\frac{\partial L}{\partial z} = -gm_1 - gm_2 \ . \tag{A.3}$$

With respect to the θ_1 direction,

$$\begin{aligned}
\frac{\partial L}{\partial \theta_1} &= l_1^2 m_2 \dot{\theta}_1^2 \cos\theta_1 \sin\theta_1 \sin^2\phi_1 - l_1^2 m_2 \dot{\phi}_1^2 \cos\theta_1 \cos^2\phi_1 \sin(\theta_1) - g l_1 m_2 \cos\phi_1 \sin\theta_1 \\
&+ l_1 m_2 \dot{z}\dot{\theta}_1 \cos\theta_1 \cos\phi_1 + l_1 m_2 \dot{x}\dot{\theta}_1 \cos\phi_1 \sin\theta_1 + l_1 m_2 \dot{x}\dot{\phi}_1 \cos\theta_1 \sin\phi_1 - l_1 m_2 \dot{y}\dot{\theta}_1 \cos\theta_1 \sin\phi_1 \\
&- l_1 m_2 \dot{y}\dot{\phi}_1 \cos\phi_1 \sin\theta_1 - l_1 m_2 \dot{z}\dot{\phi}_1 \sin\theta_1 \sin\phi_1 - l_1^2 m_2 \dot{\theta}_1 \dot{\phi}_1 \cos^2\theta_1 \cos\phi_1 \sin\phi_1 \\
&+ l_1^2 m_2 \dot{\theta}_1 \dot{\phi}_1 \cos\phi_1 \sin^2\theta_1 \sin\phi_1 + l_1 l_2 m_2 \dot{\theta}_1 \dot{\theta}_2 \cos\theta_1 \sin\phi_1 \sin\theta_2 \sin\phi_2 \\
&+ l_1 l_2 m_2 \dot{\theta}_1 \dot{\phi}_2 \cos\phi_1 \sin\theta_1 \sin\theta_2 \sin\phi_2 + l_1 l_2 m_2 \dot{\phi}_1 \dot{\theta}_2 \cos\phi_1 \sin\theta_1 \sin\theta_2 \sin\phi_2 \\
&- l_1 l_2 m_2 \dot{\phi}_1 \dot{\theta}_2 \cos\phi_2 \sin\theta_1 \sin\phi_1 \sin\theta_2 + l_1 l_2 m_2 \dot{\phi}_1 \dot{\phi}_2 \cos\theta_1 \sin\phi_1 \sin\theta_2 \sin\phi_2 \\
&- l_1 l_2 m_2 \dot{\phi}_1 \dot{\phi}_2 \cos\theta_2 \sin\theta_1 \sin\phi_1 \sin\phi_2 + l_1 l_2 m_2 \dot{\theta}_1 \dot{\theta}_2 \cos\theta_1 \cos\phi_1 \cos\phi_2 \sin\theta_2 \\
&- l_1 l_2 m_2 \dot{\theta}_1 \dot{\theta}_2 \cos\phi_1 \cos\theta_2 \cos\phi_2 \sin\theta_1 + l_1 l_2 m_2 \dot{\theta}_1 \dot{\phi}_2 \cos\theta_1 \cos\phi_1 \cos\theta_2 \sin\phi_2 \\
&- l_1 l_2 m_2 \dot{\theta}_1 \dot{\phi}_2 \cos\theta_1 \cos\theta_2 \cos\phi_2 \sin\phi_1 - l_1 l_2 m_2 \dot{\phi}_1 \dot{\theta}_2 \cos\theta_1 \cos\theta_2 \cos\phi_2 \sin\phi_1 \\
&- l_1 l_2 m_2 \dot{\phi}_1 \dot{\phi}_2 \cos\phi_1 \cos\theta_2 \cos\phi_2 \sin\theta_1 \ .
\end{aligned} \tag{A.4}$$

With respect to the ϕ_1 direction,

$$\begin{aligned}\frac{\partial L}{\partial \phi_1} &= l_1^2 m_2 \dot{\phi}_1^2 \cos\phi_1 \sin^2\theta_1 \sin\phi_1 - l_1^2 m_2 \dot{\theta}_1^2 \cos^2\theta_1 \cos\phi_1 \sin\phi_1 - g l_1 m_2 \cos\theta_1 \sin\phi_1 \\ &+ l_1 m_2 \dot{z}\dot{\phi}_1 \cos\theta_1 \cos\phi_1 + l_1 m_2 \dot{x}\dot{\theta}_1 \cos\theta_1 \sin\phi_1 + l_1 m_2 \dot{x}\dot{\phi}_1 \cos\phi_1 \sin\theta_1 - l_1 m_2 \dot{y}\dot{\theta}_1 \cos\phi_1 \sin\theta_1 \\ &- l_1 m_2 \dot{y}\dot{\phi}_1 \cos\theta_1 \sin\phi_1 - l_1 m_2 \dot{z}\dot{\theta}_1 \sin\theta_1 \sin\phi_1 - l_1^2 m_2 \dot{\theta}_1 \dot{\phi}_1 \cos\theta_1 \cos^2\phi_1 \sin\theta_1 \\ &+ l_1^2 m_2 \dot{\theta}_1 \dot{\phi}_1 \cos\theta_1 \sin\theta_1 \sin^2\phi_1 + l_1 l_2 m_2 \dot{\theta}_1 \dot{\theta}_2 \cos\phi_1 \sin\theta_1 \sin\theta_2 \sin\phi_2 \\ &- l_1 l_2 m_2 \dot{\theta}_1 \dot{\theta}_2 \cos\phi_2 \sin\theta_1 \sin\phi_1 \sin\theta_2 + l_1 l_2 m_2 \dot{\theta}_1 \dot{\phi}_2 \cos\theta_1 \sin\phi_1 \sin\theta_2 \sin\phi_2 \\ &- l_1 l_2 m_2 \dot{\theta}_1 \dot{\phi}_2 \cos\theta_2 \sin\theta_1 \sin\phi_1 \sin\phi_2 + l_1 l_2 m_2 \dot{\phi}_1 \dot{\theta}_2 \cos\theta_1 \sin\phi_1 \sin\theta_2 \sin\phi_2 \\ &+ l_1 l_2 m_2 \dot{\phi}_1 \dot{\phi}_2 \cos\phi_1 \sin\theta_1 \sin\theta_2 \sin\phi_2 - l_1 l_2 m_2 \dot{\theta}_1 \dot{\theta}_2 \cos\theta_1 \cos\theta_2 \cos\phi_2 \sin\phi_1 \\ &- l_1 l_2 m_2 \dot{\theta}_1 \dot{\phi}_2 \cos\phi_1 \cos\theta_2 \cos\phi_2 \sin\theta_1 + l_1 l_2 m_2 \dot{\phi}_1 \dot{\theta}_2 \cos\theta_1 \cos\phi_1 \cos\phi_2 \sin\theta_2 \\ &- l_1 l_2 m_2 \dot{\phi}_1 \dot{\theta}_2 \cos\phi_1 \cos\theta_2 \cos\phi_2 \sin\theta_1 + l_1 l_2 m_2 \dot{\phi}_1 \dot{\phi}_2 \cos\theta_1 \cos\phi_1 \cos\theta_2 \sin\phi_2 \\ &- l_1 l_2 m_2 \dot{\phi}_1 \dot{\phi}_2 \cos\theta_1 \cos\theta_2 \cos\phi_2 \sin\phi_1 \ . \end{aligned} \tag{A.5}$$

With respect to the ψ_1 direction,

$$\frac{\partial L}{\partial \psi_1} = 0 \ . \tag{A.6}$$

With respect to the θ_2 direction,

$$\frac{\partial L}{\partial \theta_2} = l_2^2 m_2 \dot{\theta}_2^2 \cos\theta_2 \sin\theta_2 \sin^2\phi_2 - l_2^2 m_2 \dot{\phi}_2^2 \cos\theta_2 \cos^2\phi_2 \sin\theta_2 - g l_2 m_2 \cos\phi_2 \sin\theta_2$$
$$+ l_2 m_2 \dot{z}\dot{\theta}_2 \cos\theta_2 \cos\phi_2 + l_2 m_2 \dot{x}\dot{\theta}_2 \cos\phi_2 \sin\theta_2 + l_2 m_2 \dot{x}\dot{\phi}_2 \cos\theta_2 \sin\phi_2 - l_2 m_2 \dot{y}\dot{\theta}_2 \cos\theta_2 \sin\phi_2$$
$$- l_2 m_2 \dot{y}\dot{\phi}_2 \cos\phi_2 \sin\theta_2 - l_2 m_2 \dot{z}\dot{\phi}_2 \sin\theta_2 \sin\phi_2 - l_2^2 m_2 \dot{\theta}_2 \dot{\phi}_2 \cos^2\theta_2 \cos\phi_2 \sin\phi_2$$
$$+ l_2^2 m_2 \dot{\theta}_2 \dot{\phi}_2 \cos\phi_2 \sin^2\theta_2 \sin\phi_2 + l_1 l_2 m_2 \dot{\theta}_1 \dot{\theta}_2 \cos\theta_2 \sin\theta_1 \sin\phi_1 \sin\phi_2$$
$$- l_1 l_2 m_2 \dot{\theta}_1 \dot{\phi}_2 \cos\phi_1 \sin\theta_1 \sin\theta_2 \sin\phi_2 + l_1 l_2 m_2 \dot{\theta}_1 \dot{\phi}_2 \cos\phi_2 \sin\theta_1 \sin\phi_1 \sin\theta_2$$
$$+ l_1 l_2 m_2 \dot{\phi}_1 \dot{\theta}_2 \cos\phi_2 \sin\theta_1 \sin\phi_1 \sin\theta_2 - l_1 l_2 m_2 \dot{\phi}_1 \dot{\phi}_2 \cos\theta_1 \sin\phi_1 \sin\theta_2 \sin\phi_2$$
$$+ l_1 l_2 m_2 \dot{\phi}_1 \dot{\phi}_2 \cos\theta_2 \sin\theta_1 \sin\phi_1 \sin\phi_2 - l_1 l_2 m_2 \dot{\theta}_1 \dot{\theta}_2 \cos\theta_1 \cos\phi_1 \cos\phi_2 \sin\theta_2$$
$$+ l_1 l_2 m_2 \dot{\theta}_1 \dot{\theta}_2 \cos\phi_1 \cos\theta_2 \cos\phi_2 \sin\theta_1 - l_1 l_2 m_2 \dot{\theta}_1 \dot{\phi}_2 \cos\theta_1 \cos\phi_1 \cos\theta_2 \sin\phi_2$$
$$- l_1 l_2 m_2 \dot{\phi}_1 \dot{\theta}_2 \cos\theta_1 \cos\phi_1 \cos\theta_2 \sin\phi_2 + l_1 l_2 m_2 \dot{\phi}_1 \dot{\theta}_2 \cos\theta_1 \cos\theta_2 \cos\phi_2 \sin\phi_1$$
$$- l_1 l_2 m_2 \dot{\phi}_1 \dot{\phi}_2 \cos\theta_1 \cos\phi_1 \cos\phi_2 \sin\theta_2 \ . \quad \text{(A.7)}$$

With respect to the ϕ_2 direction,

$$\frac{\partial L}{\partial \phi_2} = l_2^2 m_2 \dot{\phi}_2^2 \cos\phi_2 \sin^2\theta_2 \sin\phi_2 - l_2^2 m_2 \dot{\theta}_2^2 \cos^2\theta_2 \cos\phi_2 \sin\phi_2 - g l_2 m_2 \cos\theta_2 \sin\phi_2$$
$$+ l_2 m_2 \dot{z}\dot{\phi}_2 \cos\theta_2 \cos\phi_2 + l_2 m_2 \dot{x}\dot{\theta}_2 \cos\theta_2 \sin\phi_2 + l_2 m_2 \dot{x}\dot{\phi}_2 \cos\phi_2 \sin\theta_2 - l_2 m_2 \dot{y}\dot{\theta}_2 \cos\phi_2 \sin\theta_2$$
$$- l_2 m_2 \dot{y}\dot{\phi}_2 \cos\theta_2 \sin\phi_2 - l_2 m_2 \dot{z}\dot{\theta}_2 \sin\theta_2 \sin\phi_2 - l_2^2 m_2 \dot{\theta}_2 \dot{\phi}_2 \cos\theta_2 \cos^2\phi_2 \sin\theta_2$$
$$+ l_2^2 m_2 \dot{\theta}_2 \dot{\phi}_2 \cos\theta_2 \sin\theta_2 \sin^2\phi_2 - l_1 l_2 m_2 \dot{\theta}_1 \dot{\theta}_2 \cos\phi_1 \sin\theta_1 \sin\theta_2 \sin\phi_2$$
$$+ l_1 l_2 m_2 \dot{\theta}_1 \dot{\theta}_2 \cos\phi_2 \sin\theta_1 \sin\phi_1 \sin\theta_2 + l_1 l_2 m_2 \dot{\theta}_1 \dot{\phi}_2 \cos\theta_2 \sin\theta_1 \sin\phi_1 \sin\phi_2$$
$$- l_1 l_2 m_2 \dot{\phi}_1 \dot{\theta}_2 \cos\theta_1 \sin\phi_1 \sin\theta_2 \sin\phi_2 + l_1 l_2 m_2 \dot{\phi}_1 \dot{\theta}_2 \cos\theta_2 \sin\theta_1 \sin\phi_1 \sin\phi_2$$
$$+ l_1 l_2 m_2 \dot{\phi}_1 \dot{\phi}_2 \cos\phi_2 \sin\theta_1 \sin\phi_1 \sin\theta_2 - l_1 l_2 m_2 \dot{\theta}_1 \dot{\theta}_2 \cos\theta_1 \cos\phi_1 \cos\theta_2 \sin\phi_2$$
$$- l_1 l_2 m_2 \dot{\theta}_1 \dot{\phi}_2 \cos\theta_1 \cos\phi_1 \cos\phi_2 \sin\theta_2 + l_1 l_2 m_2 \dot{\theta}_1 \dot{\phi}_2 \cos\phi_1 \cos\theta_2 \cos\phi_2 \sin\theta_1$$
$$- l_1 l_2 m_2 \dot{\phi}_1 \dot{\theta}_2 \cos\theta_1 \cos\phi_1 \cos\phi_2 \sin\theta_2 - l_1 l_2 m_2 \dot{\phi}_1 \dot{\phi}_2 \cos\theta_1 \cos\phi_1 \cos\theta_2 \sin\phi_2$$
$$+ l_1 l_2 m_2 \dot{\phi}_1 \dot{\phi}_2 \cos\theta_1 \cos\theta_2 \cos\phi_2 \sin\phi_1 \ . \quad \text{(A.8)}$$

A.3 3D Equations of Motion

The equations below are the nonlinear equations of motion for the 3D quadrotor with dynamic inertia referred to in Chapter 3.

With respect to the x direction,

$$\begin{aligned} &l_1 m_2 \cos\phi_1 \sin\theta_1 \dot{\theta}_1^2 + 2 l_1 m_2 \cos\theta_1 \sin\phi_1 \dot{\theta}_1 \dot{\phi}_1 + l_1 m_2 \cos\phi_1 \sin\theta_1 \dot{\phi}_1^2 \\ &+ l_2 m_2 \cos\phi_2 \sin\theta_2 \dot{\theta}_2^2 + 2 l_2 m_2 \cos\theta_2 \sin\phi_2 \dot{\theta}_2 \dot{\phi}_2 + l_2 m_2 \cos\phi_2 \sin\theta_2 \dot{\phi}_2^2 + m_1 \ddot{x} + m_2 \ddot{x} \\ &- l_1 m_2 \ddot{\theta}_1 \cos\theta_1 \cos\phi_1 - l_2 m_2 \ddot{\theta}_2 \cos\theta_2 \cos\phi_2 + l_1 m_2 \ddot{\phi}_1 \sin\theta_1 \sin\phi_1 + l_2 m_2 \ddot{\phi}_2 \sin\theta_2 \sin\phi_2 \\ &= u1 \sin\theta_1 \cos\phi_1 \cos(\psi_1) \end{aligned} \quad \text{(A.9)}$$

In the y direction,

$$\begin{aligned} &- l_1 m_2 \cos\theta_1 \sin\phi_1 \dot{\theta}_1^2 - 2 l_1 m_2 \cos\phi_1 \sin\theta_1 \dot{\theta}_1 \dot{\phi}_1 - l_1 m_2 \cos\theta_1 \sin\phi_1 \dot{\phi}_1^2 \\ &- l_2 m_2 \cos\theta_2 \sin\phi_2 \dot{\theta}_2^2 - 2 l_2 m_2 \cos\phi_2 \sin\theta_2 \dot{\theta}_2 \dot{\phi}_2 - l_2 m_2 \cos\theta_2 \sin\phi_2 \dot{\phi}_2^2 + m_1 \ddot{y} + m_2 \ddot{y} \\ &+ l_1 m_2 \ddot{\phi}_1 \cos\theta_1 \cos\phi_1 + l_2 m_2 \ddot{\phi}_2 \cos\theta_2 \cos\phi_2 - l_1 m_2 \ddot{\theta}_1 \sin\theta_1 \sin\phi_1 - l_2 m_2 \ddot{\theta}_2 \sin\theta_2 \sin\phi_2 \\ &= -u1 \cos\theta_1 \sin\phi_1 \cos(\psi_1) \end{aligned} \quad \text{(A.10)}$$

In the z direction,

$$\begin{aligned} &l_1 m_2 \cos\theta_1 \cos\phi_1 \dot{\theta}_1^2 - 2 l_1 m_2 \sin\theta_1 \sin\phi_1 \dot{\theta}_1 \dot{\phi}_1 + l_1 m_2 \cos\theta_1 \cos\phi_1 \dot{\phi}_1^2 \\ &+ l_2 m_2 \cos\theta_2 \cos\phi_2 \dot{\theta}_2^2 - 2 l_2 m_2 \sin\theta_2 \sin\phi_2 \dot{\theta}_2 \dot{\phi}_2 + l_2 m_2 \cos\theta_2 \cos\phi_2 \dot{\phi}_2^2 \\ &+ g m_1 + g m_2 + m_1 \ddot{z} + m_2 \ddot{z} + l_1 m_2 \ddot{\theta}_1 \cos\phi_1 \sin\theta_1 + l_1 m_2 \ddot{\phi}_1 \cos\theta_1 \sin\phi_1 \\ &+ l_2 m_2 \ddot{\theta}_2 \cos\phi_2 \sin\theta_2 + l_2 m_2 \ddot{\phi}_2 \cos\theta_2 \sin\phi_2 = u1 \cos\theta_1 \cos\phi_1 \end{aligned} \quad \text{(A.11)}$$

In the ψ_1 direction,

$$I_{1z} \ddot{\psi}_1 = u(4) \quad \text{(A.12)}$$

In the θ_1 direction,

$$
\begin{aligned}
&I_{1y}\ddot{\theta}_1 - l_1 m_2 \ddot{x}\cos\theta_1\cos\phi_1 + g l_1 m_2 \cos\phi_1\sin\theta_1 + l_1 m_2 \ddot{z}\cos\phi_1\sin\theta_1 + l_1^2 m_2 \ddot{\theta}_1\cos^2\theta_1\cos^2\phi_1 \\
&- l_1 m_2 \ddot{y}\sin\theta_1\sin\phi_1 + l_1^2 m_2 \ddot{\theta}_1\cos^2\phi_1\sin^2\theta_1 + l_1^2 m_2 \ddot{\theta}_1\sin^2\theta_1\sin^2\phi_1 + l_1^2 m_2 \dot{\theta}_1^2\cos\theta_1\sin\theta_1\sin^2\phi_1 \\
&+ l_1^2 m_2 \dot{\phi}_1^2\cos\theta_1\sin\theta_1\sin^2\phi_1 - 2 l_1^2 m_2 \dot{\theta}_1\dot{\phi}_1\cos^2\theta_1\cos\phi_1\sin\phi_1 - l_1^2 m_2 \ddot{\phi}_1\cos\theta_1\cos\phi_1\sin\theta_1\sin\phi_1 \\
&+ l_1 l_2 m_2 \ddot{\theta}_2\cos\theta_1\cos\phi_1\cos\theta_2\cos\phi_2 + l_1 l_2 m_2 \ddot{\theta}_2\cos\phi_1\cos\phi_2\sin\theta_1\sin\theta_2 \\
&- l_1 l_2 m_2 \ddot{\phi}_2\cos\theta_1\cos\phi_1\sin\theta_2\sin\phi_2 + l_1 l_2 m_2 \ddot{\phi}_2\cos\phi_1\cos\theta_2\sin\theta_1\sin\phi_2 \\
&- l_1 l_2 m_2 \ddot{\phi}_2\cos\theta_2\cos\phi_2\sin\theta_1\sin\phi_1 + l_1 l_2 m_2 \ddot{\theta}_2\sin\theta_1\sin\phi_1\sin\theta_2\sin\phi_2 \\
&- l_1 l_2 m_2 \dot{\theta}_2^2\cos\theta_1\cos\phi_1\cos\phi_2\sin\theta_2 + l_1 l_2 m_2 \dot{\theta}_2^2\cos\phi_1\cos\theta_2\cos\phi_2\sin\theta_1 \\
&- l_1 l_2 m_2 \dot{\phi}_2^2\cos\theta_1\cos\phi_1\cos\phi_2\sin\theta_2 + l_1 l_2 m_2 \dot{\phi}_2^2\cos\phi_1\cos\theta_2\cos\phi_2\sin\theta_1 \\
&+ l_1 l_2 m_2 \dot{\theta}_2^2\cos\theta_2\sin\theta_1\sin\phi_1\sin\phi_2 + l_1 l_2 m_2 \dot{\phi}_2^2\cos\theta_2\sin\theta_1\sin\phi_1\sin\phi_2 \\
&- 2 l_1 l_2 m_2 \dot{\theta}_2\dot{\phi}_2\cos\phi_1\sin\theta_1\sin\theta_2\sin\phi_2 + 2 l_1 l_2 m_2 \dot{\theta}_2\dot{\phi}_2\cos\phi_2\sin\theta_1\sin\phi_1\sin\theta_2 \\
&- 2 l_1 l_2 m_2 \dot{\theta}_2\dot{\phi}_2\cos\theta_1\cos\phi_1\cos\theta_2\sin\phi_2 = -u(2)
\end{aligned}
\tag{A.13}
$$

In the ϕ_1 direction,

$$
\begin{aligned}
&I_{1x}\ddot{\phi}_1 + l_1 m_2 \ddot{y}\cos\theta_1\cos\phi_1 + g l_1 m_2 \cos\theta_1\sin\phi_1 + l_1 m_2 \ddot{z}\cos\theta_1\sin\phi_1 \\
&+ l_1^2 m_2 \ddot{\phi}_1\cos^2\theta_1\cos^2\phi_1 + l_1 m_2 \ddot{x}\sin\theta_1\sin\phi_1 + l_1^2 m_2 \ddot{\phi}_1\cos^2\theta_1\sin^2\phi_1 \\
&+ l_1^2 m_2 \ddot{\phi}_1\sin^2\theta_1\sin^2\phi_1 + l_1^2 m_2 \dot{\theta}_1^2\cos\phi_1\sin^2\theta_1\sin\phi_1 + l_1^2 m_2 \dot{\phi}_1^2\cos\phi_1\sin^2\theta_1\sin\phi_1 \\
&- 2 l_1^2 m_2 \dot{\theta}_1\dot{\phi}_1\cos\theta_1\cos^2\phi_1\sin\theta_1 - l_1^2 m_2 \ddot{\theta}_1\cos\theta_1\cos\phi_1\sin\theta_1\sin\phi_1 \\
&+ l_1 l_2 m_2 \ddot{\phi}_2\cos\theta_1\cos\phi_1\cos\theta_2\cos\phi_2 - l_1 l_2 m_2 \ddot{\theta}_2\cos\theta_1\cos\phi_1\sin\theta_2\sin\phi_2 \\
&+ l_1 l_2 m_2 \ddot{\theta}_2\cos\theta_1\cos\phi_2\sin\phi_1\sin\theta_2 - l_1 l_2 m_2 \ddot{\theta}_2\cos\theta_2\cos\phi_2\sin\theta_1\sin\phi_1 \\
&+ l_1 l_2 m_2 \ddot{\phi}_2\cos\theta_1\cos\theta_2\sin\phi_1\sin\phi_2 + l_1 l_2 m_2 \ddot{\phi}_2\sin\theta_1\sin\phi_1\sin\theta_2\sin\phi_2 \\
&- l_1 l_2 m_2 \dot{\theta}_2^2\cos\theta_1\cos\phi_1\cos\theta_2\sin\phi_2 + l_1 l_2 m_2 \dot{\theta}_2^2\cos\theta_1\cos\theta_2\cos\phi_2\sin\phi_1 \\
&- l_1 l_2 m_2 \dot{\phi}_2^2\cos\theta_1\cos\phi_1\cos\theta_2\sin\phi_2 + l_1 l_2 m_2 \dot{\phi}_2^2\cos\theta_1\cos\theta_2\cos\phi_2\sin\phi_1 \\
&+ l_1 l_2 m_2 \dot{\theta}_2^2\cos\phi_2\sin\theta_1\sin\phi_1\sin\theta_2 + l_1 l_2 m_2 \dot{\phi}_2^2\cos\phi_2\sin\theta_1\sin\phi_1\sin\theta_2 \\
&- 2 l_1 l_2 m_2 \dot{\theta}_2\dot{\phi}_2\cos\theta_1\sin\phi_1\sin\theta_2\sin\phi_2 + 2 l_1 l_2 m_2 \dot{\theta}_2\dot{\phi}_2\cos\theta_2\sin\theta_1\sin\phi_1\sin\phi_2 \\
&- 2 l_1 l_2 m_2 \dot{\theta}_2\dot{\phi}_2\cos\theta_1\cos\phi_1\cos\phi_2\sin\theta_2 = -u(3)
\end{aligned}
\tag{A.14}
$$

In the θ_2 direction,

$$
\begin{aligned}
&I_{2y}\ddot{\theta}_2 - l_2 m_2 \ddot{x}\cos\theta_2\cos\phi_2 + g l_2 m_2\cos\phi_2\sin\theta_2 + l_2 m_2 \ddot{z}\cos\phi_2\sin\theta_2 \\
&+ l_2^2 m_2\ddot{\theta}_2\cos^2\theta_2\cos^2\phi_2 - l_2 m_2\ddot{y}\sin\theta_2\sin\phi_2 + l_2^2 m_2\ddot{\theta}_2\cos^2\phi_2\sin^2\theta_2 + l_2^2 m_2\ddot{\theta}_2\sin^2\theta_2\sin^2\phi_2 \\
&+ l_2^2 m_2\dot{\theta}_2^2\cos\theta_2\sin\theta_2\sin^2\phi_2 + l_2^2 m_2\dot{\phi}_2^2\cos\theta_2\sin\theta_2\sin^2\phi_2 - 2l_2^2 m_2\dot{\theta}_2\dot{\phi}_2\cos^2\theta_2\cos\phi_2\sin\phi_2 \\
&- l_2^2 m_2\ddot{\phi}_2\cos\theta_2\cos\phi_2\sin\theta_2\sin\phi_2 + l_1 l_2 m_2\ddot{\theta}_1\cos\theta_1\cos\phi_1\cos\theta_2\cos\phi_2 \\
&+ l_1 l_2 m_2\ddot{\theta}_1\cos\phi_1\cos\phi_2\sin\theta_1\sin\theta_2 - l_1 l_2 m_2\ddot{\phi}_1\cos\theta_1\cos\phi_1\sin\theta_2\sin\phi_2 \\
&+ l_1 l_2 m_2\ddot{\phi}_1\cos\theta_1\cos\phi_2\sin\phi_1\sin\theta_2 - l_1 l_2 m_2\ddot{\phi}_1\cos\theta_2\cos\phi_2\sin\theta_1\sin\phi_1 \\
&+ l_1 l_2 m_2\ddot{\theta}_1\sin\theta_1\sin\phi_1\sin\theta_2\sin\phi_2 + l_1 l_2 m_2\dot{\theta}_1^2\cos\theta_1\cos\phi_1\cos\phi_2\sin\theta_2 \\
&- l_1 l_2 m_2\dot{\theta}_1^2\cos\phi_1\cos\theta_2\cos\phi_2\sin\theta_1 + l_1 l_2 m_2\dot{\phi}_1^2\cos\theta_1\cos\phi_1\cos\phi_2\sin\theta_2 \\
&- l_1 l_2 m_2\dot{\phi}_1^2\cos\phi_1\cos\theta_2\cos\phi_2\sin\theta_1 + l_1 l_2 m_2\dot{\theta}_1^2\cos\theta_1\sin\phi_1\sin\theta_2\sin\phi_2 \\
&+ l_1 l_2 m_2\dot{\phi}_1^2\cos\theta_1\sin\phi_1\sin\theta_2\sin\phi_2 + 2l_1 l_2 m_2\dot{\theta}_1\dot{\phi}_1\cos\phi_1\sin\theta_1\sin\theta_2\sin\phi_2 \\
&- 2l_1 l_2 m_2\dot{\theta}_1\dot{\phi}_1\cos\phi_2\sin\theta_1\sin\phi_1\sin\theta_2 - 2l_1 l_2 m_2\dot{\theta}_1\dot{\phi}_1\cos\theta_1\cos\theta_2\cos\phi_2\sin\phi_1 = u(2)
\end{aligned}
\tag{A.15}
$$

In the ϕ_2 direction,

$$
\begin{aligned}
&I_{2x}\ddot{\phi}_2 + l_2 m_2 \ddot{y}\cos\theta_2\cos\phi_2 + g l_2 m_2\cos\theta_2\sin\phi_2 + l_2 m_2 \ddot{z}\cos\theta_2\sin\phi_2 \\
&\quad + l_2^2 m_2\ddot{\phi}_2\cos^2\theta_2\cos^2\phi_2 + l_2 m_2\ddot{x}\sin\theta_2\sin\phi_2 + l_2^2 m_2\ddot{\phi}_2\cos^2\theta_2\sin^2\phi_2 \\
&\quad + l_2^2 m_2\ddot{\phi}_2\sin^2\theta_2\sin^2\phi_2 + l_2^2 m_2\dot{\theta}_2^2\cos\phi_2\sin^2\theta_2\sin\phi_2 + l_2^2 m_2\dot{\phi}_2^2\cos\phi_2\sin^2\theta_2\sin\phi_2 \\
&\quad - 2l_2^2 m_2\dot{\theta}_2\dot{\phi}_2\cos\theta_2\cos^2\phi_2\sin\theta_2 - l_2^2 m_2\ddot{\theta}_2\cos\theta_2\cos\phi_2\sin\theta_2\sin\phi_2 \\
&\quad + l_1 l_2 m_2\ddot{\phi}_1\cos\theta_1\cos\phi_1\cos\theta_2\cos\phi_2 - l_1 l_2 m_2\ddot{\theta}_1\cos\theta_1\cos\phi_1\sin\theta_2\sin\phi_2 \\
&\quad + l_1 l_2 m_2\ddot{\theta}_1\cos\phi_1\cos\theta_2\sin\theta_1\sin\phi_2 - l_1 l_2 m_2\ddot{\theta}_1\cos\theta_2\cos\phi_2\sin\theta_1\sin\phi_1 \\
&\quad + l_1 l_2 m_2\ddot{\phi}_1\cos\theta_1\cos\theta_2\sin\phi_1\sin\phi_2 + l_1 l_2 m_2\ddot{\phi}_1\sin\theta_1\sin\phi_1\sin\theta_2\sin\phi_2 \\
&\quad + l_1 l_2 m_2\dot{\theta}_1^2\cos\theta_1\cos\phi_1\cos\theta_2\sin\phi_2 - l_1 l_2 m_2\dot{\theta}_1^2\cos\theta_1\cos\theta_2\cos\phi_2\sin\phi_1 \\
&\quad + l_1 l_2 m_2\dot{\phi}_1^2\cos\theta_1\cos\phi_1\cos\theta_2\sin\phi_2 - l_1 l_2 m_2\dot{\phi}_1^2\cos\theta_1\cos\theta_2\cos\phi_2\sin\phi_1 \\
&\quad + l_1 l_2 m_2\dot{\theta}_1^2\cos\phi_1\sin\theta_1\sin\theta_2\sin\phi_2 + l_1 l_2 m_2\dot{\phi}_1^2\cos\phi_1\sin\theta_1\sin\theta_2\sin\phi_2 \\
&\quad + 2l_1 l_2 m_2\dot{\theta}_1\dot{\phi}_1\cos\theta_1\sin\phi_1\sin\theta_2\sin\phi_2 - 2l_1 l_2 m_2\dot{\theta}_1\dot{\phi}_1\cos\theta_2\sin\theta_1\sin\phi_1\sin\phi_2 \\
&\quad - 2l_1 l_2 m_2\dot{\theta}_1\dot{\phi}_1\cos\phi_1\cos\theta_2\cos\phi_2\sin\theta_1 = u(3) \quad \text{(A.16)}
\end{aligned}
$$

Appendix B

LINEARIZED MATRICES AND GAIN MATRIX

B.1 Linarized A and B matrices

Below are the linearized A and B matrices for the 2D planar quadrotor model in symbollic form referred to in Chapter 4.

$$\mathbf{A} = \begin{bmatrix} 0 & 0 & 0 & 0 & 1 & 0 & 0 & 0 \\ 0 & 0 & 0 & 0 & 0 & 1 & 0 & 0 \\ 0 & 0 & 0 & 0 & 0 & 0 & 1 & 0 \\ 0 & 0 & 0 & 0 & 0 & 0 & 0 & 1 \\ 0 & 0 & \frac{I_2 g m_1 l_1^2 m_2 + I_1 g l_2^2 m_2 (m_1+m_2) + I_1 I_2 g (m_1+m_2)}{m_1 m_2 (I_2 l_1^2 + I_1 l_2^2) + I_1 I_2 (m_1+m_2)} & \frac{-I_1 g l_2^2 m_2^2}{m_1 m_2 (I_2 l_1^2 + I_1 l_2^2) + I_1 I_2 (m_1+m_2)} & 0 & 0 & 0 & 0 \\ 0 & 0 & 0 & 0 & 0 & 0 & 0 & 0 \\ 0 & 0 & \frac{-g l_1 l_2^2 m_1 m_2^2}{m_1 m_2 (I_2 l_1^2 + I_1 l_2^2) + I_1 I_2 (m_1+m_2)} & \frac{g l_1 l_2^2 m_1 m_2^2}{m_1 m_2 (I_2 l_1^2 + I_1 l_2^2) + I_1 I_2 (m_1+m_2)} & 0 & 0 & 0 & 0 \\ 0 & 0 & \frac{g l_2 m_2 (m_1 m_2 l_1^2 + I_1 m_1 + I_1 m_2)}{m_1 m_2 (I_2 l_1^2 + I_1 l_2^2) + I_1 I_2 (m_1+m_2)} & \frac{-g l_2 m_2 (m_1 m_2 l_1^2 + I_1 m_1 + I_1 m_2)}{m_1 m_2 (I_2 l_1^2 + I_1 l_2^2) + I_1 I_2 (m_1+m_2)} & 0 & 0 & 0 & 0 \end{bmatrix} \tag{B.1}$$

$$\mathbf{B} = \begin{bmatrix} 0 & 0 \\ 0 & 0 \\ 0 & 0 \\ 0 & 0 \\ 0 & \frac{I_1 l_2 m_2 - I_2 l_1 m_2}{m_1 m_2 (I_2 l_1^2 + I_1 l_2^2) + I_1 I_2 (m_1+m_2)} \\ \frac{1}{m_1+m_2} & 0 \\ 0 & \frac{-m_1 m_2 (l_2^2 + l_1 l_2) + I_2 (m_1+m_2)}{m_1 m_2 (I_2 l_1^2 + I_1 l_2^2) + I_1 I_2 (m_1+m_2)} \\ 0 & \frac{m_1 m_2 (l_1^2 + l_2 l_1) + I_1 (m_1+m_2)}{m_1 m_2 (I_2 l_1^2 + I_1 l_2^2) + I_1 I_2 (m_1+m_2)} \end{bmatrix}. \tag{B.2}$$

When the planar A and B matrices in (B.1) and (B.2) are evaluated using the quadrotor parameters in Table 4.1, the result is

A =

0	0	0	0	1.0000	0	0	0
0	0	0	0	0	1.0000	0	0
0	0	0	0	0	0	1.0000	0
0	0	0	0	0	0	0	1.0000
0	0	11.0582	-1.2482	0	0	0	0
0	0	0	0	0	0	0	0
0	0	-3.6862	3.6862	0	0	0	0
0	0	55.6598	-55.6598	0	0	0	0

B =

0	0
0	0
0	0
0	0
0	5.8095
1.1364	0
0	-234.2972
0	302.4772

The A and B matrices for the 3D nonlinear quadrotor model evaluated using the parameters in 4.1 are

```
A =

  Columns 1 through 8

         0         0         0         0         0         0         0         0
         0         0         0         0         0         0         0         0
         0         0         0         0         0         0         0         0
         0         0         0         0         0         0         0         0
         0         0         0         0         0         0         0         0
         0         0         0         0         0         0         0         0
         0         0         0         0         0         0         0         0
         0         0         0         0         0         0         0         0
         0         0         0   11.0270         0         0   -1.2170         0
         0         0         0         0  -11.0270         0         0    1.2170
         0         0         0         0         0         0         0         0
         0         0         0   -3.6997         0         0    3.6997         0
         0         0         0         0   -3.6997         0         0    3.6997
         0         0         0         0         0         0         0         0
         0         0         0   55.5050         0         0  -55.5050         0
         0         0         0         0   55.5050         0         0  -55.5050

  Columns 9 through 16

    1.0000         0         0         0         0         0         0         0
         0    1.0000         0         0         0         0         0         0
         0         0    1.0000         0         0         0         0         0
         0         0         0    1.0000         0         0         0         0
         0         0         0         0    1.0000         0         0         0
         0         0         0         0         0    1.0000         0         0
         0         0         0         0         0         0    1.0000         0
         0         0         0         0         0         0         0    1.0000
         0         0         0         0         0         0         0         0
         0         0         0         0         0         0         0         0
         0         0         0         0         0         0         0         0
         0         0         0         0         0         0         0         0
         0         0         0         0         0         0         0         0
         0         0         0         0         0         0         0         0
         0         0         0         0         0         0         0         0
```

B =

```
         0         0         0         0
         0         0         0         0
         0         0         0         0
         0         0         0         0
         0         0         0         0
         0         0         0         0
         0         0         0         0
         0         0         0         0
         0    5.6641         0         0
         0         0   -5.6641         0
    1.1111         0         0         0
         0 -234.3598         0         0
         0         0 -234.3598         0
         0         0         0  122.1374
         0  301.7565         0         0
         0         0  301.7565         0
```

B.2 Optimal Feedback Gain Matrix

The optimal feedback gain computed for the 3D quadrotor model according to the development in Chapter 4 is:

```
K =

  Columns 1 through 9

   -0.0000   -0.0000   47.6731    0.0000    0.0000   -0.0000   -0.0000    0.0000   -0.0000
   -2.5318   -0.0000    0.0000  -15.1356    0.0000    0.0000    4.4131    0.0000   -2.4851
    0.0000    2.5318   -0.0000    0.0000  -15.1356   -0.0000   -0.0000    4.4131    0.0000
   -0.0000   -0.0000   -0.0000   -0.0000    0.0000    1.0000    0.0000   -0.0000   -0.0000

  Columns 10 through 16

   -0.0000   10.4182    0.0000    0.0000   -0.0000    0.0000    0.0000
   -0.0000   -0.0000   -2.0385    0.0000    0.0000   -0.4713    0.0000
    2.4851   -0.0000    0.0000   -2.0385   -0.0000    0.0000   -0.4713
   -0.0000   -0.0000   -0.0000    0.0000    1.0082   -0.0000    0.0000
```

Appendix C

QUADROTOR WITHOUT DYNAMIC INERTIA

In order to evaluate the quadrotor with dynamic inertia, the tracking performance of the quadrotor with dynamic inertia is compared to the tracking of performance controlled with traditional differential thrust inputs. To develop a quadrotor model using traditional differential thrust control begin with the nonlinear equations of motion for the quadrotor with dynamic inertia (3.12). Because there is no dynamic mass, substitute the states associated with the dynamic mass with zero, $m_2 = \theta_2 = \phi_2 = 0$. The last two equations of motion corresponding to the angular position of the dynamic mass evaluate to zero, leaving

$$\begin{aligned} m_1\ddot{x} &= -T\sin\theta_1\cos\phi_1\cos\psi_1 \\ m_1\ddot{y} &= T\cos\theta_1\sin\phi_1\cos\psi_1 \\ m_1\ddot{z} + gm_1 &= T\cos\theta_1\cos\phi_1 \\ I_{1_y}\ddot{\theta}_1 &= -\tau_1 \\ I_{1_x}\ddot{\phi}_1 &= -\tau_2 \\ I_{1_z}\ddot{\psi}_1 &= \tau_3 \end{aligned}$$

The Ascending Technology Hummingbird quadrotor has an inner loop controller that controls the RPM of each of the four motors to generate rotational moments on the vehicle. In other words the user does not provide individual motor RPM as an input, but simply the desired roll, pitch, or yaw angle. Therefore, let the control inputs be thrust, pitch, roll, and yaw

$$u_1 = T \qquad u_2 = \theta_1 \qquad u_3 = \phi_1 \qquad u_4 = \psi_1 \ .$$

Substituting the control inputs into the original equations of motion produces,

$$\begin{aligned} m_1\ddot{x} &= -u_1 \sin u_2 \cos u_3 \cos u_4 \\ m_1\ddot{y} &= u_1 \cos u_2 \sin u_3 \cos u_4 \\ m_1\ddot{z} + gm_1 &= u_1 \cos u_2 \cos u_3 \ . \end{aligned} \tag{C.1}$$

To develop an LQR controller for this quadrotor model the equations of motion are linearized about the hovering flight condition using the small perturbation linearization method. Once again, the linearization conditions are

$$\begin{aligned} x_0 &= 0 & y_0 &= 0 & z_0 &= 0 \\ u_{1_0} &= g * m_1 & u_{2_0} &= 0 & u_{3_0} &= 0 \ . \end{aligned}$$

The resulting linearized equations of motion for the three dimensional quadrotor without dynamic inertia are

$$\begin{bmatrix} m_1 & 0 & 0 \\ 0 & m_1 & 0 \\ 0 & 0 & m_1 \end{bmatrix} \begin{bmatrix} \delta\ddot{x} \\ \delta\ddot{y} \\ \delta\ddot{z} \end{bmatrix} = \begin{bmatrix} 0 & -u_{1_0} & 0 & 0 \\ 0 & 0 & u_{1_0} & 0 \\ 1 & 0 & 0 & 0 \end{bmatrix} \begin{bmatrix} \delta u_1 \\ \delta u_2 \\ \delta u_3 \\ \delta u_3 \end{bmatrix} \ . \tag{C.2}$$

The weighting matrices used to develop the LQR controller are

$$\mathbf{Q} = \begin{bmatrix} 10 & 0 & 0 & 0 & 0 & 0 \\ 0 & 10 & 0 & 0 & 0 & 0 \\ 0 & 0 & 100 & 0 & 0 & 0 \\ 0 & 0 & 0 & 1 & 0 & 0 \\ 0 & 0 & 0 & 0 & 1 & 0 \\ 0 & 0 & 0 & 0 & 0 & 1 \end{bmatrix} \qquad \mathbf{R} = \begin{bmatrix} 0.044 & 0 & 0 & 0 \\ 0 & 1 & 0 & 0 \\ 0 & 0 & 1 & 0 \\ 0 & 0 & 0 & 1 \end{bmatrix} \ .$$

In a similar way, a planar quadrotor model without dynamic inertia was developed as well. Beginning withe nonlinear equations of motion for the quadrotor with dynamic inertia (3.13), the states associated with the dynamic mass are set equal to

zero resulting in the planar nonlinear equations for the quadrotor without dynamic inertia:

$$\begin{aligned} m\ddot{x} &= -u_1 \sin u_2 \\ m\ddot{z} + gm &= u_1 \cos u_2 \ . \end{aligned} \tag{C.3}$$

Once again, small perturbation analysis is used to linearize the nonlinear equations of motion, where the linearization conditions are $u_{1_0} = gm$ and $u_{2_0} = 0$. The result of this process is linearized planar quadrotor model without dynamic inertia:

$$\begin{bmatrix} m_1 & 0 \\ 0 & m_1 \end{bmatrix} \begin{bmatrix} \delta\ddot{x} \\ \delta\ddot{z} \end{bmatrix} = \begin{bmatrix} 0 & -u_{1_0} \\ 1 & 0 \end{bmatrix} \begin{bmatrix} \delta u_1 \\ \delta u_2 \end{bmatrix} \ . \tag{C.4}$$

The weighting matrices used to develop the LQR controller are

$$\mathbf{Q} = \begin{bmatrix} 10 & 0 & 0 & 0 \\ 0 & 100 & 0 & 0 \\ 0 & 0 & 1 & 0 \\ 0 & 0 & 0 & 1 \end{bmatrix} \qquad \mathbf{R} = \begin{bmatrix} 0.044 & 0 \\ 0 & 1 \end{bmatrix} \ .$$